國立交通大學

機械工程學系

碩士論文

整數階與分數階變革式心搏系統的渾沌及其同步與

反控制

Chaos, Its Synchronization and Anticontrol of Integral and Fractional Order Modified Heartbeat Systems

研 究 生： 張安瑞

指導教授： 戈正銘 教授

中華民國九十五年六月

整數階與分數階變革式心搏系統的渾沌及其同步與反控制

Chaos, Its Synchronization and Anticontrol of Integral and Fractional Order Modified Heartbeat Systems

研 究 生： 張安瑞　　Student：An-Ray Zhang
指導教授： 戈正銘　　Advisor：Zheng-Ming Ge

國 立 交 通 大 學
機 械 工 程 學 系

碩 士 論 文

A Thesis
Submitted to Department of Mechanical Engineering
College of Engineering
National Chiao Tung University
In Partial Fulfillment of the Requirements
For the Degree of Master of Science
In
Mechanical Engineering
June 2006
Hsinchu, Taiwan, Republic of China

中華民國九十五年六月

整數階與分數階變革式心搏系統的渾沌及其同步與反控制

學生：張安瑞　　　　　　　　　　　　　　　　指導教授：戈正銘

摘　　　要

本篇論文探討有關整數階與分數階變革式心搏系統的渾沌、渾沌同步及其反控制。藉由相圖、龐卡萊圖及分歧圖等數值模擬結果，可以得知週期及渾沌的現象。另外經由參數激發法使得兩個非耦合的整數階或分數階變革式心搏系統達到同步。並透過外加常數項或非線性項獲得分數階變革式心搏系統的反控制。最後，成功的利用參數激發的方式，讓整數階與分數階的變革式心搏系統達到渾沌化。

Chaos, Its Synchronization and Anticontrol of Integral and Fractional Order Modified Heartbeat Systems

Student：An-Ray Zhang Advisor：Zheng-Ming Ge

Department of Mechanical Engineering
National Chiao Tung University

Abstract

Chaos, chaos synchronization and anticontrol for integral and fractional modified heartbeat systems are studied in the thesis. By applying numerical results, phase portrait, Poincaré maps and bifurcation diagrams, a variety of the phenomena of the periodic and chaotic motion can be presented. The synchronizations of two uncoupled integral and fractional order chaotic modified heartbeat systems are accomplished by parameter excited synchronization. Anticontrol of chaos of fractional order modified heartbeat systems can be obtained by addition of a constant term and addition of a nonlinear term. Chaotization of integral and fractional order modified heartbeat systems by parameter excited method, replacement of the parameter of first system by the function of the chaotic state variables of a second chaotic system, is successfully accomplished.

ACKNOWLEDGMENT

利用兩年的時間完成了本篇論文及碩士學位，其中最感謝的不外乎是給予耐心指導與教誨的　戈正銘教授。教授不僅傳授在專業領域上的知識，更藉由與教授的相處，使得學生無論是在看待事物的態度或是在處理事情的方法都有明顯的改變。此外，教授無論是在專業領域或是文學、史學甚至哲學的博學讓學生深感佩服，並領會到老師的真智慧。

在研究的兩年當中，感謝學長陳炎生、楊振雄、張晉銘在渾沌方面知識的指導與程式的應用。尤其感謝張晉銘學長的大力幫忙，使得本篇論文得以更加完善。其次感謝同學易昌賢與歐展義無論在課業上或是論文研討方面的幫忙，使得學生做起事來事半功倍，充分展現團結的力量。另外，感謝實驗室其他的成員對學生在各方面的支持與幫忙，讓學生可以心無旁騖專心致力於課業與論文的研究。

在二十幾年來的求學過程中，感謝父母及兩位姐姐在生活上給予全力的支持，雖然在求學過程中有著諸多的崎嶇，但他們都無怨無悔的付出，讓學生可以不必擔心課業以外的事與物，得以全心衝刺以造就現今的我。最後，感謝忠翰、柏豪、俊明、佩珊與依萍，謝謝你們分享我的喜怒哀樂，讓我的心情得以宣洩。再一次感謝大家的幫忙與支持，在此獻上十二萬分的敬意。

CONTENTS

LIST OF FIGURES

Chapter 1
Introduction

Chaos is desirable under certain circumstances and chaotic phenomena are quite useful in many applications such as fluid mixing [1], human brain [2], and heart beat regulation [3], etc. But like many other theories in science, the theory of chaos did not get enough attention for almost two decades, ever since Edward Lorenz reported his discovery of the theory in 1963. However, the invention of high-speed computers in the late 1970s and early 1980s brought about a major revolution in nonlinear dynamical theories in general, and chaos theory in particular that is why chaos theory developed in the natural sciences during the 1970s, and the social sciences during the 1980s.

Chaos synchronization [4-12] is a very important topic in the nonlinear [13-15] science and it has been developed extensively. Recently many scientists in various fields have been attracted to investigate chaos synchronization due to its application in a variety of fields such as secure communications, chemical, physical, and biological systems, neural networks, etc. So various synchronization schemes, such as variable structure control [16], parameters adaptive control [17-24], observer based control [25, 26], active control [27-33], nonlinear control [34, 35] and so on have been successfully applied to the chaos synchronization.

Fractional calculus is a 300-year-old mathematical topic. Although it has a long history, the applications of fractional calculus to physics and engineering are just a recent focus of interest [36]. In recent years, many scholars have devoted themselves to study the applications of the fractional order system to physics and engineering such as viscoelastic systems [37], dielectric polarization, and electromagnetic waves. More recently, there is a new trend to investigate the control [38] and dynamics [39-46] of the fractional order dynamical systems [47-49]. In [37] it has been shown that nonlinear chaotic systems still have chaotic behavior when their models become fractional. In [47], chaos control was investigated for fractional chaotic systems by the ‘‘back-stepping’’ method of nonlinear control design. In [48] and [49], it was found that chaos exists in a fractional order Chen system with order less than 3. Linear feedback control of chaos in this system was also studied. In [41], chaos synchronization of fractional order chaotic systems was studied. The existence and uniqueness of solutions of initial value problems for fractional order differential equations have been studied in the literature [50-53].

In addition, anticontrol [54-60] of chaos have received great attention for many research activities in recent years and it is an interesting, new and challenging phenomenon [61-63]. As a reverse process of suppressing or eliminating chaotic behaviors in order to reduce the complexity of an individual system or a coupled system, anticontrol of chaos aims at creating or enhancing the system complexity for some special applications. More precisely, anticontrolling chaos is to generate some chaotic behaviors from a given system, which is non-chaotic or even is stable originally. By fully exploiting the intrinsic nonlinearity, this "control" technique provides another dimension for feedback systems design. Its potential applications can be easily found in many fields, including typically physics, biology, engineering, and medical as well as social sciences.

In this thesis, integral and fractional order modified heartbeat systems, i.e., van der Pol systems, are investigated. Chapter 2 presents a fractional derivative and the model of modified Van der Pol system. In Chapter 3, the dynamics of integral and fractional order modified van der Pol systems are investigated and the numerical results of periodic and chaotic phenomena are presented. The synchronizations of two uncoupled integral and fractional order chaotic modified van der Pol systems are achieved by parameter excited synchronization in Chapter 4. Anticontrol of chaos of fractional order modified van der Pol systems by addition of a constant term and addition of k|x|sinx term are discussed in Chapter 5. The parameter excited chaotization of integral and fractional order modified van der Pol systems is studied in Chapter 6. Finally, the conclusions are draw.

Chapter 2

A Fractional Derivative and a Modified Heartbeat System

2.1 A fractional derivative and its approximation

There are several definitions of fractional derivatives. The commonly used definition for a general fractional derivative is the Riemann-Liouville definition [64], which is given by

$$\frac{d^q f(t)}{dt^q} = \frac{1}{\Gamma(n-q)} \frac{d^n}{dt^n} \int_0^t \frac{f(\tau)}{(t-\tau)^{q-n+1}} d\tau \tag{2.1}$$

where $\Gamma(\cdot)$ is the gamma function and n is an integer such that $n-1<q<n$. This definition is different from the usual intuitive definition of derivative. Fortunately, the basic engineering tool for analyzing linear systems, the Laplace transform, is still applicable and works as one would expect:

$$L\left\{\frac{d^q f(t)}{dt^q}\right\} = s^q L\{f(t)\} - \sum_{k=0}^{n-1} s^k \left[\frac{d^{q-1-k} f(t)}{dt^{q-1-k}}\right]_{t=0}, \quad \text{for all } q, \tag{2.2}$$

where n is an integer such that $n-1<q<n$. Upon considering the initial conditions to be zero, this formula reduces to the more expected form

$$L\left\{\frac{d^q f(t)}{dt^q}\right\} = s^q L\{f(t)\}. \tag{2.3}$$

An efficient method is to approximate fractional operators by using standard integer order operators. In [65-69], an effective algorithm is developed to approximate fractional order transfer functions. Basically the idea is to approximate the system behavior based on frequency domain arguments. By utilizing frequency domain techniques based on Bode diagrams, one can obtain a linear approximation of the fractional order integrator, the order of which depends on the desired bandwidth and discrepancy between the actual and the approximate magnitude Bode diagrams. In Table 1 (See Appendix) of [70], approximations for $\frac{1}{s^q}$ with q = 0.1 ~ 0.9 in steps 0.1 are given, with errors of approximately 2 dB. These approximations are used in the following simulations.

2.2 A modified heartbeat system and the corresponding fractional order system

Firstly, a heartbeat system, i.e. a van der Pol oscillator[71-73], driven by a periodic force is considered. The equation of motion can be written as:

$$\ddot{x} + \varphi x + a\dot{x}(x^2 - 1) - b\sin\omega t = 0 \tag{2.4}$$

In Eq. (2.4), the linear term stands for a conservative harmonic force which determines the intrinsic oscillation frequency. The self-sustaining mechanism which is responsible for the perpetual oscillation rests on the nonlinear term. Energy exchange with the external agent depends on the magnitude of displacement |x| and on the sign of velocity $\dot{x}$. During a complete cycle of oscillation, the energy is dissipated if displacement x(t) is large than one, and that energy is fed-in if |x| < 1. The time-dependent term stands for the external driving force with amplitude b and frequency ω.Eq. (2.4) can be rewritten as two first order equations:

$$\begin{cases} \dot{x} = y \\ \dot{y} = -\varphi x + a(1 - x^2)y + b\sin\omega t \end{cases} \tag{2.5}$$

The modified heartbeat system, i.e. the modified van der Pol system, and its fractional order system studied in this paper are

$$\begin{cases} \dfrac{d^\alpha x}{dt^\alpha} = y \\ \dfrac{d^\beta y}{dt^\beta} = -x + a(1-x^2)y + bz \\ \dot{z} = w \\ \dot{w} = -cz - dz^3 \end{cases} \tag{2.6}$$

where α, β are integer numbers and fractional numbers respectively.

System (2.6) can be separated into two parts:

$$\begin{cases} \dfrac{d^\alpha x}{dt^\alpha} = y \\ \dfrac{d^\beta y}{dt^\beta} = -x + a(1-x^2)y + bz \end{cases} \tag{2.7}$$

and

$$\begin{cases} \dot{z} = w \\ \dot{w} = -cz - dz^3 \end{cases} \tag{2.8}$$

In Eq. (2.5) changing the integral order derivatives to the fractional order derivations and replaceing $\sin \omega t$ by z which is the periodic time function solution of the nonlinear oscillator (2.8), we obtain system (2.7). In Eq. (2.8) if d = 0, z is a sinusoidal function of time. Now d $\neq$ 0, z is a periodic motion of time but not a sinusoidal function of time. As a result, system (2.7) can be considered as a nonautonomous system with two states, while system (2.6) consisting of Eq. (2.7) and Eq. (2.8) can be considered as an autonomous system with four states. When $\alpha = \beta = 1$, Eq.(2.6) is the modified van der Pol system.

Chapter 3

Chaos in a Modified Heartbeat System and in Its Fractional Order Systems

Chaos in a modified van der Pol system and in its fractional order systems is studied in this chapter. It is found that chaos exists both in the system and in the fractional order systems with total order from 1.8 down to 0.8 much less than the number of states of the system, two. By phase portraits, Poincaré maps and bifurcation diagrams, the chaotic behaviors of integral and fractional order modified van der Pol systems are presented.

In this chapter, phase portraits and bifurcation diagrams are studied for system (2.6) for $\alpha + \beta \leq 2$ and three parameters *a, c, d* are chosen as *a* = 5, *c* = 0.01, *d* = 0.001. A time step of 0.001 is used.

3.1 Chaos in a integral order modified heartbeat system

Let $\alpha = \beta = 1$. Fig. 3.1 shows the bifurcation diagram of the 2 order system. It is shown that chaos exists when $b \in [0, 1.0]$. Fig. 3.2 is the phase portrait of chaotic motion with *b* = 1.0. Fig. 3.3 ~ 3.5 are phase portraits of periodic motions with $b = 1.1$, 1.5, 3, respectively.

3.2 Chaos in a fractional order modified heartbeat system

Case 1 Let $\alpha = 0.9$, $\beta = 0.9$.

Fig. 3.6 shows the bifurcation diagram of the 1.8 order system. It is shown that chaos exists when $b \in [0, 9.7]$. Fig. 3.7 is the phase portrait of chaotic motion with *b* = 9.7. Fig. 3.8 ~ 3.11 are phase portraits of periodic motions with $b = 9.8$, 14, 23, 40 respectively.

Case 2 Let $\alpha = 0.9$, $\beta = 0.8$.

Fig. 3.12 shows the bifurcation diagram of the 1.7 order system. It is shown that chaos exists when $b \in [0, 9.8]$. Fig. 3.13 is the phase portrait of chaotic motion with *b* = 9.8. Fig. 3.14 ~ 3.17 are phase portraits of periodic motions with $b = 9.9$, 12, 25, 30, respectively.

Case 3 Let $\alpha = 0.8$, $\beta = 0.9$.

Fig. 3.18 shows the bifurcation diagram of the 1.7 order system. It is shown that chaos exists when $b \in [0, 10.1]$. Fig. 3.19 is the phase portrait of chaotic motion with b = 10.1. Fig. 3.20 ~ 3.24 are phase portraits of periodic motions with $b = 10.2$, 15, 23, 30, 45 respectively.

Case 4 Let $\alpha = 0.8$, $\beta = 0.8$.

Fig. 3.25 shows the bifurcation diagram of the 1.6 order system. It is shown that chaos exists when $b \in [0, 10.1]$. Fig. 3.26 is the phase portrait of chaotic motion with b = 10.1. Fig. 3.27 ~ 3.31 are phase portraits of periodic motions with $b = 10.2$, 14.5, 20, 35, 40 respectively.

Case 5 Let $\alpha = 0.7$, $\beta = 0.7$.

Fig. 3.32 shows the bifurcation diagram of the 1.4 order system. It is shown that chaos exists when $b \in [0, 7.9]$. Fig. 3.33 is the phase portrait of chaotic motion with b = 7.9. Fig. 3.34 ~ 3.37 are phase portraits of periodic motions with $b = 8.0$, 15, 35, 40 respectively.

Case 6 Let $\alpha = 0.6$, $\beta = 0.6$.

Fig. 3.38 shows the bifurcation diagram of the 1.2 order system. It is shown that chaos exists when $b \in [0, 6.0]$. Fig. 3.39 is the phase portrait of chaotic motion with b = 6.0. Fig. 3.40 ~ 3.44 are phase portraits of periodic motions with $b = 6.1$, 6.5, 9.5, 20, 45 respectively.

Case 7 Let $\alpha = 0.5$, $\beta = 0.5$.

Fig. 3.45 shows the bifurcation diagram of the 1.0 order system. It is shown that chaos exists when $b \in [0, 4.2]$. Fig. 3.46 is the phase portrait of chaotic motion with b = 2. Fig. 3.47 ~ 3.49 are phase portraits of periodic motions with $b = 6.0$, 10, 15 respectively.

Case 8 Let $\alpha = 0.4$, $\beta = 0.4$.

Fig. 3.50 shows the bifurcation diagram of the 0.8 order system. It is shown that chaos exists when $b \in [0, 1.8]$. Fig. 3.51 is the phase portrait of chaotic motion with b = 0.7. Fig. 3.52 、 Fig. 3.53 are phase portraits of periodic motions with $b = 0.7$, 1.3 respectively. When we tried to reduce the total order to 0.6, the phase portraits become periodic motions, as shown in Fig. 3.54 and Fig. 3.55, for any *b* value.

Chaos in modified van der Pol system and in its fractional order systems is studied in this chapter. It is found that the range of the chaos in the system gradually decreases as the total order number $\alpha + \beta$ decreases. Nine cases for $0.8 \le (\alpha + \beta) \le 2.0$ are studied. The lowest total order for chaos existence in the system is found to be 0.8.

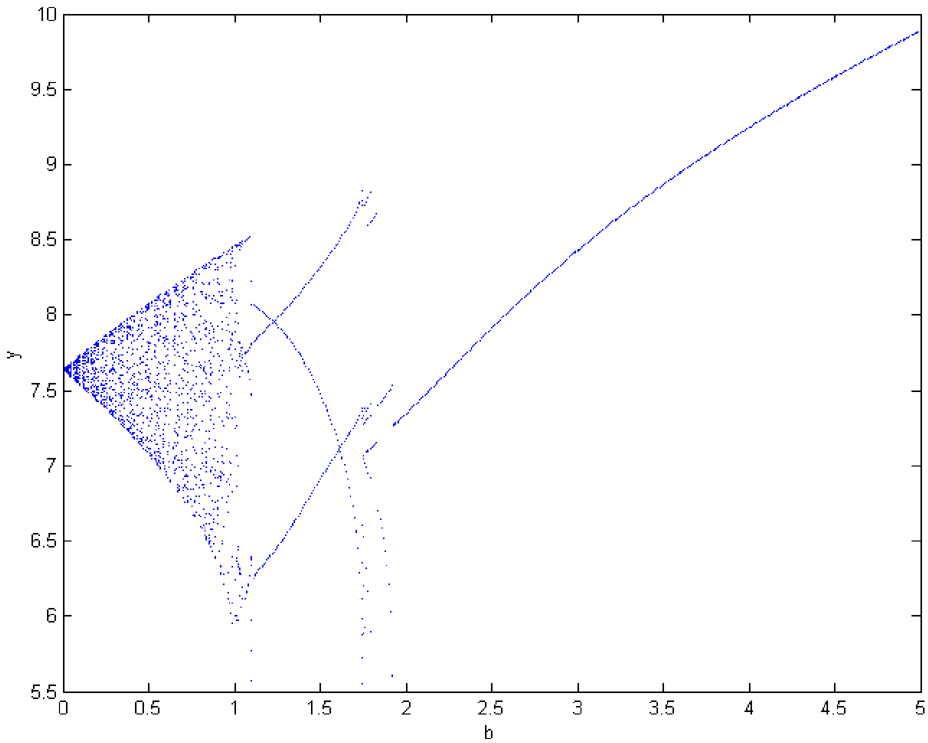

Fig. 3.1 The bifurcation diagram for $\alpha = \beta = 1$.

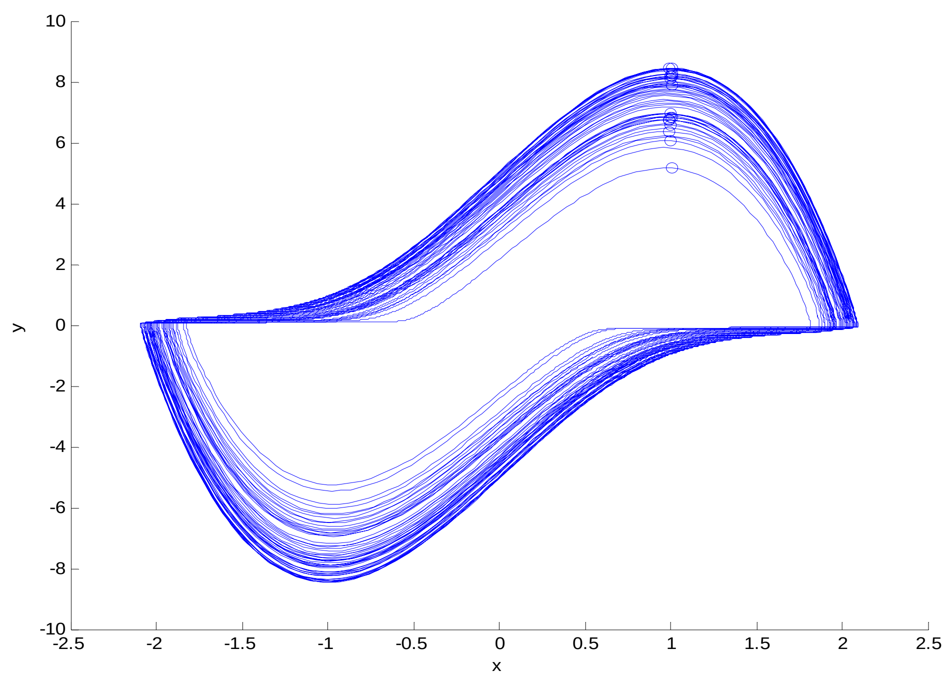

Fig. 3.2 The phase portrait for $\alpha = \beta = 1$, b=1.0.

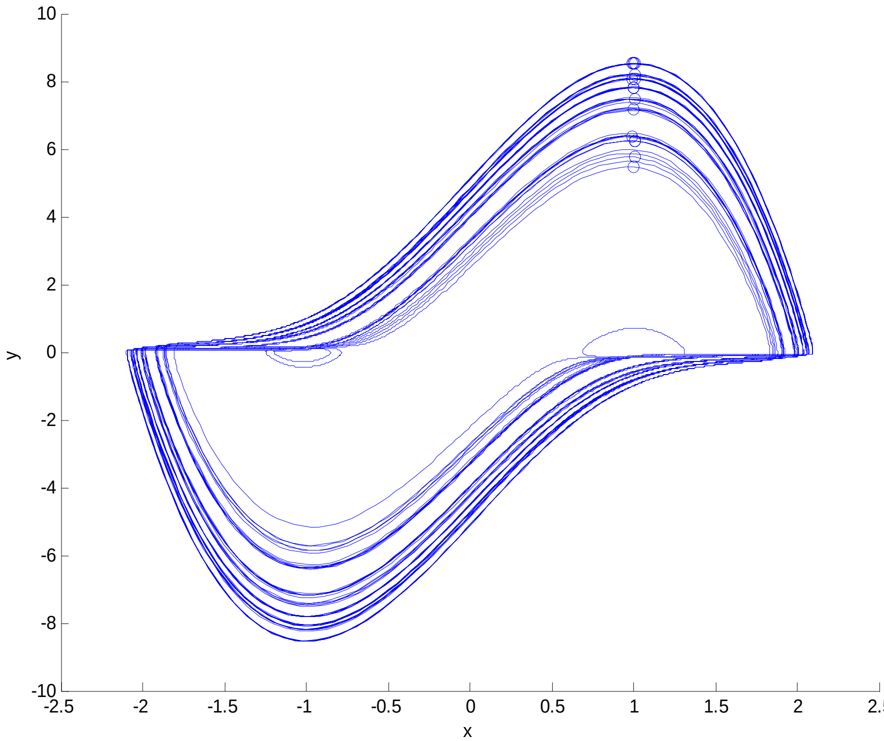

Fig. 3.3 The phase portrait for $\alpha = \beta = 1$, b=1.1.

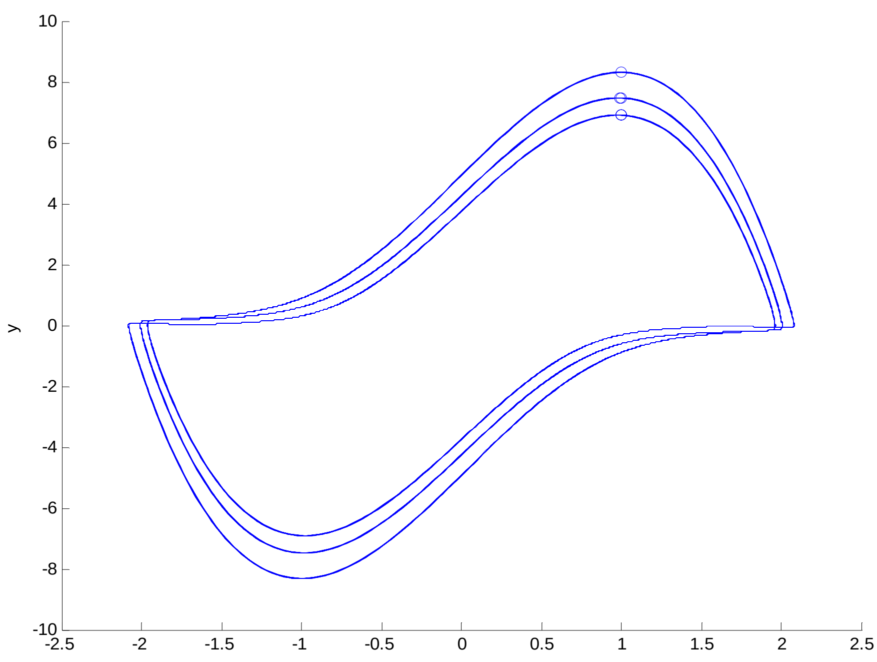

Fig. 3.4 The phase portrait for $\alpha = \beta = 1$, b=1.5.

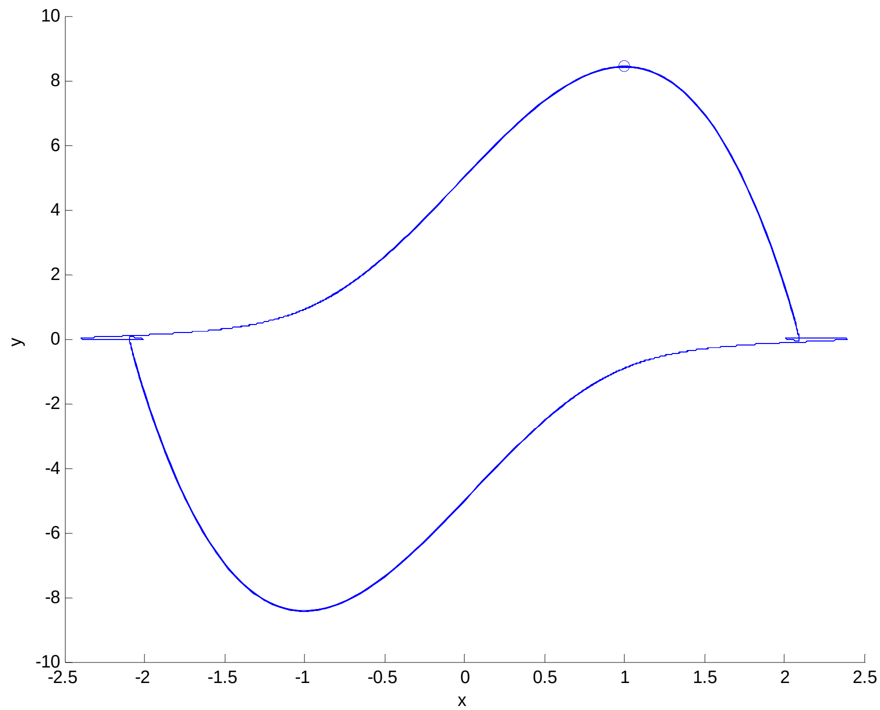

Fig. 3.5 The phase portrait for $\alpha = \beta = 1$, b=3.

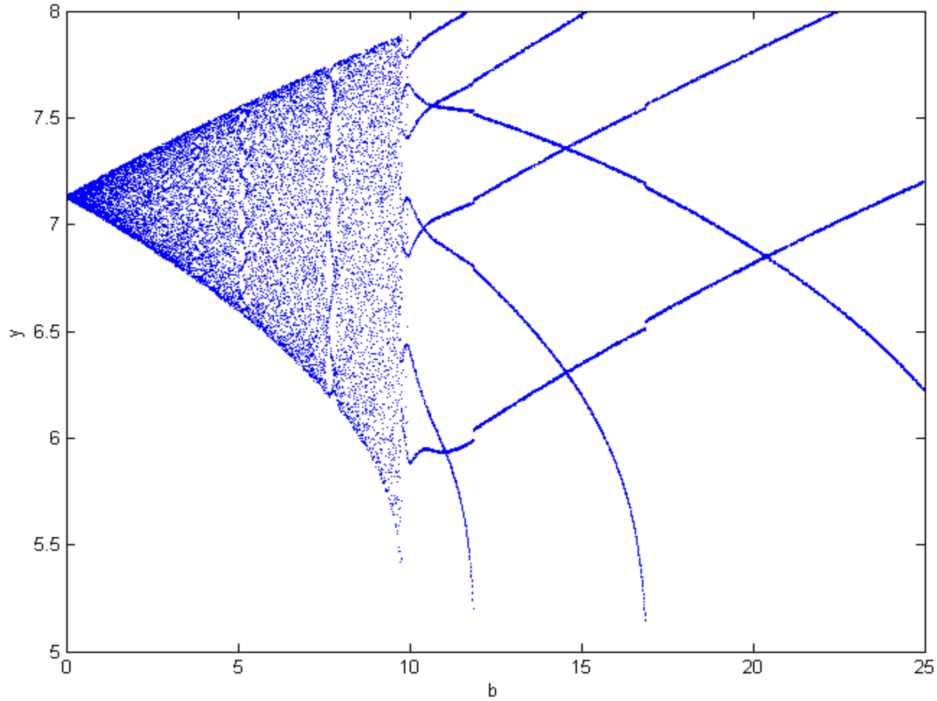

Fig. 3.6 The bifurcation diagram for $\alpha = 0.9$, $\beta = 0.9$.

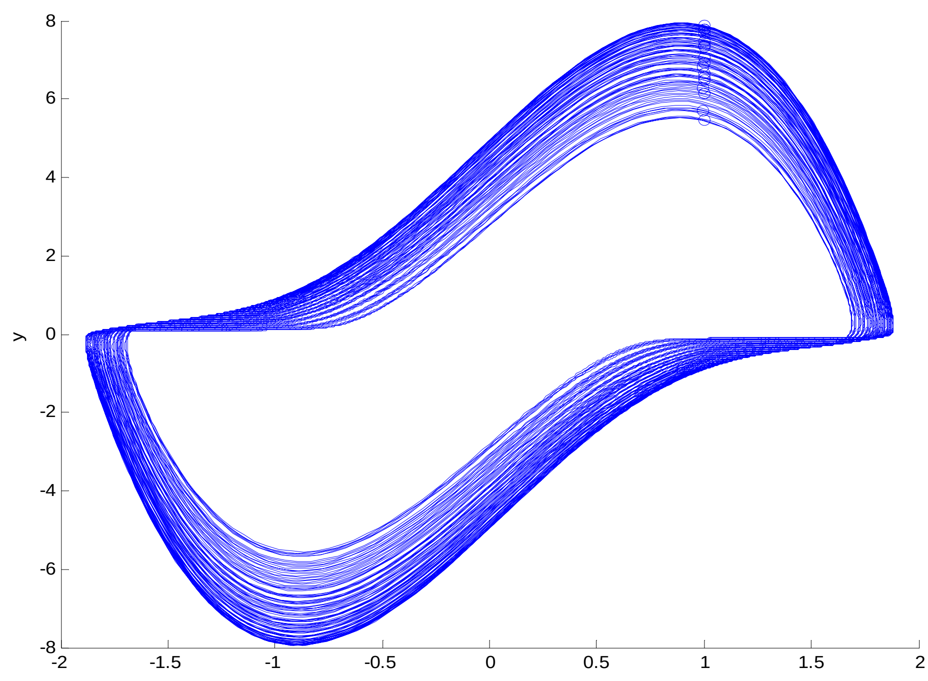

Fig. 3.7 The phase portrait for $\alpha = 0.9$, $\beta = 0.9$, $b = 9.7$.

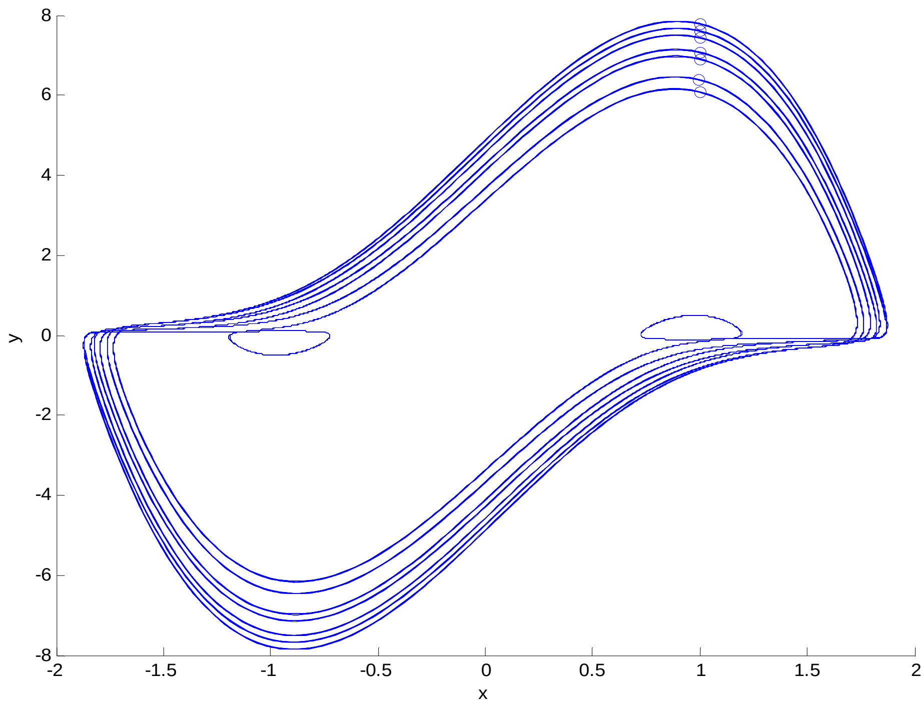

Fig. 3.8 The phase portrait for $\alpha = 0.9$, $\beta = 0.9$, b = 9.8.

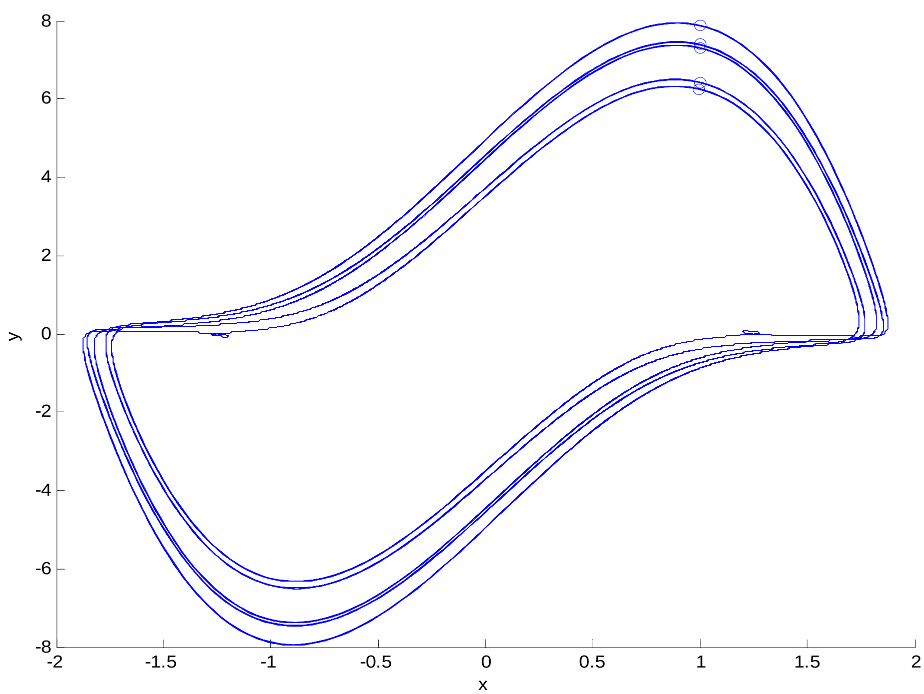

Fig. 3.9 The phase portrait for $\alpha = 0.9$, $\beta = 0.9$, b = 14.

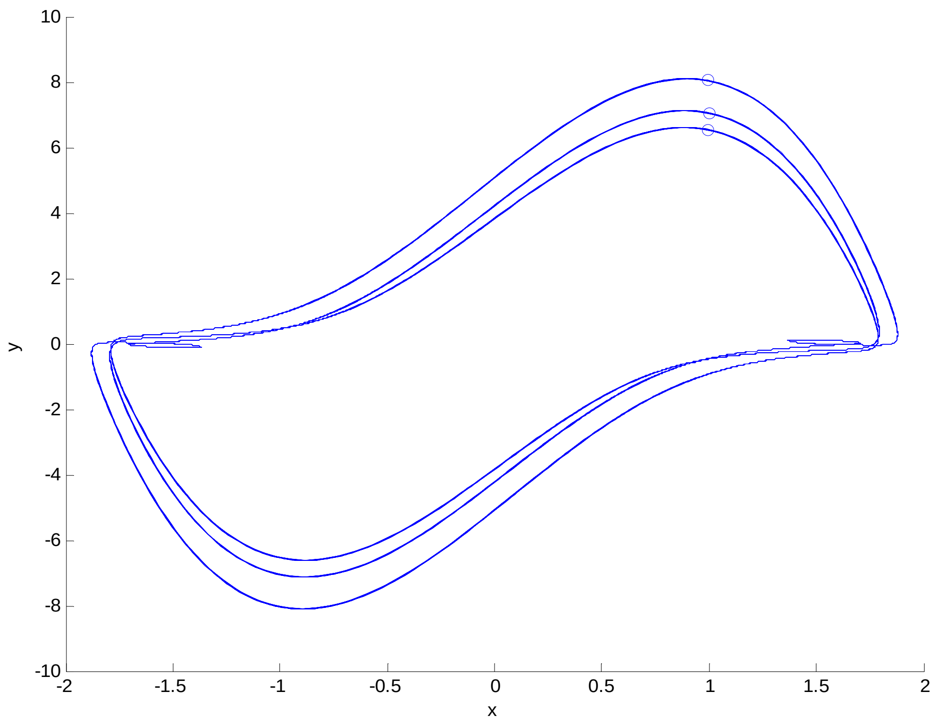

Fig. 3.10 The phase portrait for $\alpha = 0.9$, $\beta = 0.9$, $b = 23$.

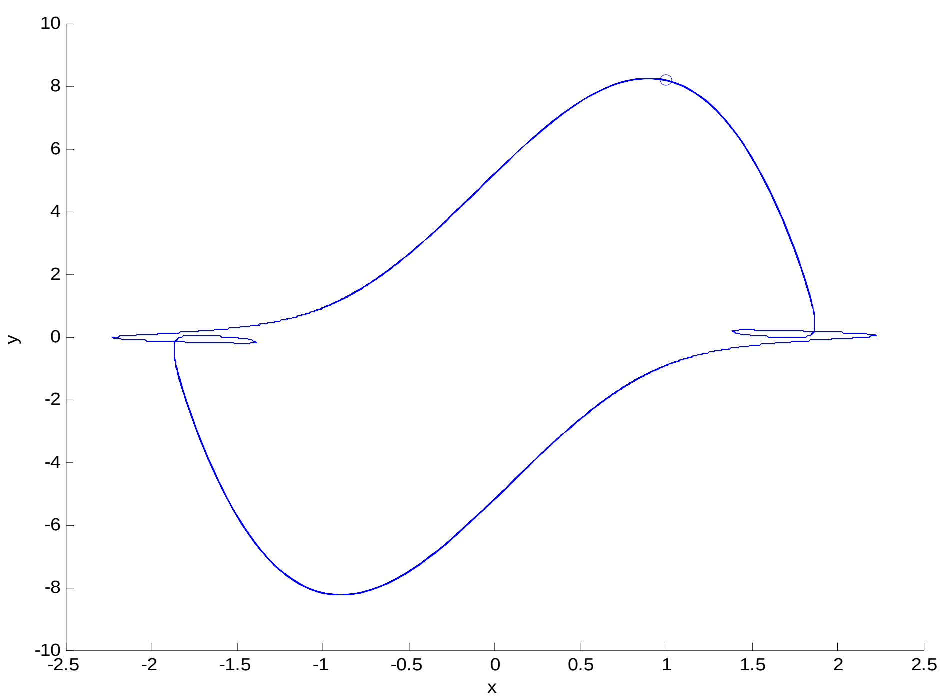

Fig. 3.11 The phase portrait for $\alpha = 0.9$, $\beta = 0.9$, $b = 40$.

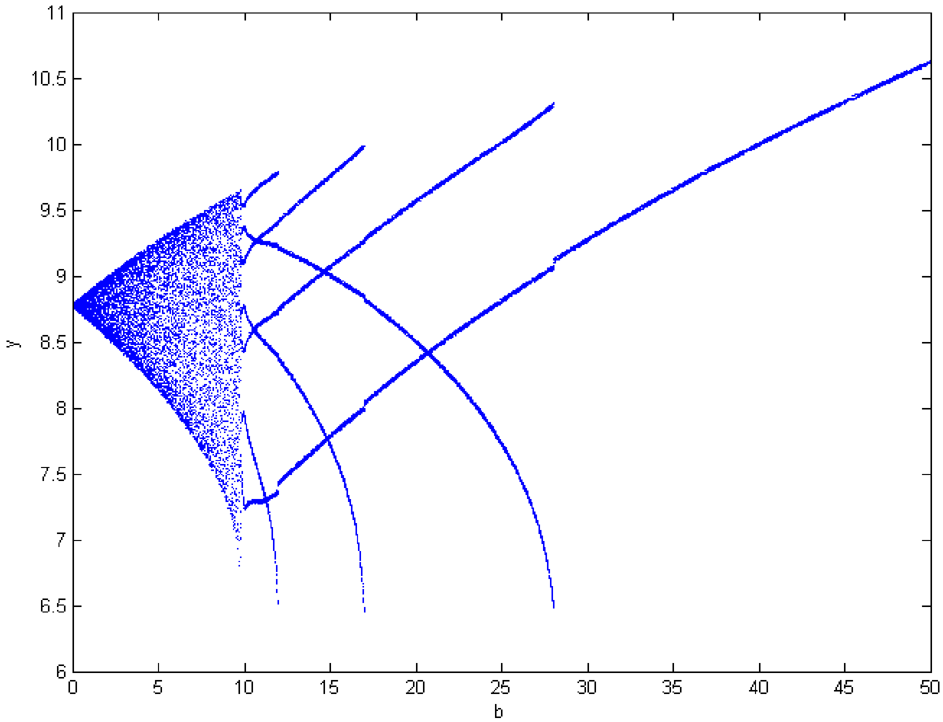

Fig. 3.12 The bifurcation diagram for $\alpha = 0.9$, $\beta = 0.8$.

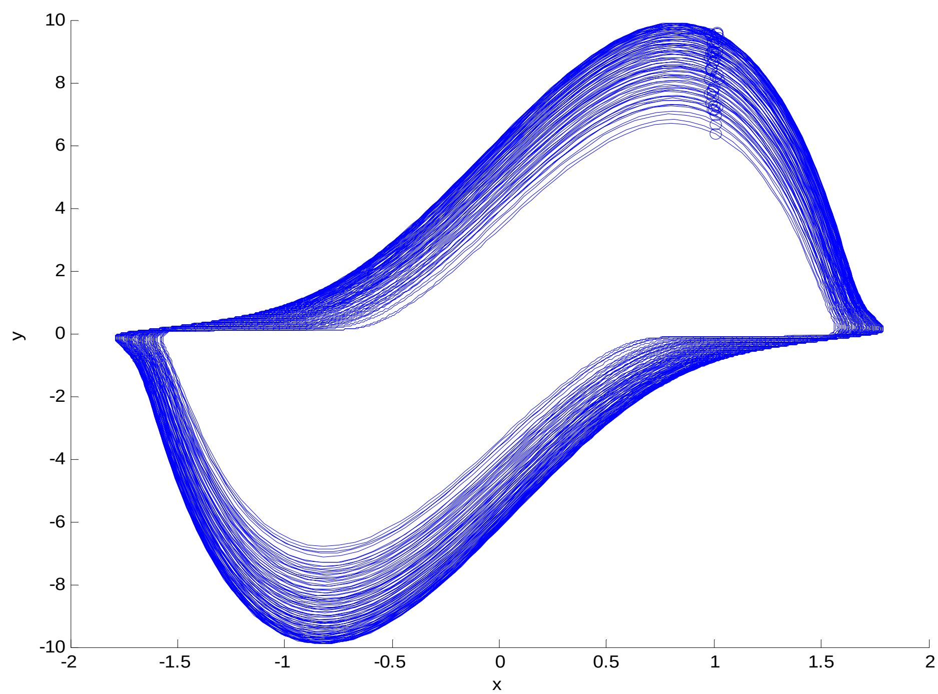

Fig 3.13 The phase portrait for $\alpha = 0.9$, $\beta = 0.8$, $b = 9.8$.

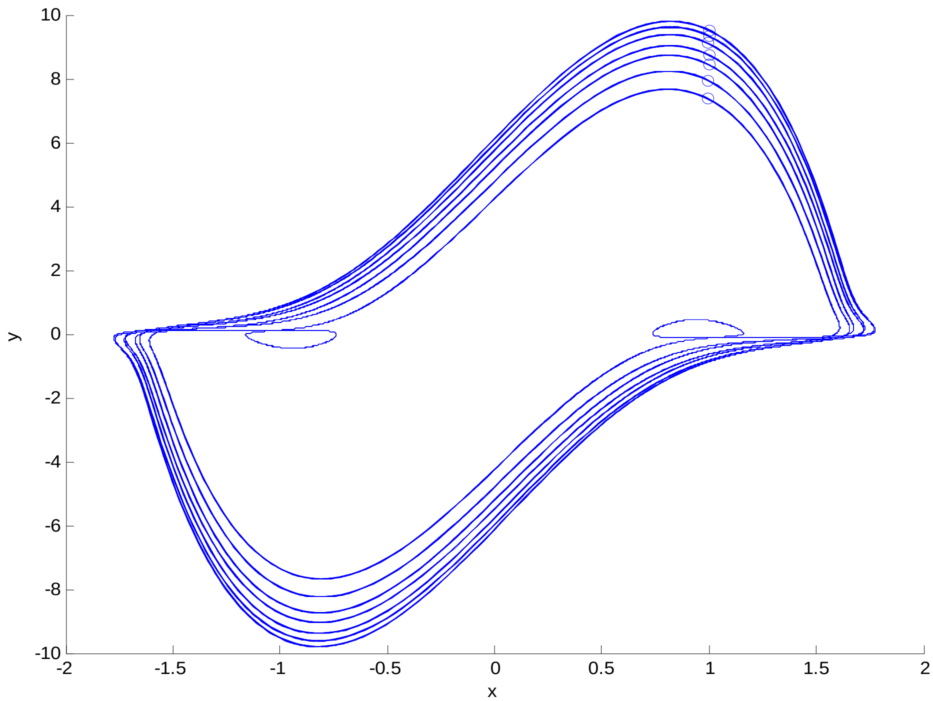

Fig. 3.14 The phase portrait for $\alpha = 0.9$, $\beta = 0.8$, $b = 9.9$.

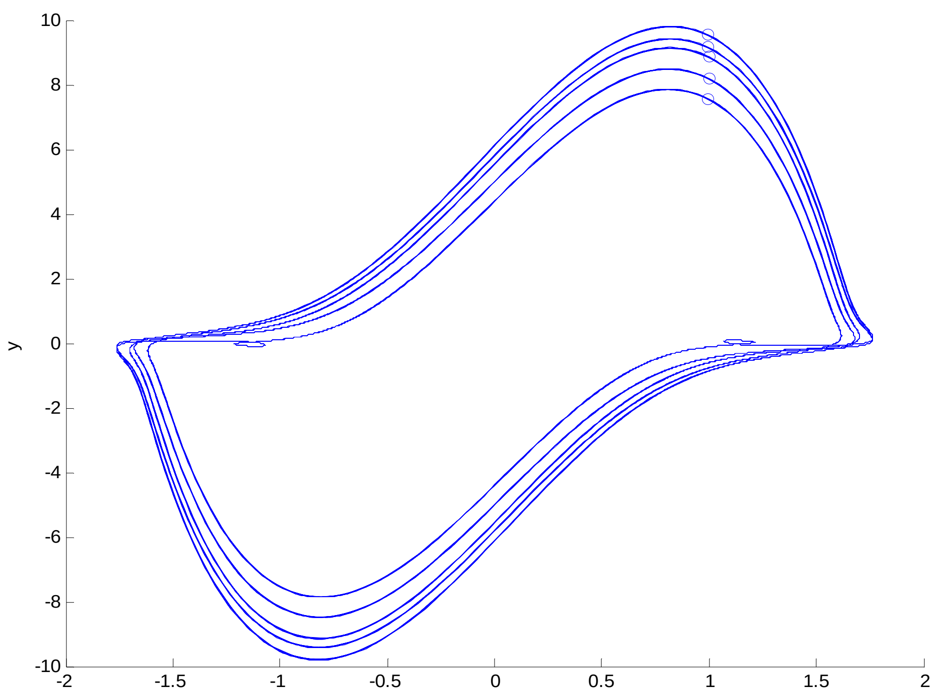

Fig. 3.15 The phase portrait for $\alpha = 0.9$, $\beta = 0.8$, $b = 12$.

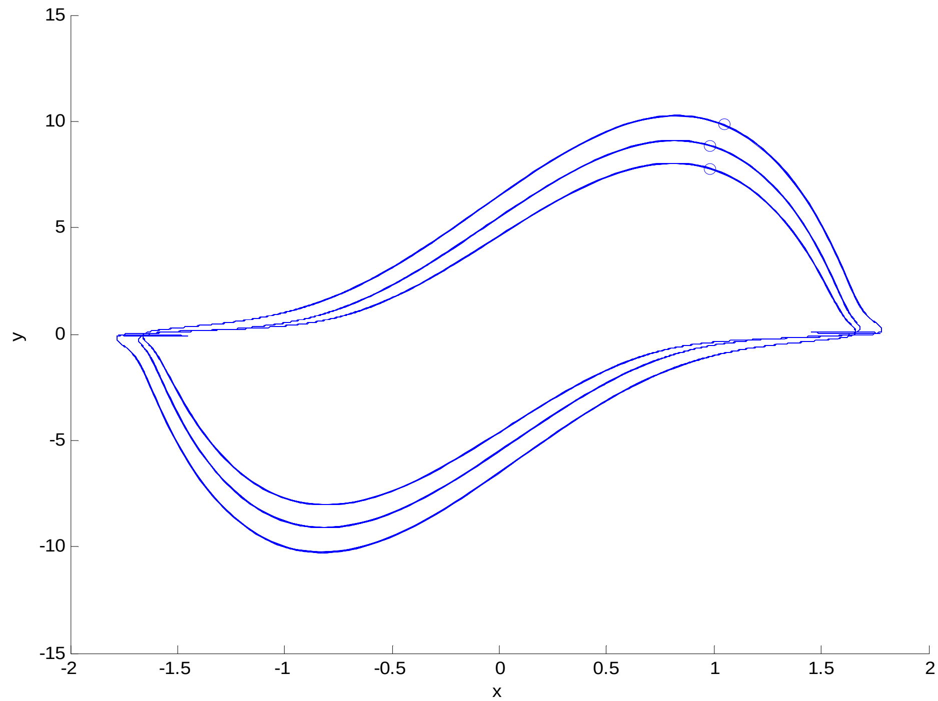

Fig. 3.16 The phase portrait for $\alpha = 0.9$, $\beta = 0.8$, $b = 25$.

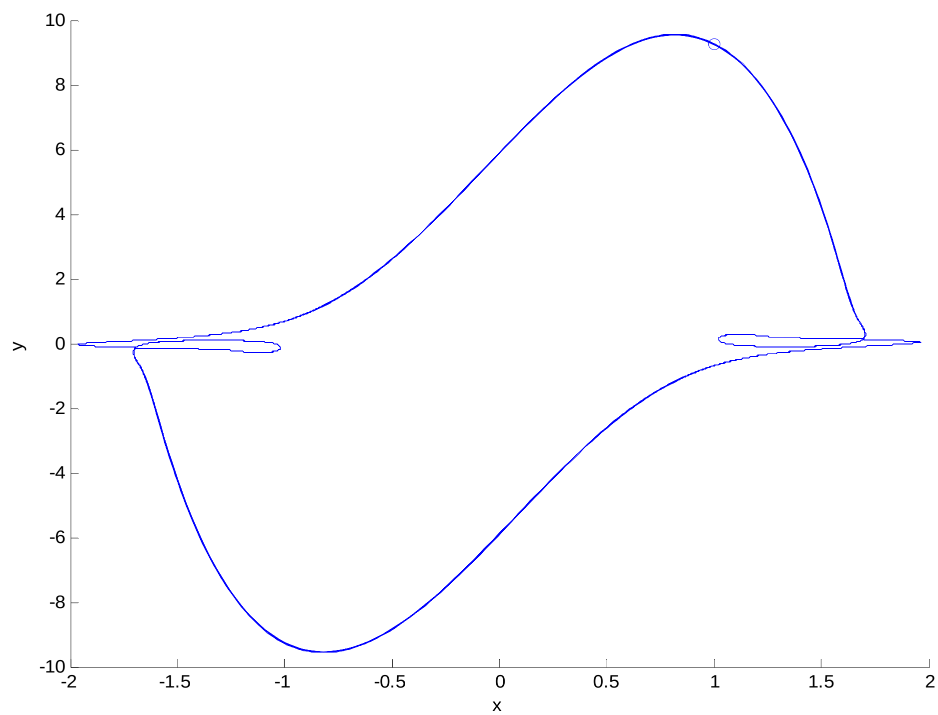

Fig. 3.17 The phase portrait for $\alpha = 0.9$, $\beta = 0.8$, $b = 30$.

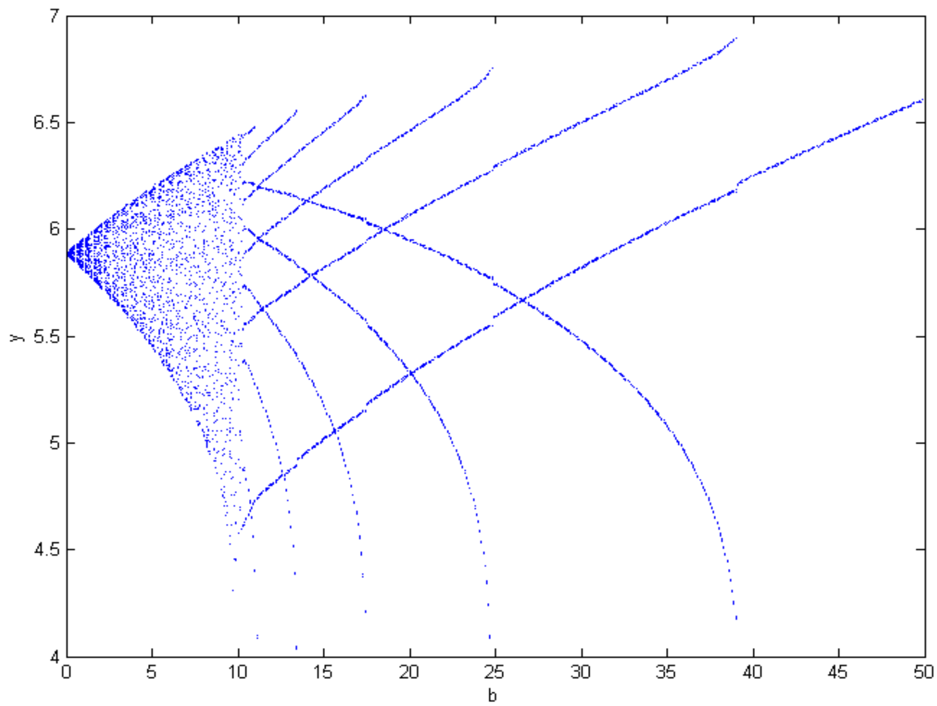

Fig. 3.18 The bifurcation diagram for $\alpha = 0.8$, $\beta = 0.9$.

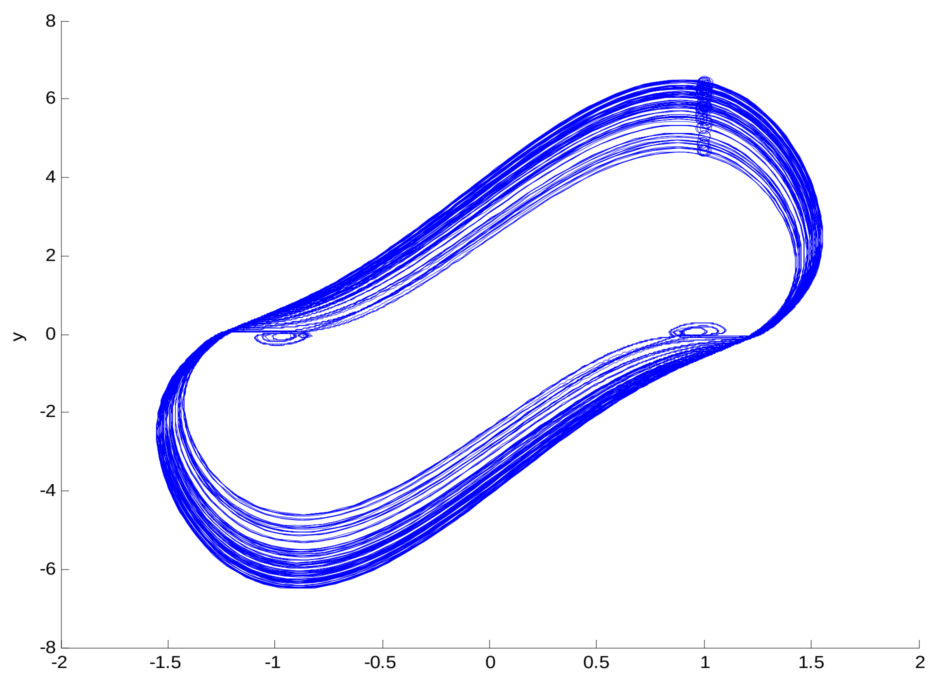

Fig. 3.19 The phase portrait for $\alpha = 0.8$, $\beta = 0.9$, $b = 10.1$.

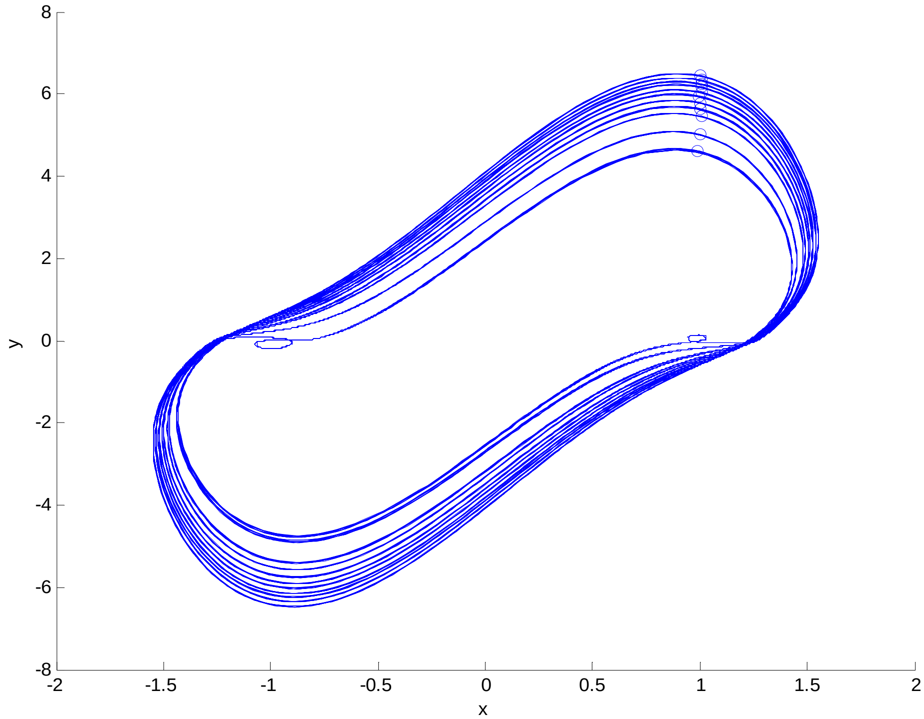

Fig. 3.20 The phase portrait for $\alpha = 0.8$, $\beta = 0.9$, $b = 10.2$.

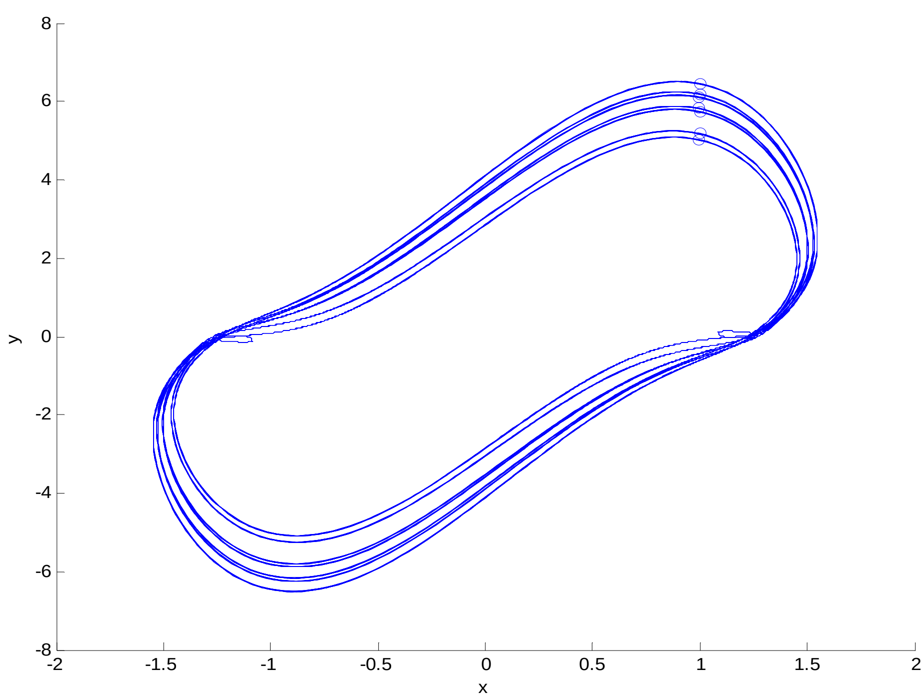

Fig. 3.21 The phase portrait for $\alpha = 0.8$, $\beta = 0.9$, $b = 15$.

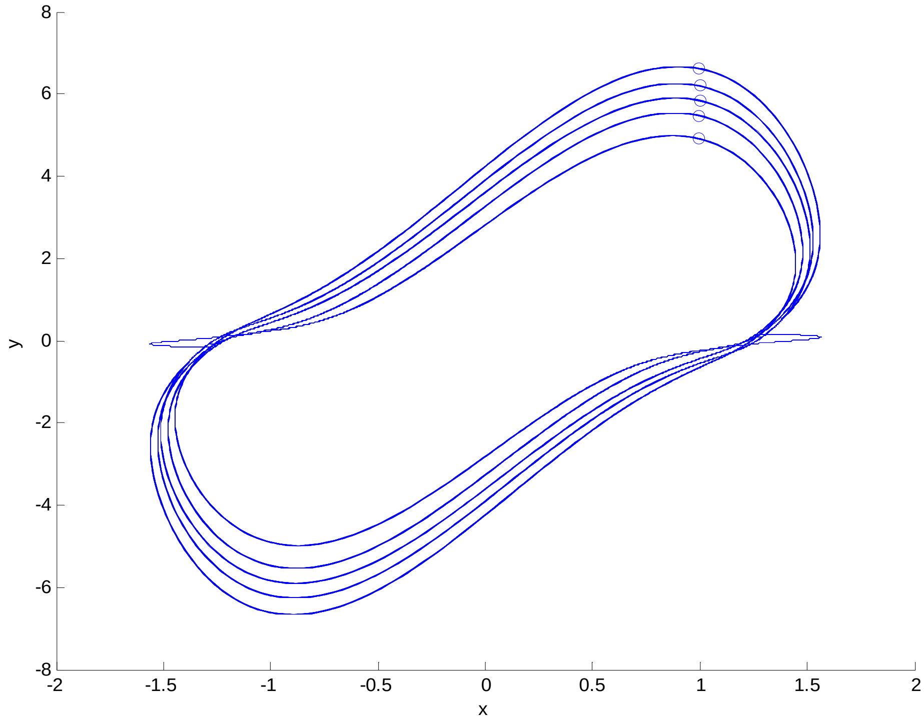

Fig. 3.22 The phase portrait for $\alpha = 0.8$, $\beta = 0.9$, $b = 23$.

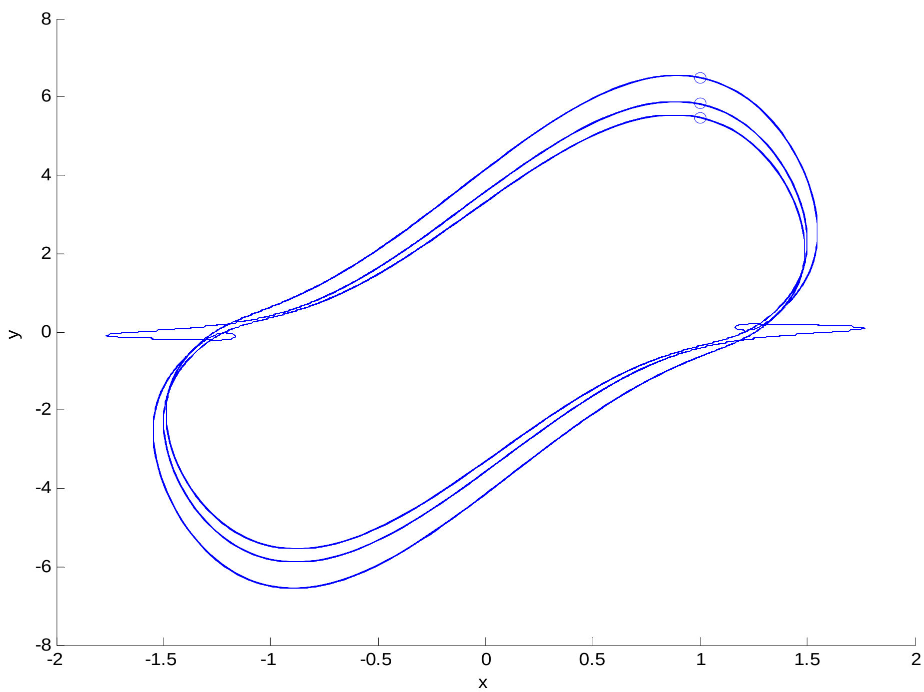

Fig. 3.23 The phase portrait for $\alpha = 0.8$, $\beta = 0.9$, $b = 30$.

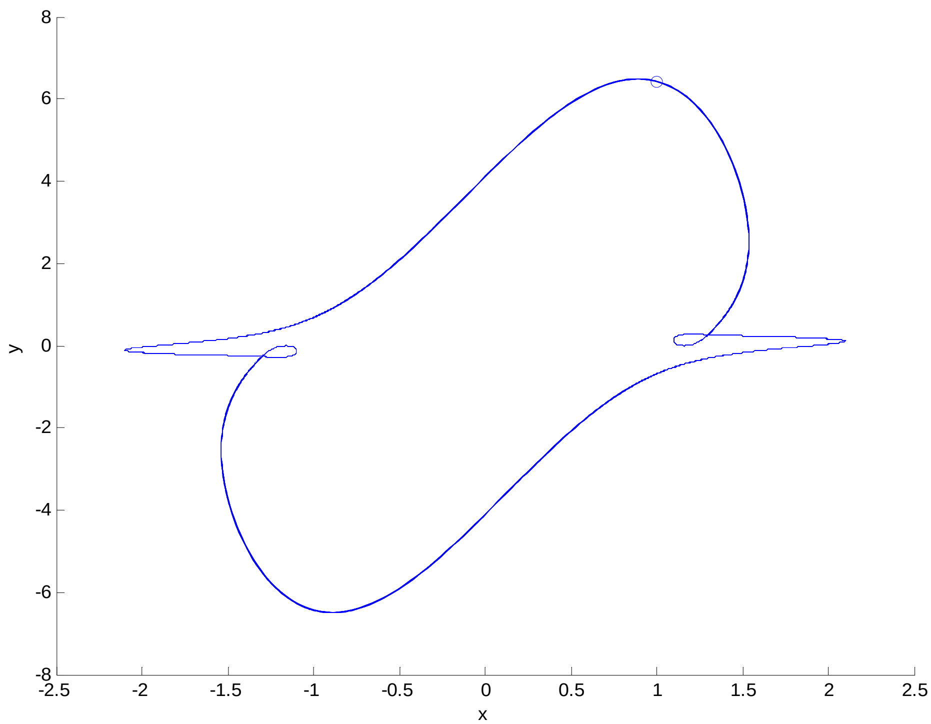

Fig. 3.24 The phase portrait for $\alpha = 0.8$, $\beta = 0.9$, $b = 45$.

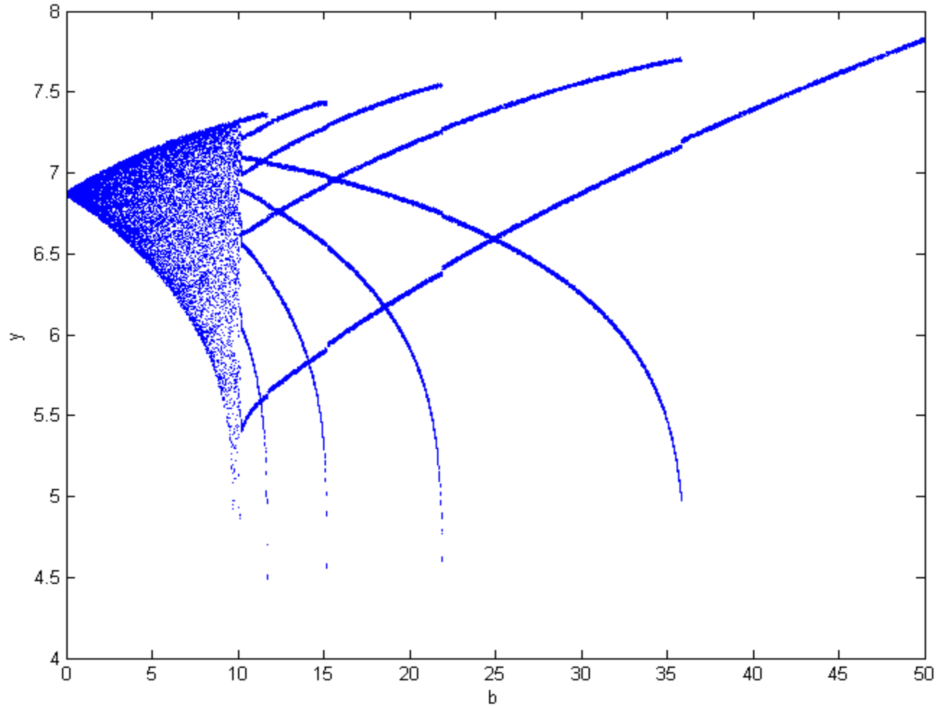

Fig. 3.25 The bifurcation diagram for $\alpha = 0.8$, $\beta = 0.8$.

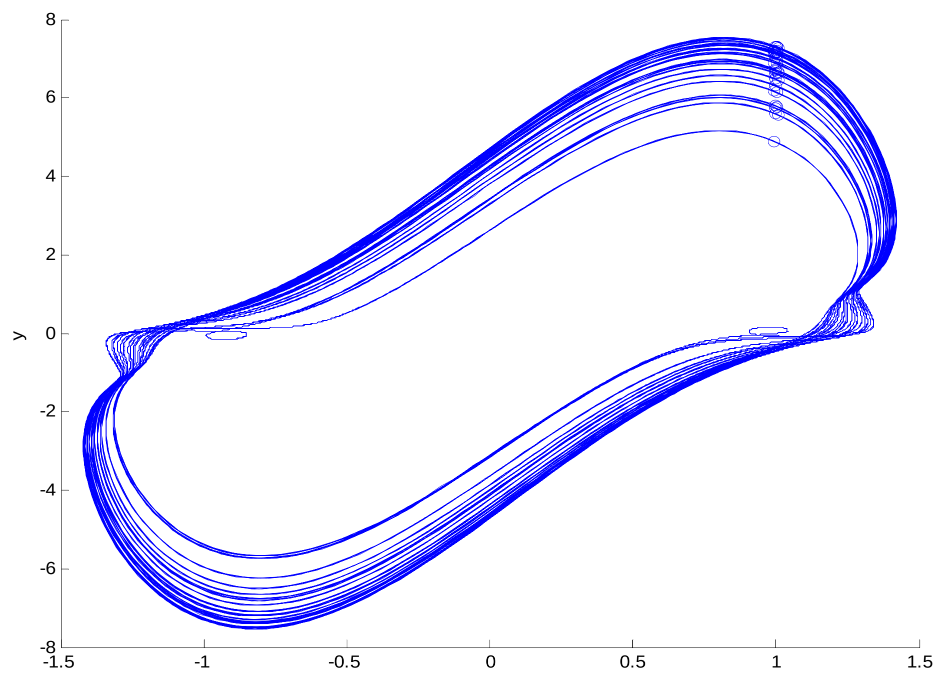

Fig. 3.26 The phase portrait for $\alpha = 0.8$, $\beta = 0.8$, $b = 10.1$.

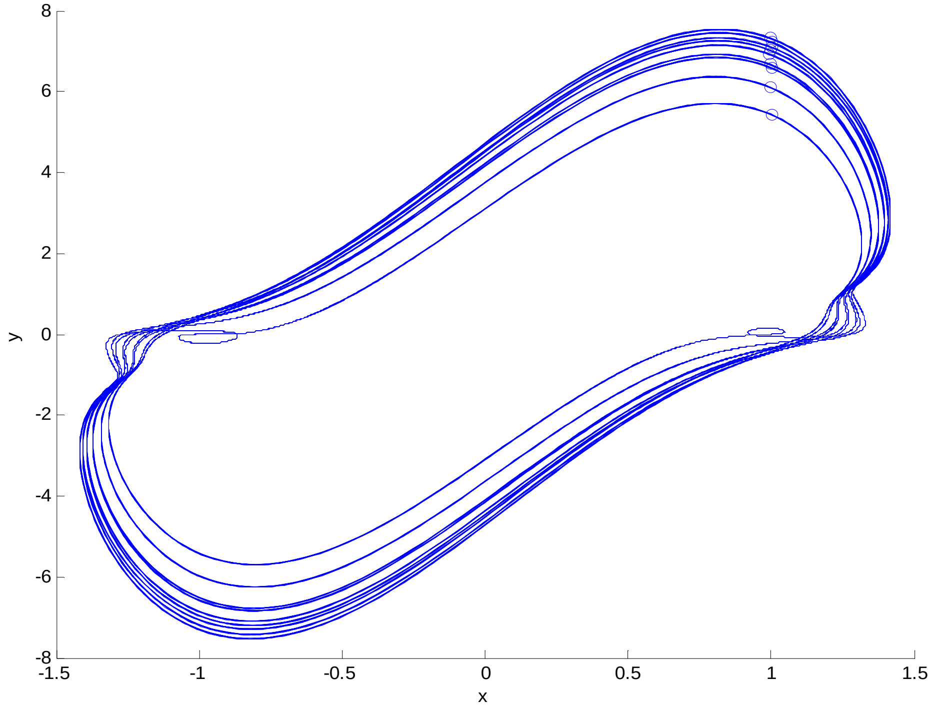

Fig. 3.27 The phase portrait for $\alpha = 0.8$, $\beta = 0.8$, $b = 10.2$.

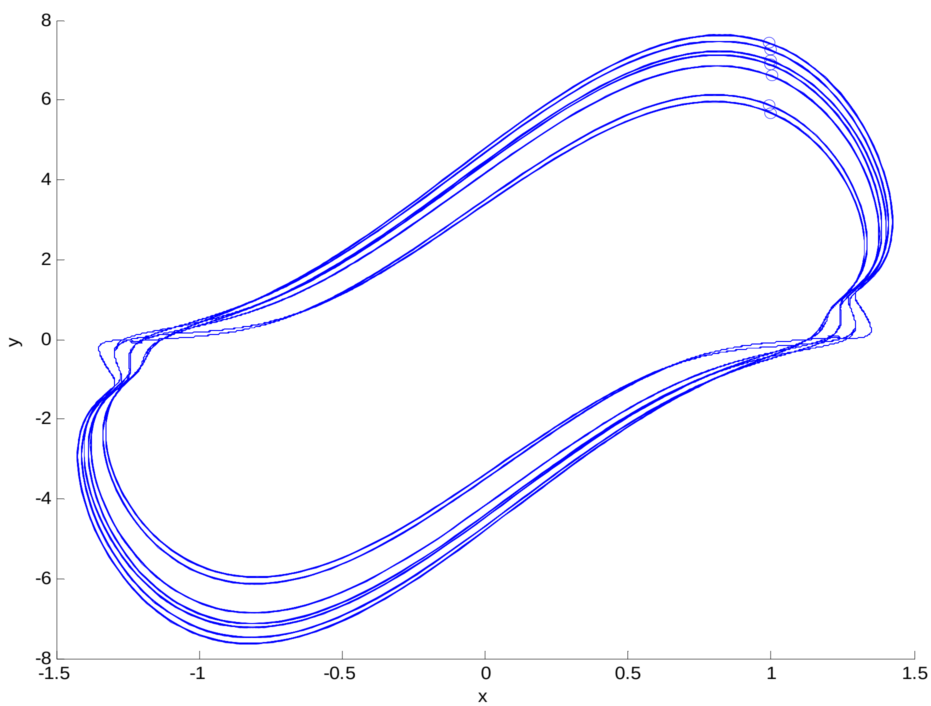

Fig. 3.28 The phase portrait for $\alpha = 0.8$, $\beta = 0.8$, $b = 14.5$.

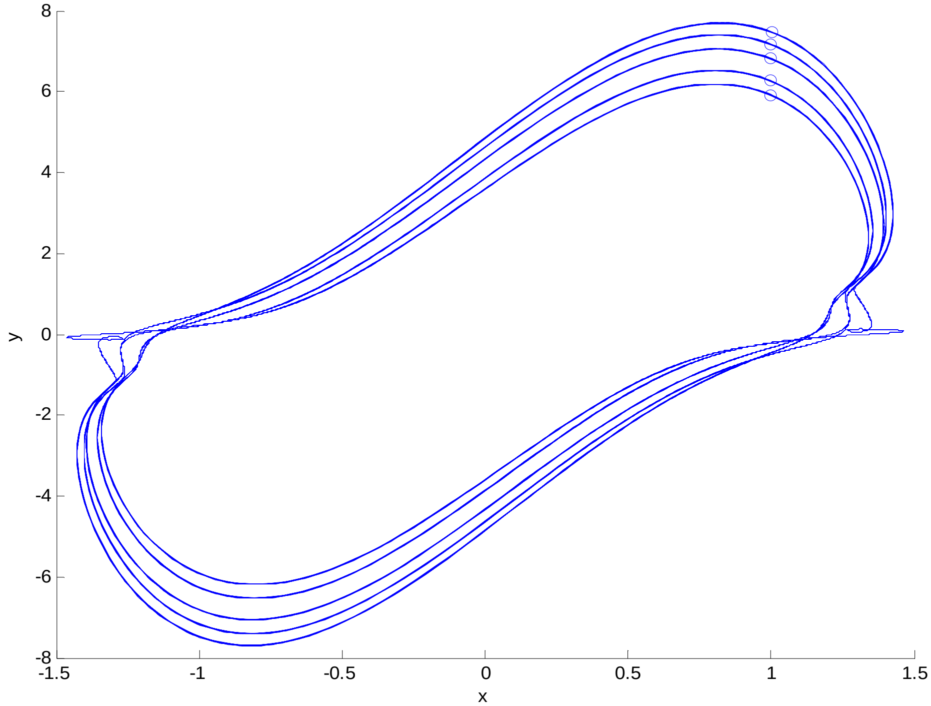

Fig. 3.29 The phase portrait for $\alpha = 0.8$, $\beta = 0.8$, b = 20.

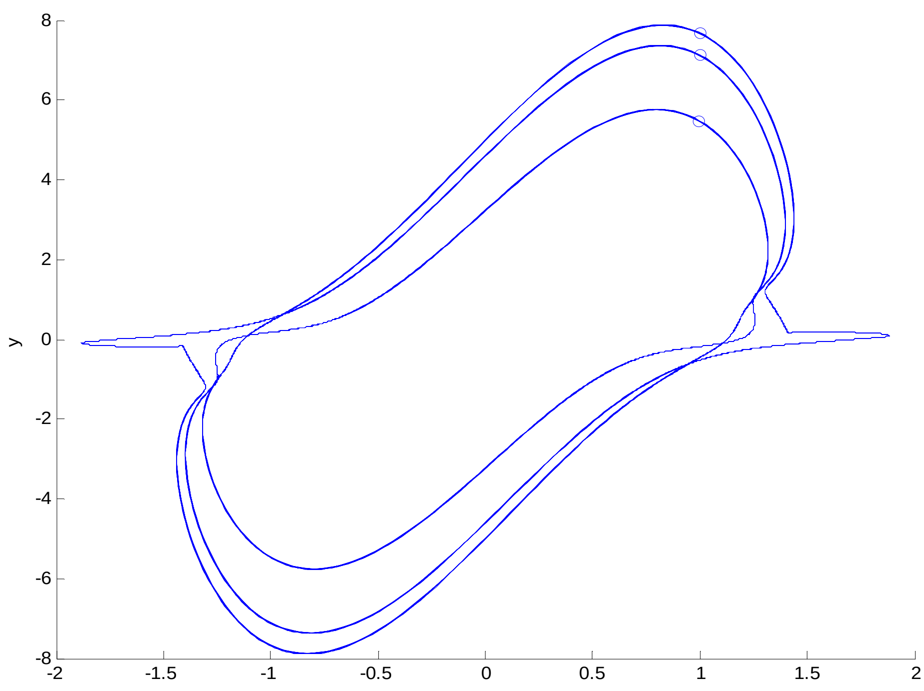

Fig. 3.30 The phase portrait for $\alpha = 0.8$, $\beta = 0.8$, b = 35.

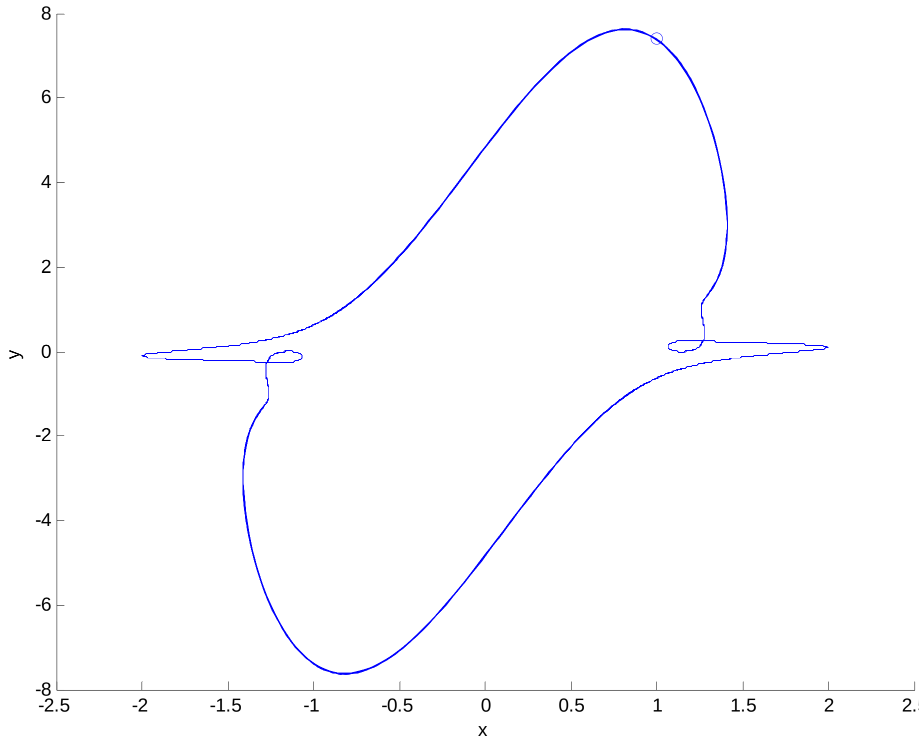

Fig. 3.31 The phase portrait for $\alpha = 0.8$, $\beta = 0.8$, $b = 40$

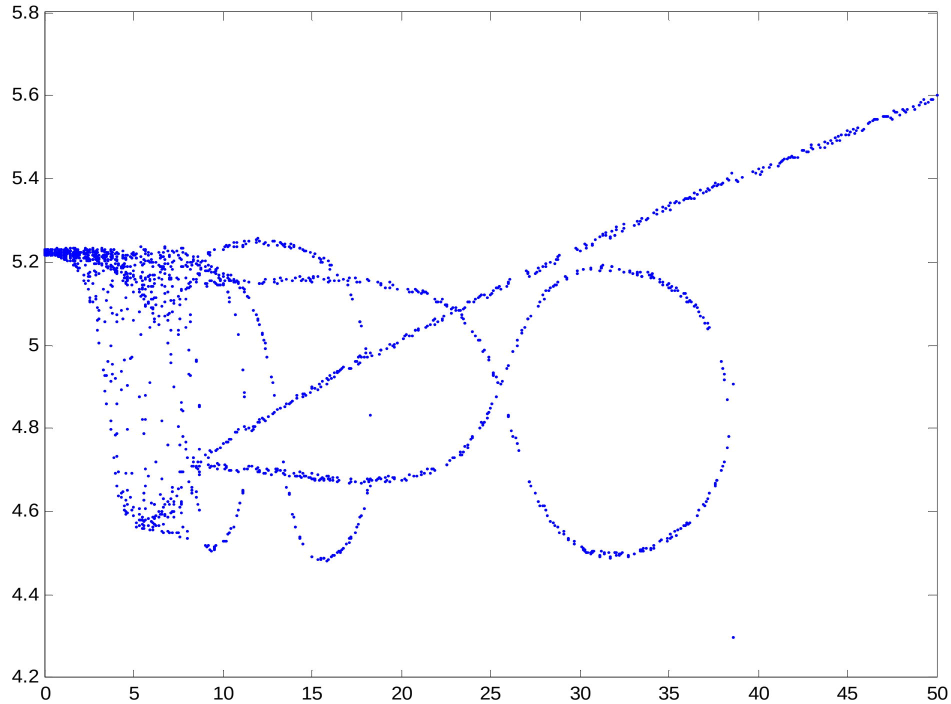

Fig. 3.32 The bifurcation diagram for $\alpha = 0.7$, $\beta = 0.7$.

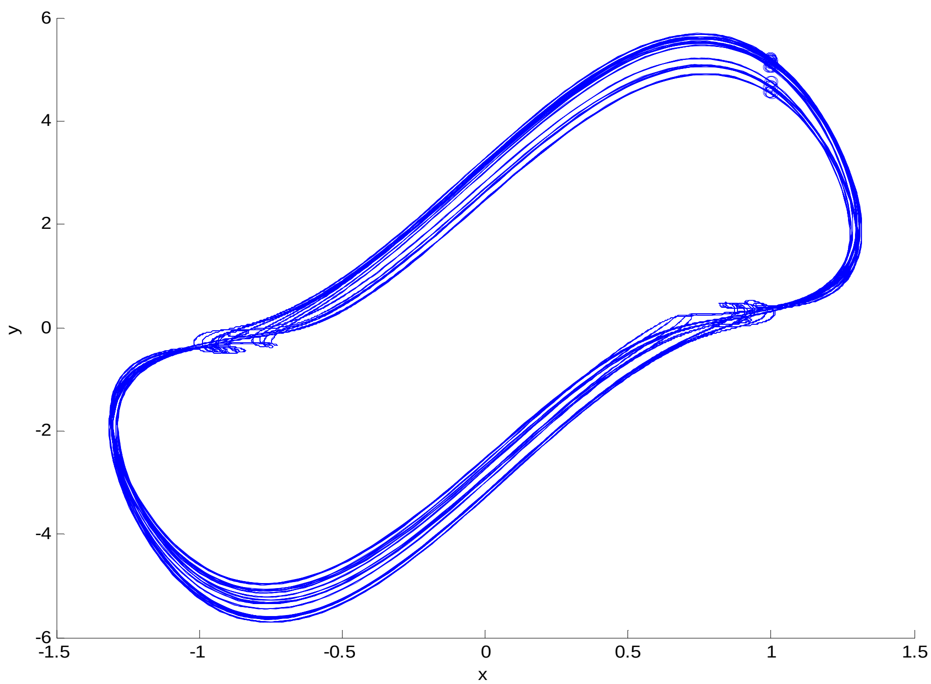

Fig. 3.33 The phase portrait for $\alpha = 0.7$, $\beta = 0.7$, $b = 7.9$.

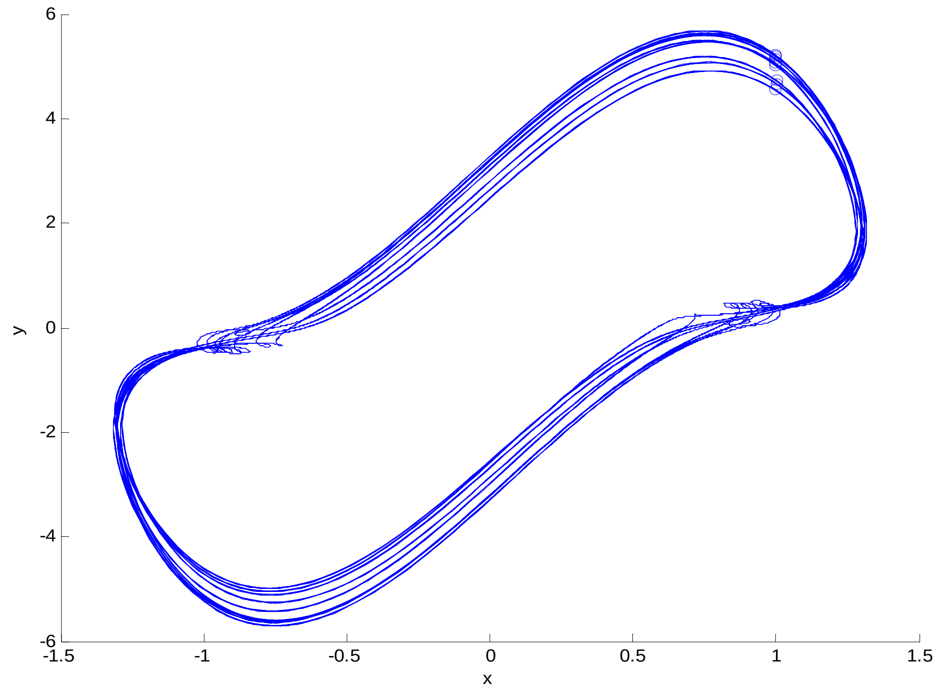

Fig. 3.34 The phase portrait for $\alpha = 0.7$, $\beta = 0.7$, b = 8.0.

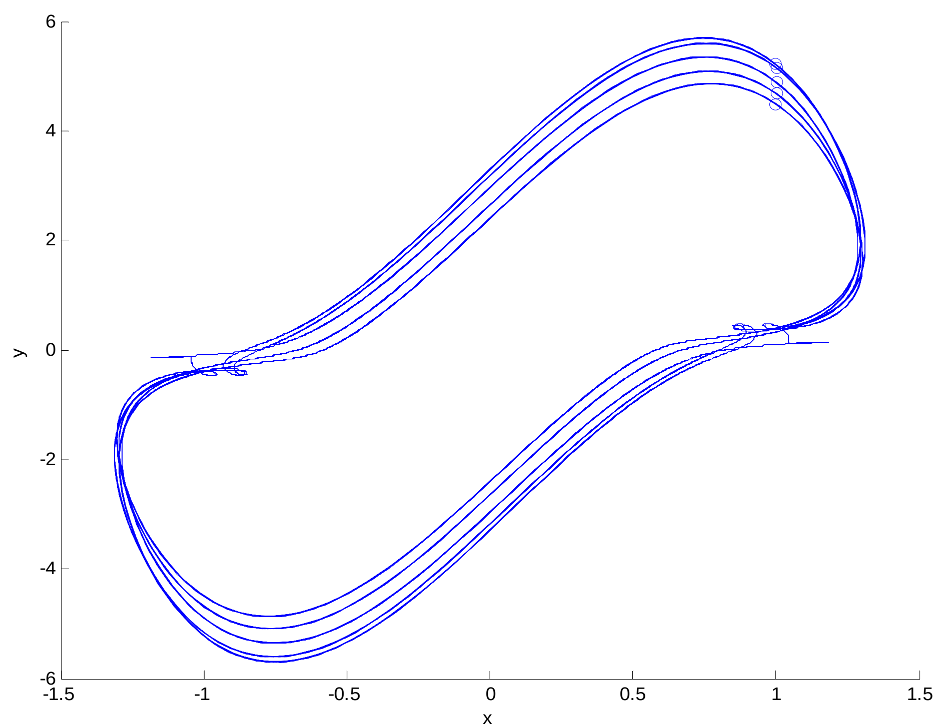

Fig. 3.35 The phase portrait for $\alpha = 0.7$, $\beta = 0.7$, b = 15.

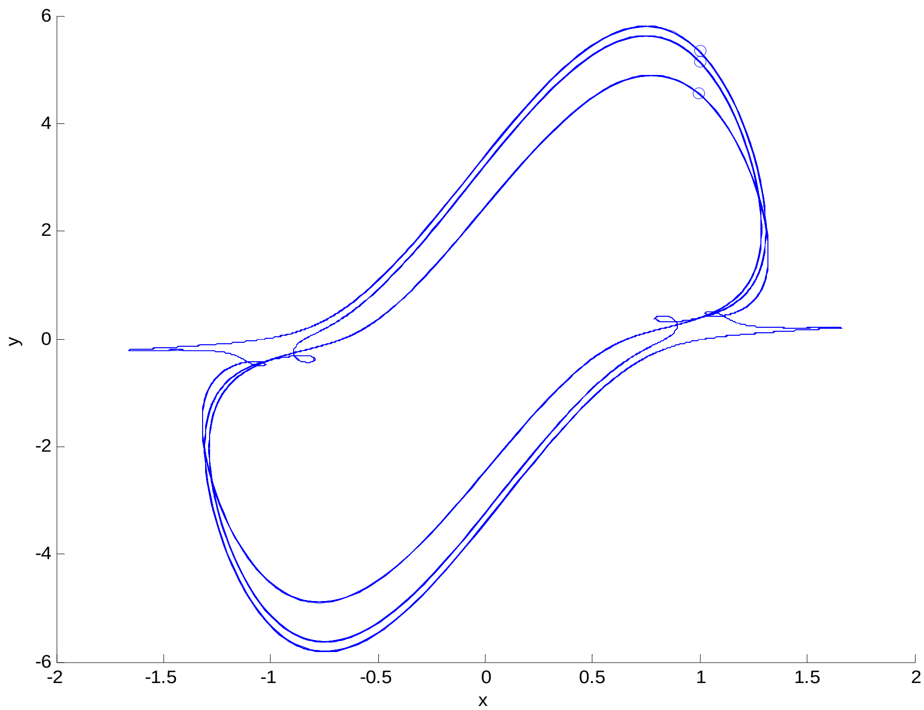

Fig. 3.36 The phase portrait for $\alpha = 0.7$, $\beta = 0.7$, b = 35.

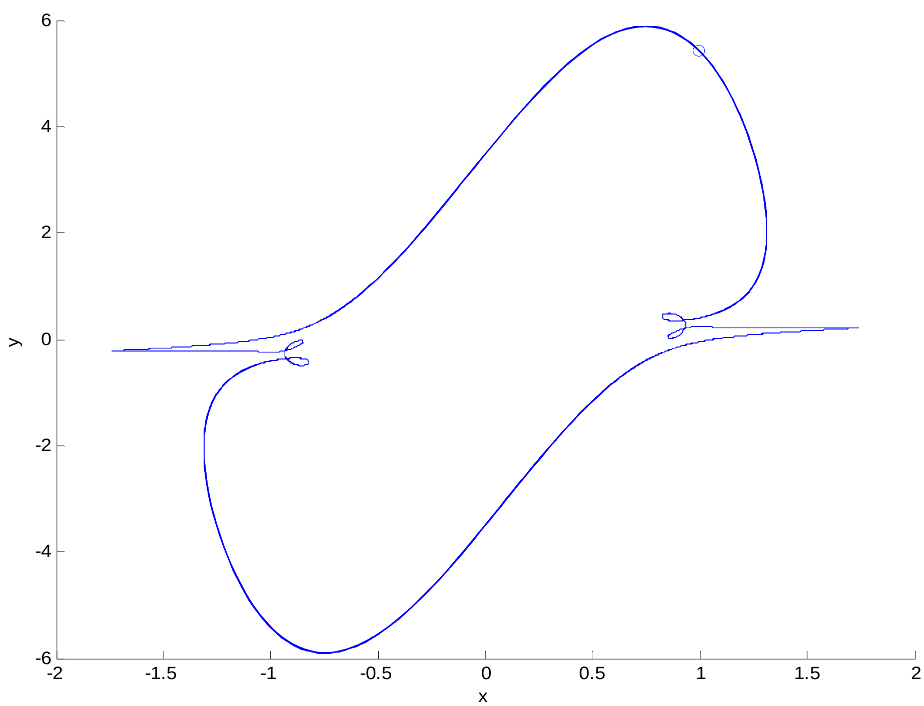

Fig. 3.37 The phase portrait for $\alpha = 0.7$, $\beta = 0.7$, b = 40.

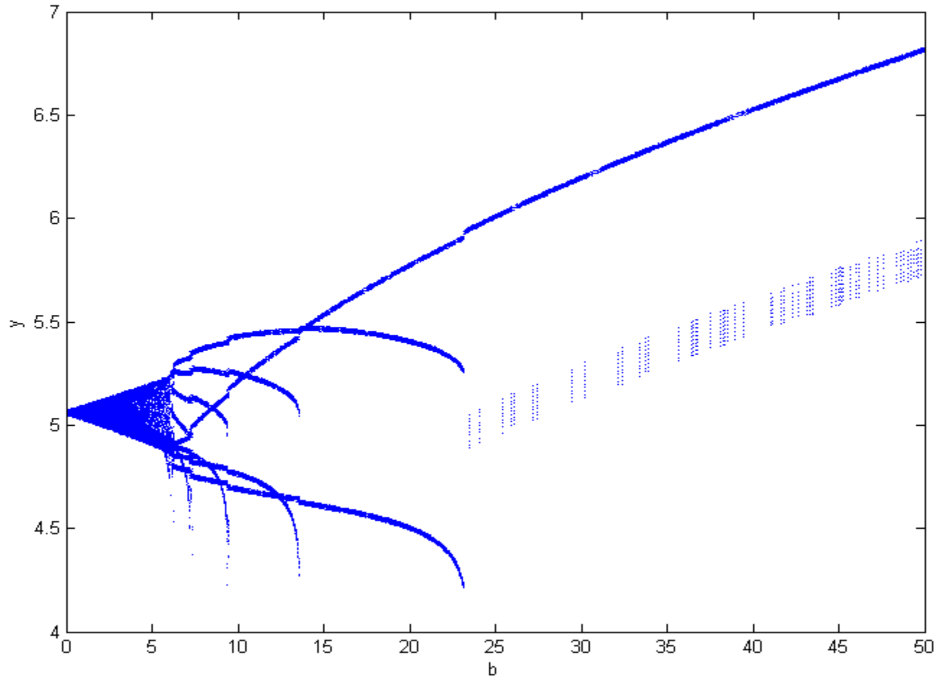

Fig. 3.38 The bifurcation diagram for $\alpha = 0.6$, $\beta = 0.6$.

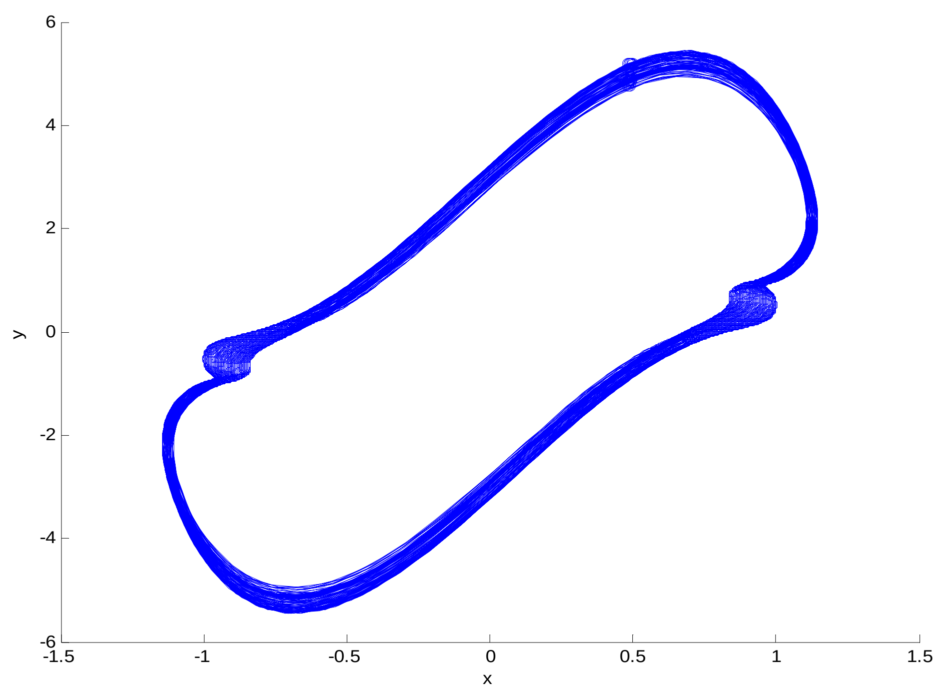

Fig. 3.39 The phase portrait for $\alpha = 0.6$, $\beta = 0.6$, $b = 6.0$.

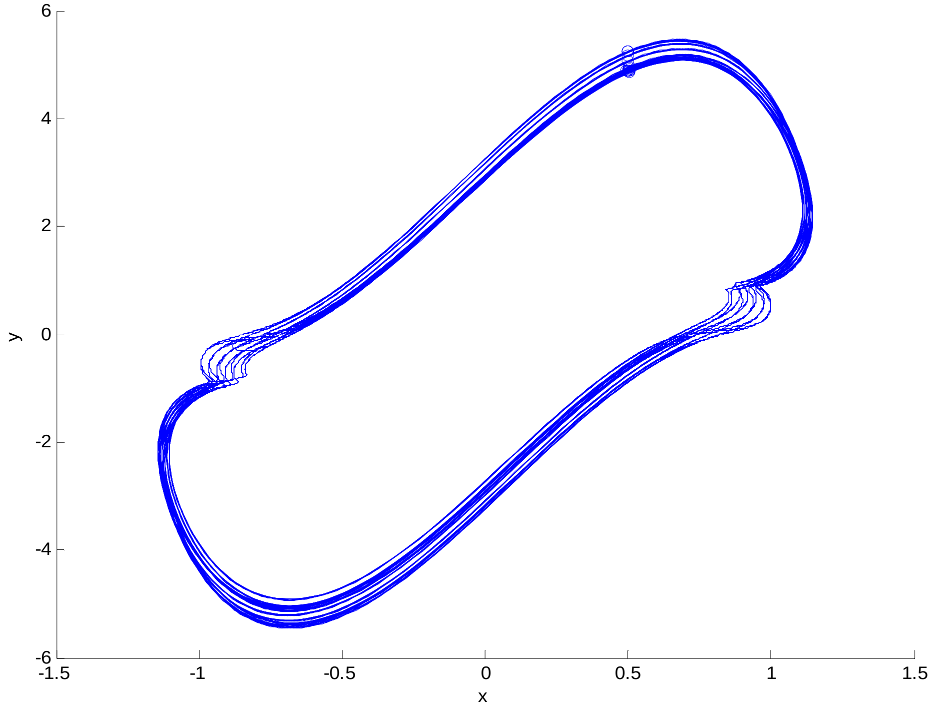

Fig. 3.40 The phase portrait for $\alpha = 0.6$, $\beta = 0.6$, $b = 6.1$.

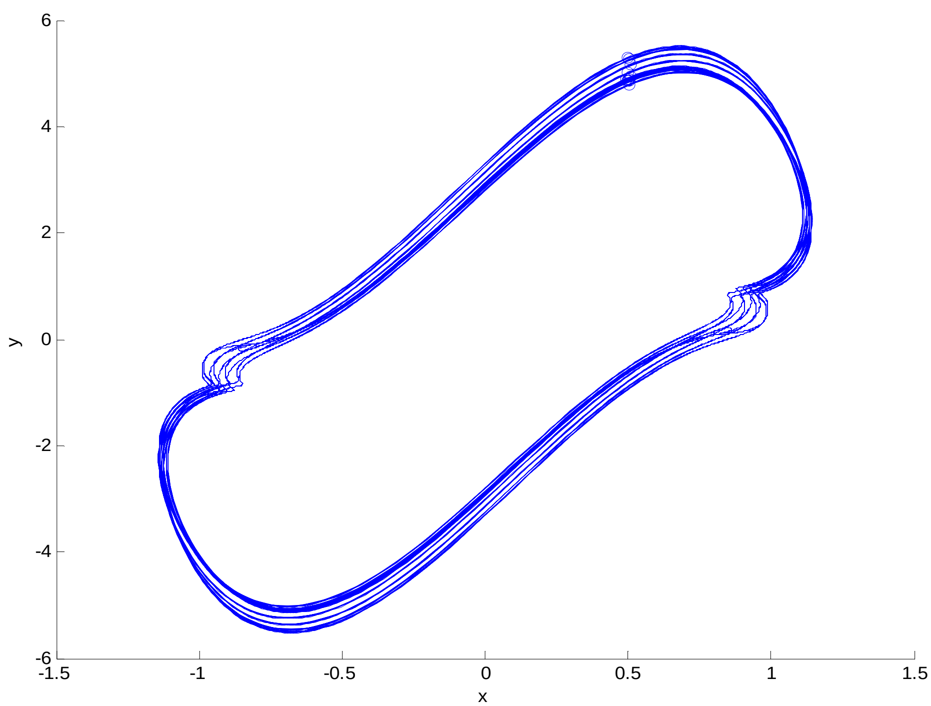

Fig. 3.41 The phase portrait for $\alpha = 0.6$, $\beta = 0.6$, $b = 6.5$.

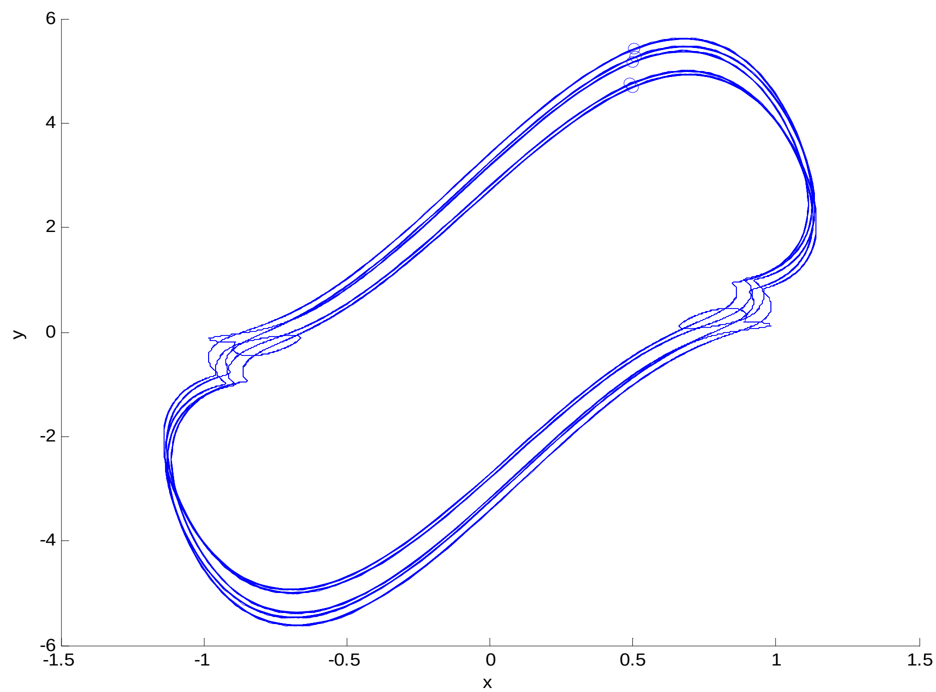

Fig. 3.42 The phase portrait for $\alpha = 0.6$, $\beta = 0.6$, $b = 9.5$.

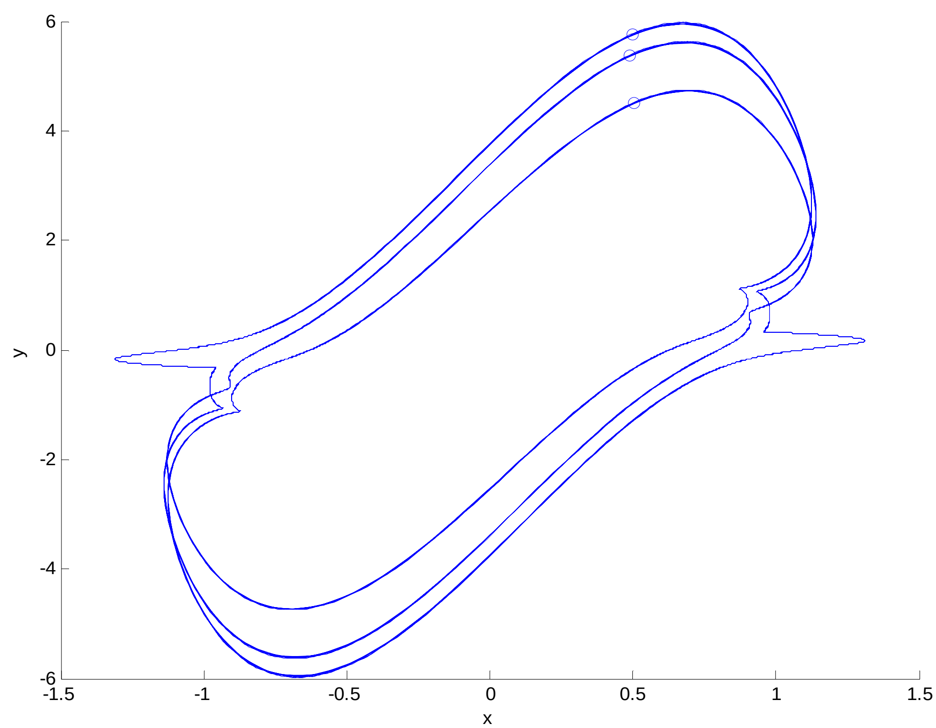

Fig. 3.43 The phase portrait for $\alpha = 0.6$, $\beta = 0.6$, $b = 20$.

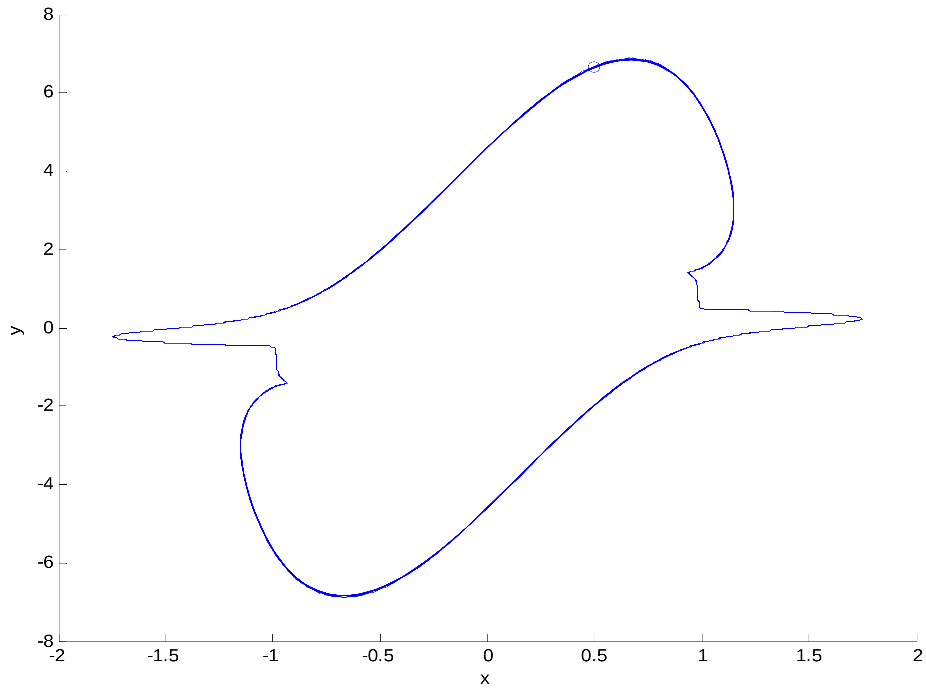

Fig. 3.44 The phase portrait for $\alpha = 0.6$, $\beta = 0.6$, $b = 45$.

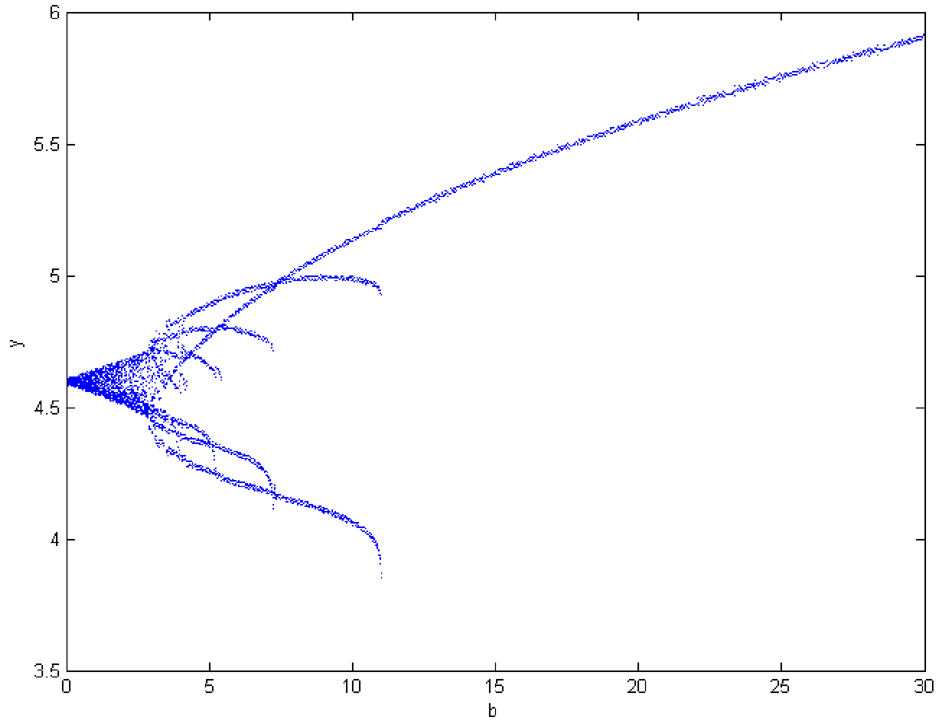

Fig. 3.45 The bifurcation diagram for $\alpha = 0.5$, $\beta = 0.5$.

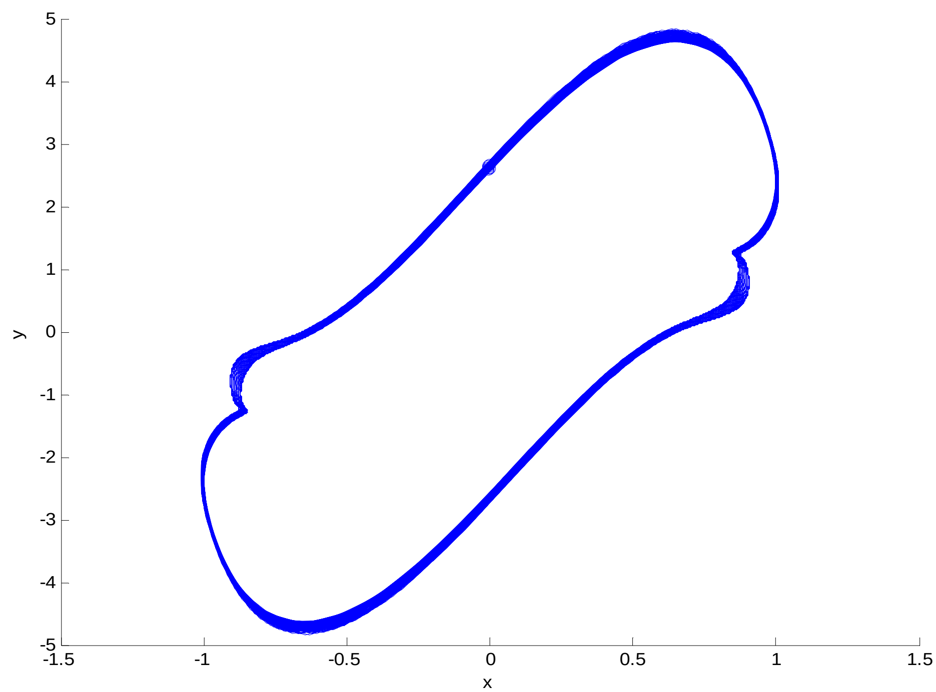

Fig. 3.46 The phase portrait for $\alpha = 0.5$, $\beta = 0.5$, $b = 2$.

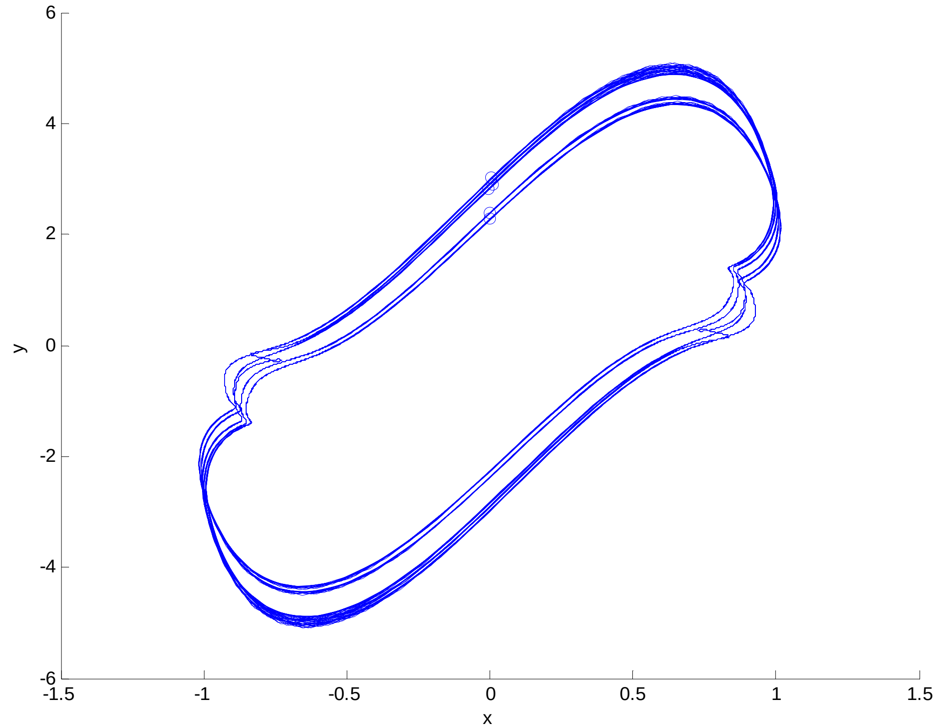

Fig. 3.47 The phase portrait for $\alpha = 0.5$, $\beta = 0.5$, $b = 6$.

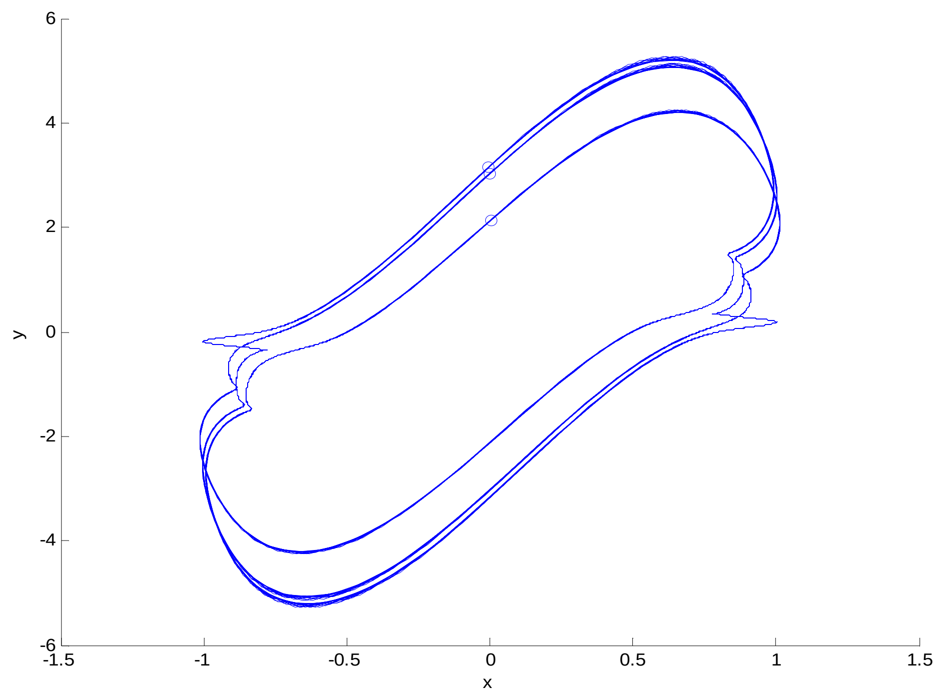

Fig. 3.48 The phase portrait for $\alpha = 0.5$, $\beta = 0.5$, $b = 10$.

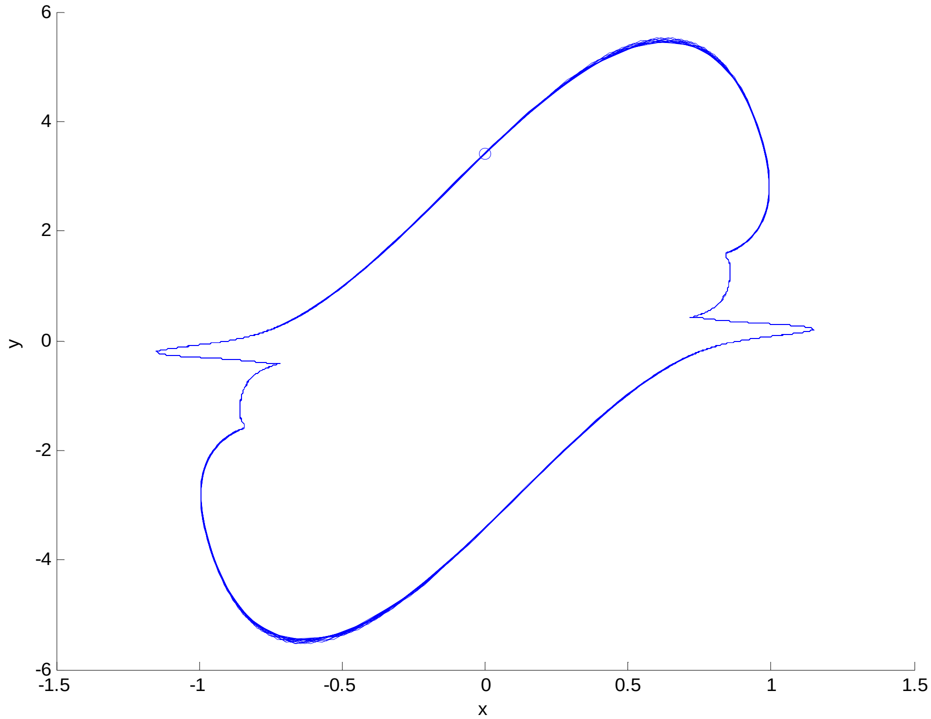

Fig. 3.49 The phase portrait for $\alpha = 0.5$, $\beta = 0.5$, $b = 15$.

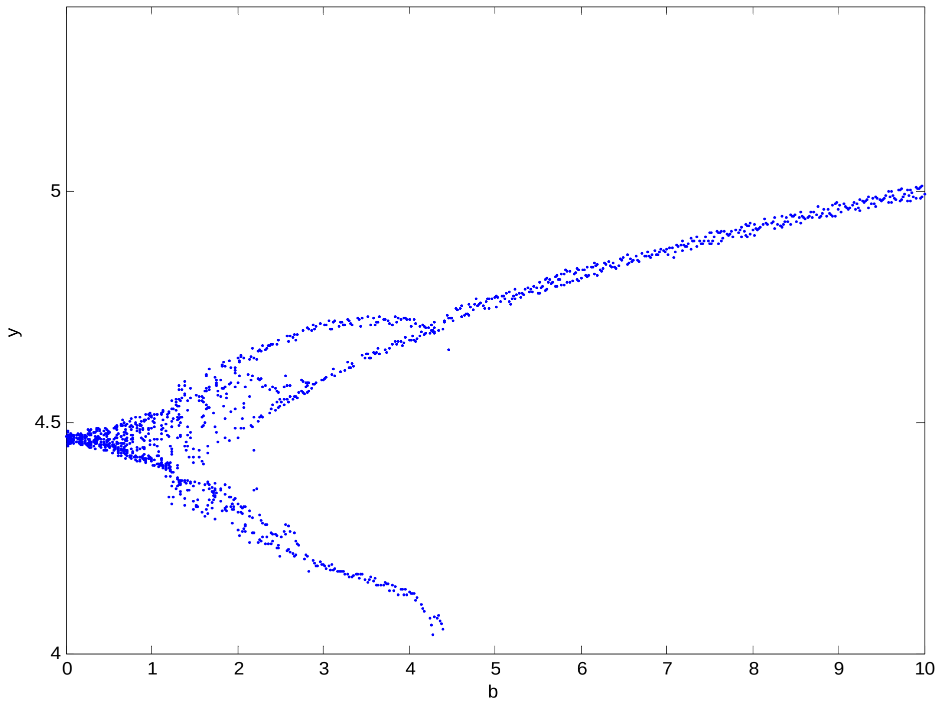

Fig. 3.50 The bifurcation diagram for $\alpha = 0.4$, $\beta = 0.4$.

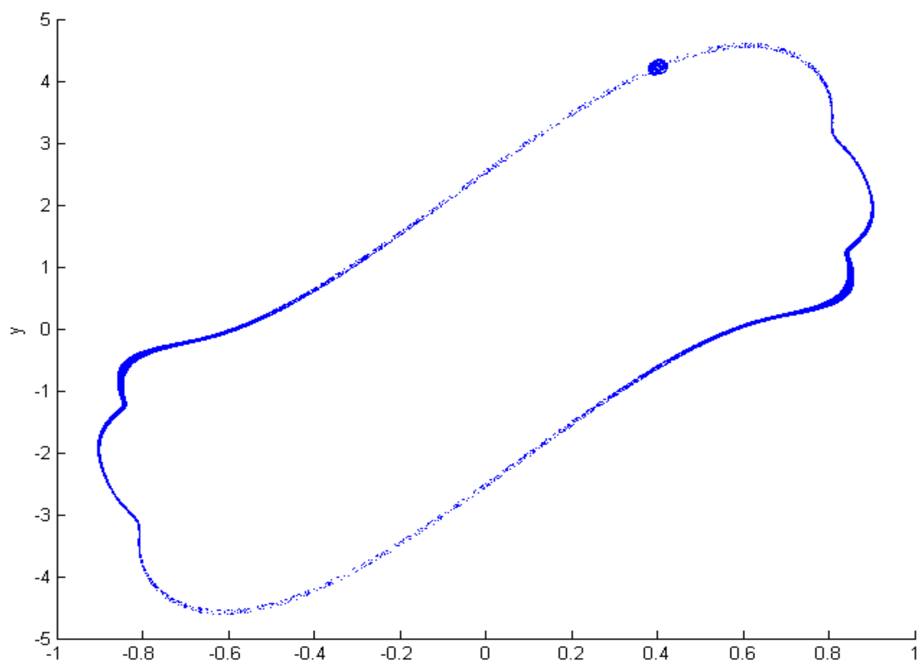

Fig. 3.51 The phase portrait for $\alpha = 0.4$, $\beta = 0.4$, $b = 0.7$.

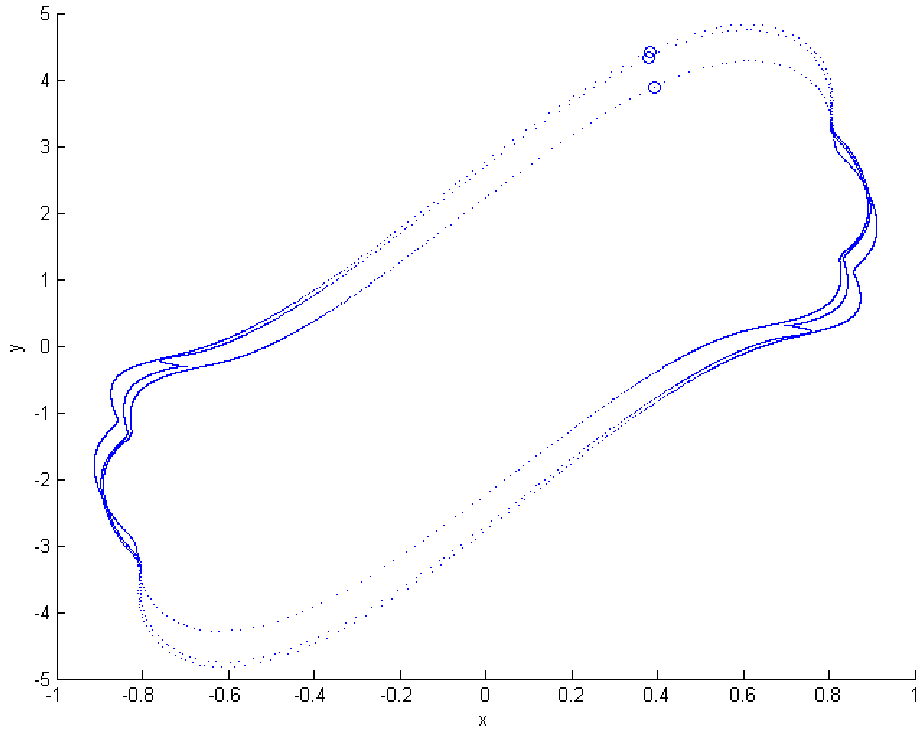

Fig. 3.52 The phase portrait for $\alpha = 0.4$, $\beta = 0.4$, $b = 3.5$.

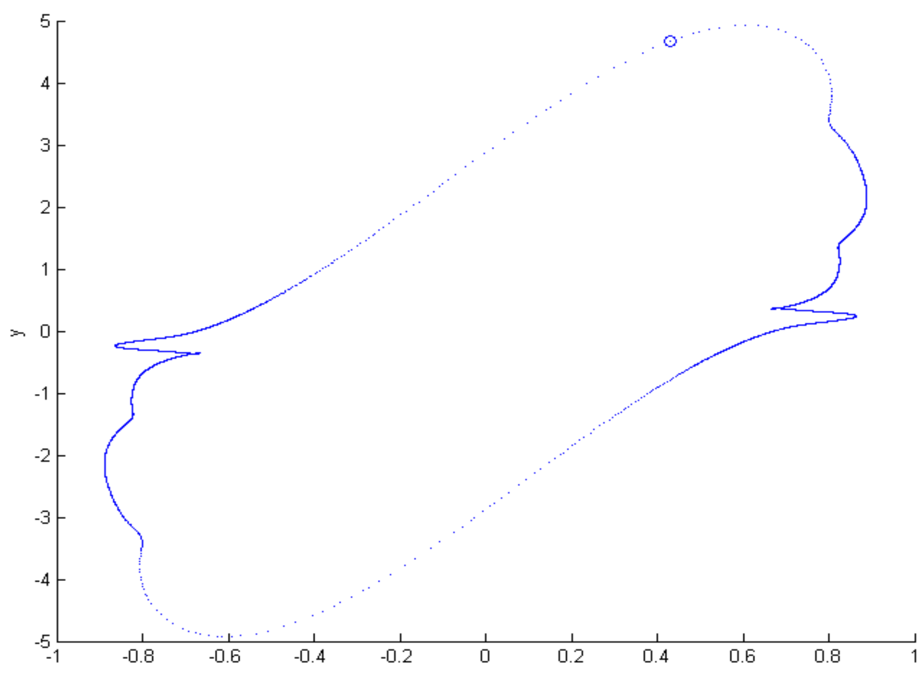

Fig. 3.53 The phase portrait for $\alpha = 0.4$, $\beta = 0.4$, $b = 6.0$

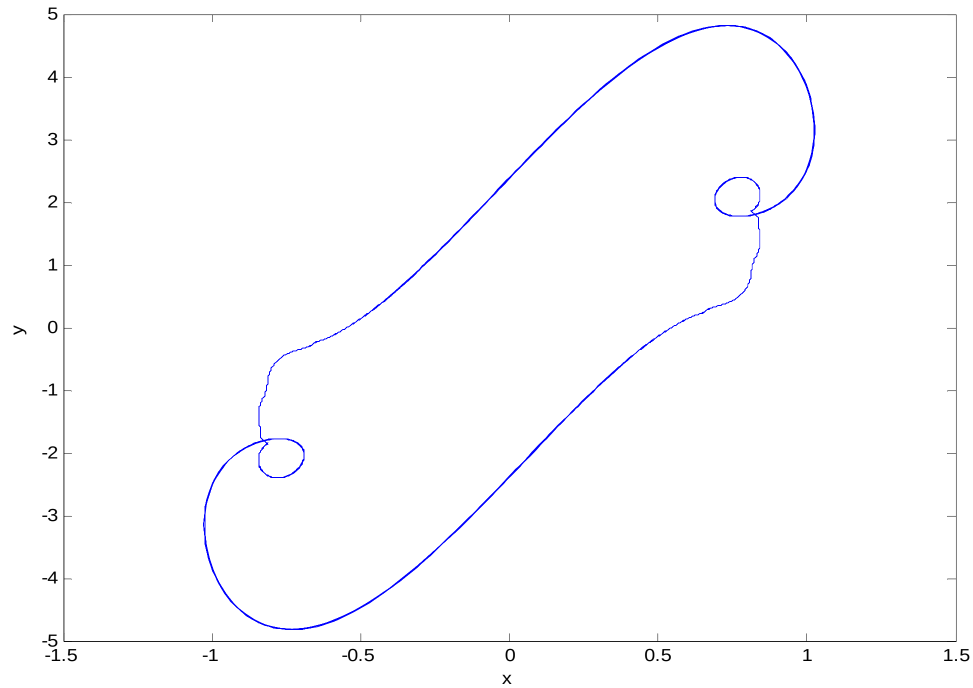

Fig. 3.54 The phase portrait for $\alpha = 0.3$, $\beta = 0.3$, $b = 0.7$.

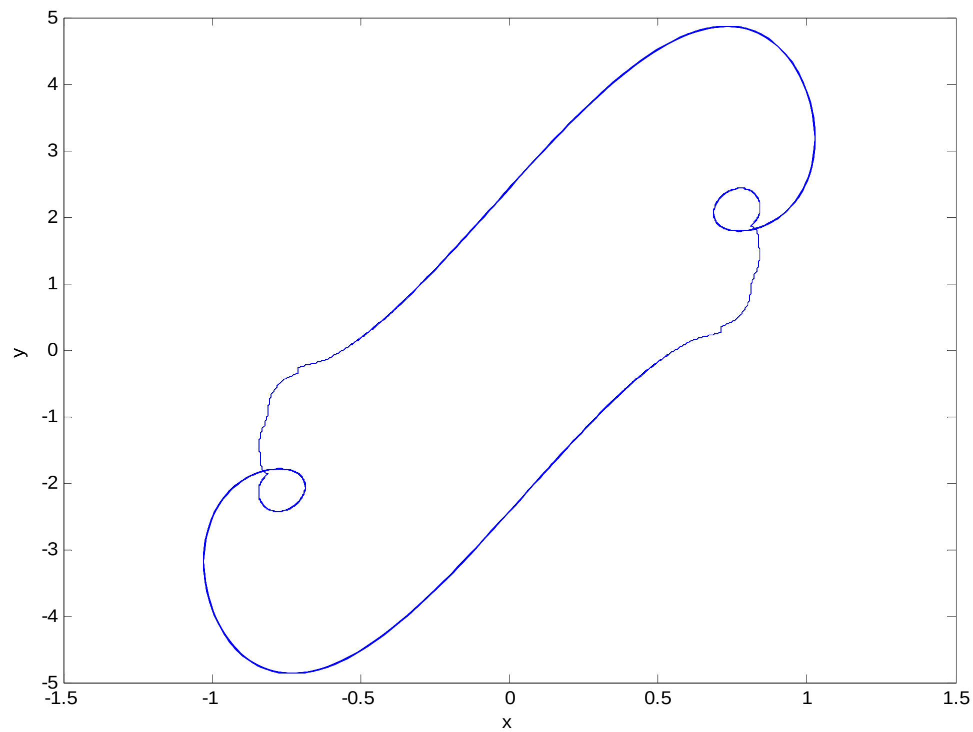

Fig. 3.55 The phase portrait for $\alpha = 0.3$, $\beta = 0.3$, $b = 1.3$.

Chapter 4

Parameter Excited Chaos Synchronizations of Integral and Fractional Order Modified Heartbeat Systems

In this chapter, the synchronizations of two uncoupled integral and fractional order chaotic modified heartbeat systems, i.e. modified van der Pol systems, are achieved by replacing the corresponding parameters of two systems by the same function of the chaotic state variables of a third chaotic system. It is named parameter excited synchronization which can be successfully obtained for very low total fractional order 0.2. Numerical simulations are illustrated by phase portraits, Poincaré maps and state error plots.

4.1 The scheme of parameter excited chaos synchronizations

In this section, both parameters b of two identical modified fractional order van der Pol systems with different initial conditions

$$\begin{cases} \dfrac{d^{\alpha} x_1}{dt^{\alpha}} = y_1 \\ \dfrac{d^{\beta} y_1}{dt^{\beta}} = -x_1 + a(1 - x_1{}^2) y_1 + b z_1 \\ \dot{z}_1 = w_1 \\ \dot{w}_1 = -c z_1 - d z_1{}^3 \end{cases} \tag{4.1}$$

$$\begin{cases} \dfrac{d^{\alpha} x_2}{dt^{\alpha}} = y_2 \\ \dfrac{d^{\beta} y_2}{dt^{\beta}} = -x_2 + a(1 - x_2{}^2) y_2 + b z_2 \\ \dot{z}_2 = w_2 \\ \dot{w}_2 = -c z_2 - d z_2{}^3 \end{cases} \tag{4.2}$$

are replaced by the same cosine function of state variables of a third system (2.6). We study the parameter excited chaos synchronization for various α, β. The parameters a, c of systems (4.1) and (4.2) are adjusted to achieve synchronization for different α and β. d = 0.001 is fixed. Errors $e_1 = x_2 - x_1$, $e_2 = y_2 - y_1$ are defined. If $e_1 \to 0$, $e_2 \to 0$

when $t \to \infty$, synchronization is obtained. A time step of 0.001 is used. Three cases are studied.

4.2 Parameter Excited Chaos Synchronizations by *kcosx*、*kcosy*、*kcosxcosy*

Then, the corresponding parameters *b* of two uncoupled identical integral and fractional order chaotic modified van der Pol systems will be replaced by *kcosx, kcosy, kcosxcosy*, where *x, y* are the states of a third identical system (2.6).

4.2.1 Parameter Excited Chaos Synchronizations by *kcosx*

Let the parameter *b* of Eqs. (4.1) and (4.2) be replaced by *kcosx* where *x* is the state variable of system (2.6). Parameter *k* is chosen as *k* = 0.5.

Case 1 Let $\alpha = \beta = 1$. Fig. 4.1 shows that the chaos exists when *a* = 2, *c* = 10. Fig. 4.2 shows the error dynamics for synchronization.

Case 2 Let $\alpha = \beta = 0.9$. Fig. 4.3 shows that the chaos exists when *a* = 5, *c* = 5. Fig. 4.4 shows the error dynamics for synchronization.

Case 3 Let $\alpha = \beta = 0.8$. Fig. 4.5 shows that the chaos exists when *a* = 5, *c* = 5. Fig. 4.6 shows the error dynamics for synchronization.

Case 4 Let $\alpha = \beta = 0.7$. Fig. 4.7 shows that the chaos exists when *a* = 2.5, *c* = 35. Fig. 4.8 shows the error dynamics for synchronization.

Case 5 Let $\alpha = \beta = 0.6$. Fig. 4.9 shows that the chaos exists when *a* = 2.5, *c* = 50. Fig. 4.10 shows the error dynamics for synchronization.

Case 6 Let $\alpha = \beta = 0.5$. Fig. 4.11 shows that the chaos exists when *a* = 2, *c* = 35. Fig. 4.12 shows the error dynamics for synchronization.

Case 7 Let $\alpha = \beta = 0.4$. Fig. 4.13 shows that the chaos exists when *a* = 2, *c* = 65. Fig. 4.14 shows the error dynamics for synchronization.

Case 8 Let $\alpha = \beta = 0.3$. Fig. 4.15 shows that the chaos exists when *a* = 10, *c* = 65. Fig. 4.16 shows the error dynamics for synchronization.

Case 9 Let $\alpha = \beta = 0.2$. Fig. 4.17 shows that the chaos exists when *a* = 20, *c* = 55. Fig. 4.18 shows the error dynamics for synchronization.

Case 10 Let $\alpha = \beta = 0.1$. Fig. 4.19 shows that the chaos exists when *a* = 10, c = 0.5. Fig. 4.20 shows the error dynamics for synchronization.

4.2.2 Parameter Excited Chaos Synchronizations by *kcosy*

Let the parameter b of Eqs. (4.1) and (4.2) be replaced by *kcosy* where *y* is the state variable of system (2.6). Parameter *k* is chosen as *k* = 0.5.

Case 1 Let $\alpha = \beta = 1$. Fig. 4.21 shows that the chaos exists when *a* = 2, *c* = 10. Fig. 4.22 shows the error dynamics for synchronization.

Case 2 Let $\alpha = \beta = 0.9$. Fig. 4.23 shows that the chaos exists when *a* = 5, *c* = 5. Fig. 4.24 shows the error dynamics for synchronization.

Case 3 Let $\alpha = \beta = 0.8$. Fig. 4.25 shows that the chaos exists when *a* = 5, *c* = 5. Fig. 4.26 shows the error dynamics for synchronization.

Case 4 Let $\alpha = \beta = 0.7$. Fig. 4.27 shows that the chaos exists when *a* = 2.5, *c* = 35. Fig. 4.28 shows the error dynamics for synchronization.

Case 5 Let $\alpha = \beta = 0.6$. Fig. 4.29 shows that the chaos exists when *a* = 2.5, *c* = 50. Fig. 4.30 shows the error dynamics for synchronization.

Case 6 Let $\alpha = \beta = 0.5$. Fig. 4.31 shows that the chaos exists when *a* = 2, *c* = 35. Fig. 4.32 shows the error dynamics for synchronization.

Case 7 Let $\alpha = \beta = 0.4$. Fig. 4.33 shows that the chaos exists when *a* = 2, *c* = 65. Fig. 4.34 shows the error dynamics for synchronization.

Case 8 Let $\alpha = \beta = 0.3$. Fig. 4.35 shows that the chaos exists when *a* = 5, *c* = 5. Fig. 4.36 shows the error dynamics for synchronization.

Case 9 Let $\alpha = \beta = 0.2$. Fig. 4.37 shows that the chaos exists when *a* = 20, *c* = 55. Fig. 4.38 shows the error dynamics for synchronization.

Case 10 Let $\alpha = \beta = 0.1$. Fig. 4.39 shows that the chaos exists when *a* = 10, *c* = 1. Fig. 4.40 shows the error dynamics for synchronization.

4.2.3 Parameter Excited Chaos Synchronizations by *kcosxcosy*

Let the parameter *b* of Eqs. (4.1) and (4.2) be replaced by *kcosxcosy* where *x*, *y* are the state variables of system (6). Parameter *k* is chosen as *k* = 0.5.

Case 1 Let $\alpha = \beta = 1$. Fig. 4.41 shows that the chaos exists when *a* = 2, *c* = 10. Fig. 4.42 shows the error dynamics for synchronization.

Case 2 Let $\alpha = \beta = 0.9$. Fig. 4.43 shows that the chaos exists when *a* = 5, *c* = 5. Fig. 4.44 shows the error dynamics for synchronization.

Case 3 Let $\alpha = \beta = 0.8$. Fig. 4.45 shows that the chaos exists when a = 10, c = 5. Fig. 4.46 shows the error dynamics for synchronization.

Case 4 Let $\alpha = \beta = 0.7$. Fig. 4.47 shows that the chaos exists when a = 2.5, c = 35. Fig. 4.48 shows the error dynamics for synchronization.

Case 5 Let $\alpha = \beta = 0.6$. Fig. 4.49 shows that the chaos exists when a = 2.5, c = 50. Fig. 4.50 shows the error dynamics for synchronization.

Case 6 Let $\alpha = \beta = 0.5$. Fig. 4.51 shows that the chaos exists when a = 5.5, c = 45. Fig. 4.52 shows the error dynamics for synchronization.

Case 7 Let $\alpha = \beta = 0.4$. Fig. 4.53 shows that the chaos exists when a = 2, c = 65. Fig. 4.54 shows the error dynamics for synchronization.

Case 8 Let $\alpha = \beta = 0.3$. Fig. 4.55 shows that the chaos exists when a = 4, c = 35. Fig. 4.56 shows the error dynamics for synchronization.

Case 9 Let $\alpha = \beta = 0.2$. Fig. 4.57 shows that the chaos exists when a = 2, c = 1. Fig. 4.58 shows the error dynamics for synchronization.

Case 10 Let $\alpha = \beta = 0.1$. Fig. 4.59 shows that the chaos exists when a = 2, c = 10. Fig. 4.60 shows the error dynamics for synchronization.

In this paper, parameter excited chaos synchronizations of uncoupled integral and fractional order modified van der Pol systems are studied by means of phase portraits, Poincaré maps and error dynamics plots. It is found that this approach is very effective even for very low total fractional order 0.2.

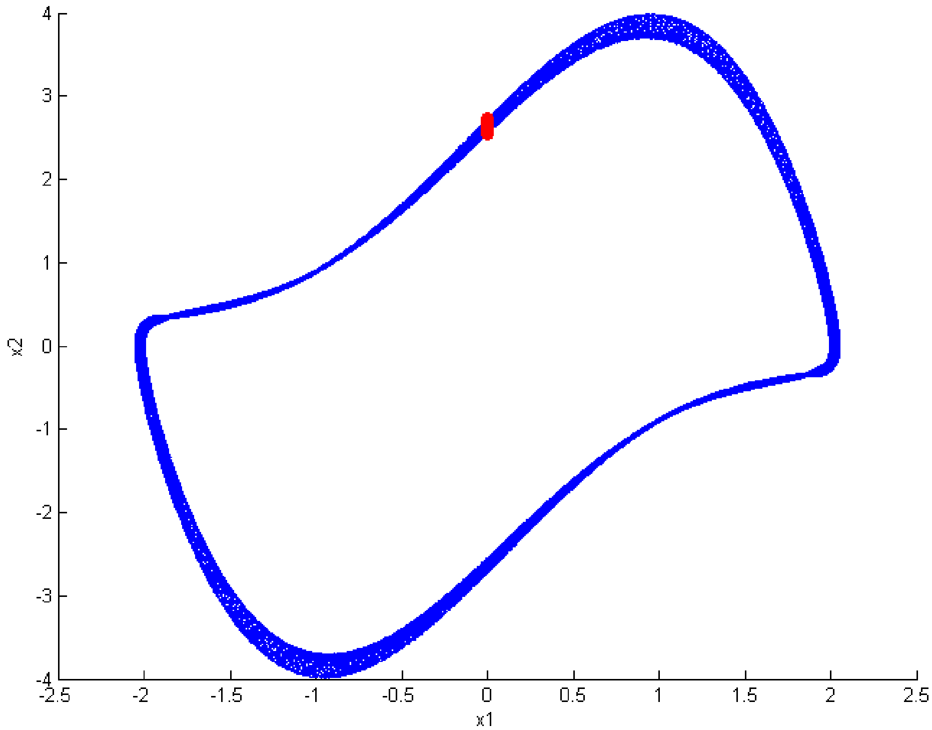

Fig. 4.1 The phase portrait for replacing b by $k\cos x$ with $\alpha = \beta = 1$, $a = 2$, $c = 10$.

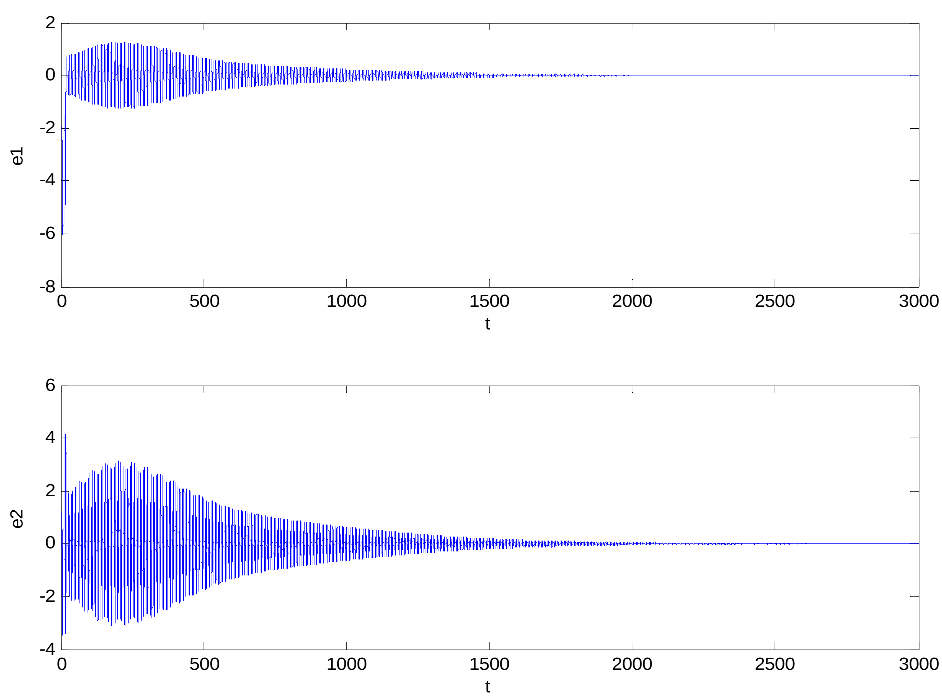

Fig. 4.2 Error dynamics for Case 1.

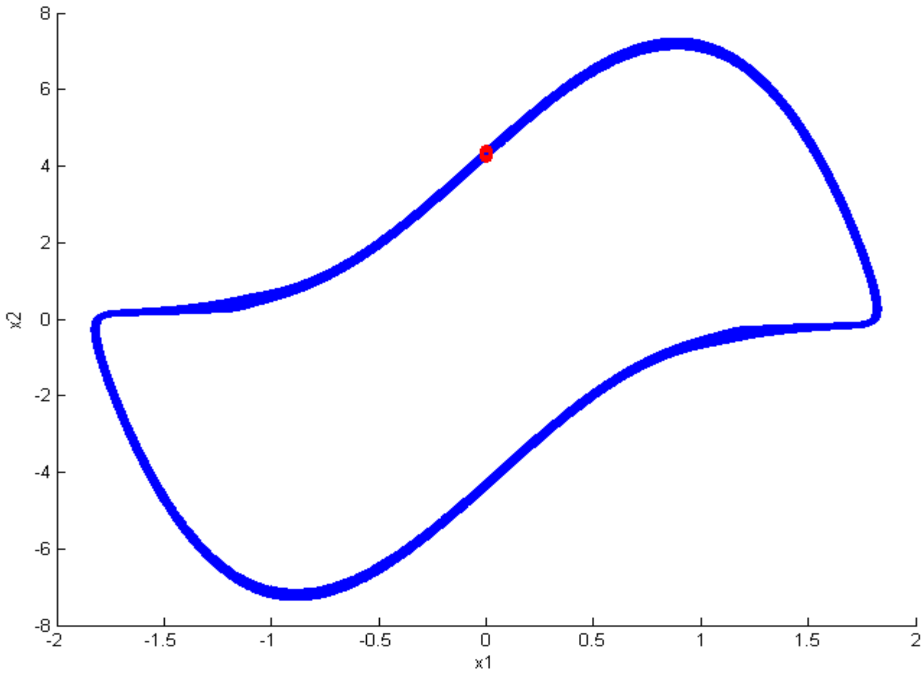

Fig. 4.3 The phase portrait for replacing b by $k\cos x$ with $\alpha = \beta = 0.9$, a = 5, c = 5.

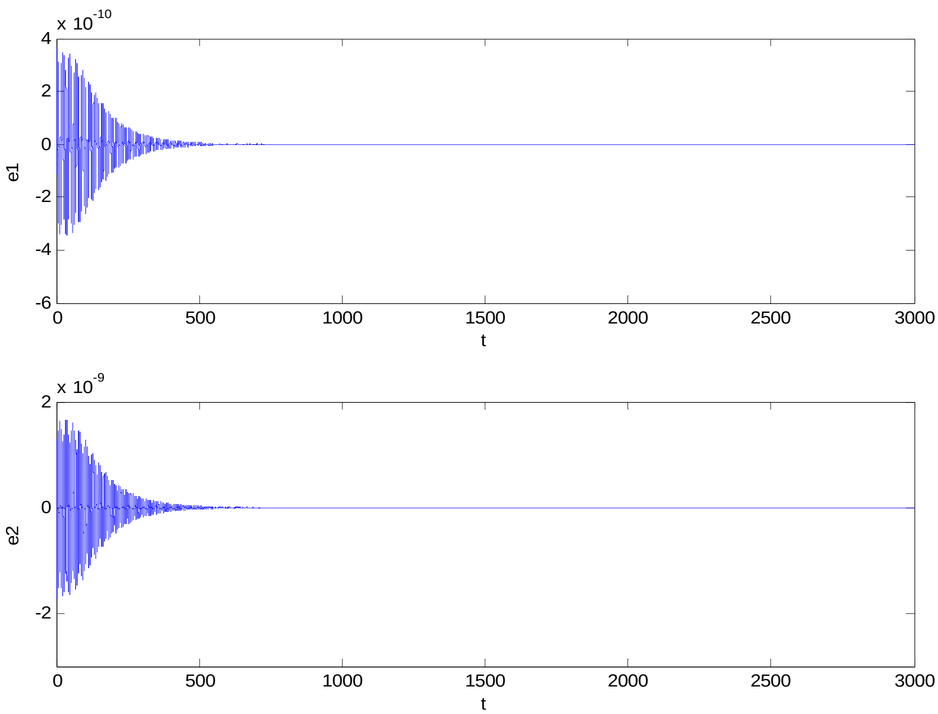

Fig. 4.4 Error dynamics for Case 2.

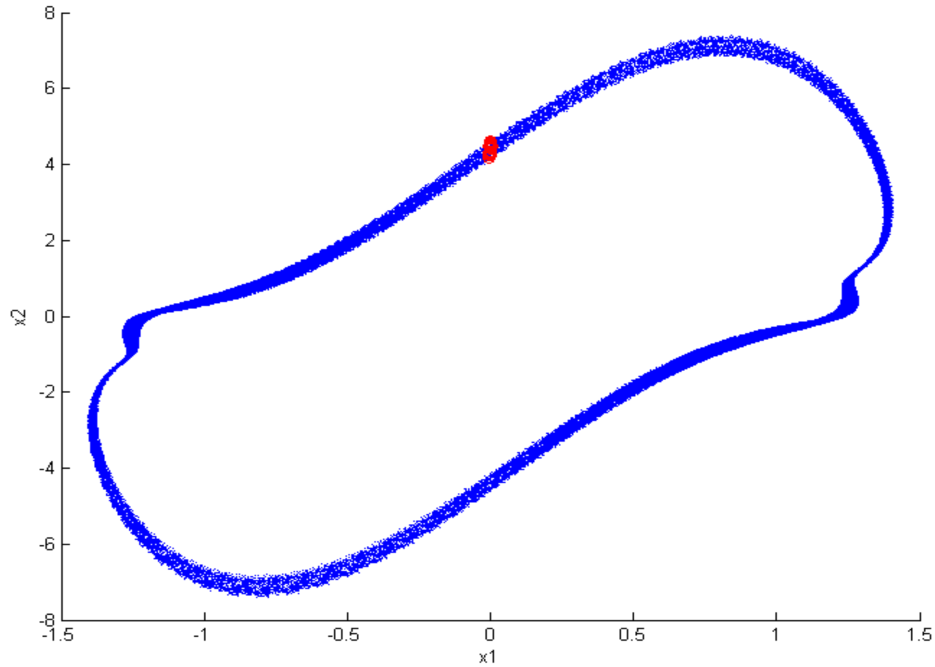

Fig. 4.5 The phase portrait for replacing *b* by *kcosx* with $\alpha = \beta = 0.8$, a = 5, c = 5.

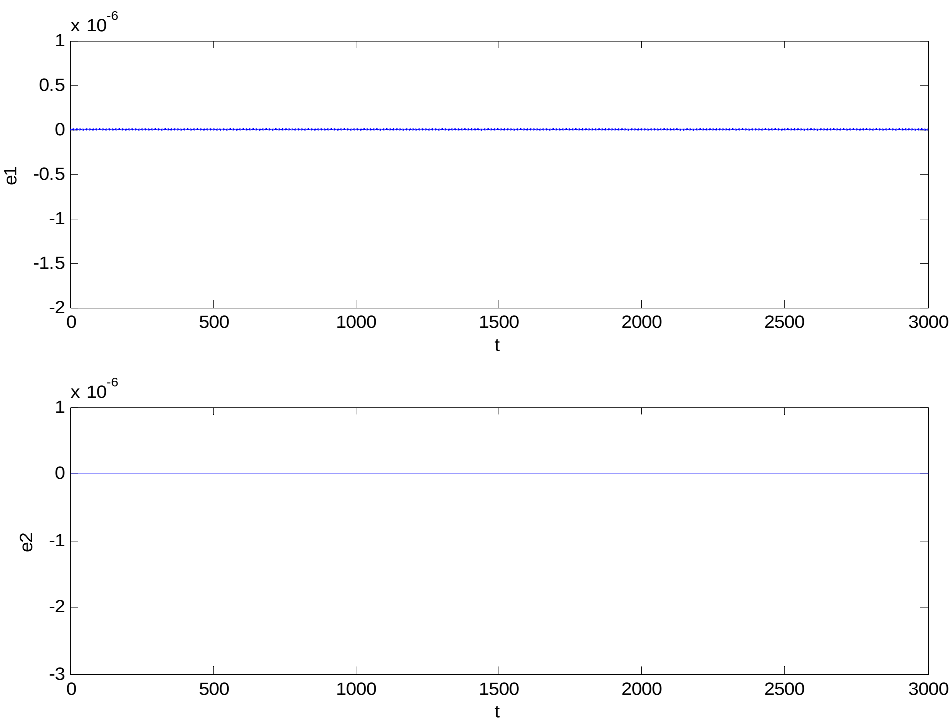

Fig. 4.6 Error dynamics for Case 3.

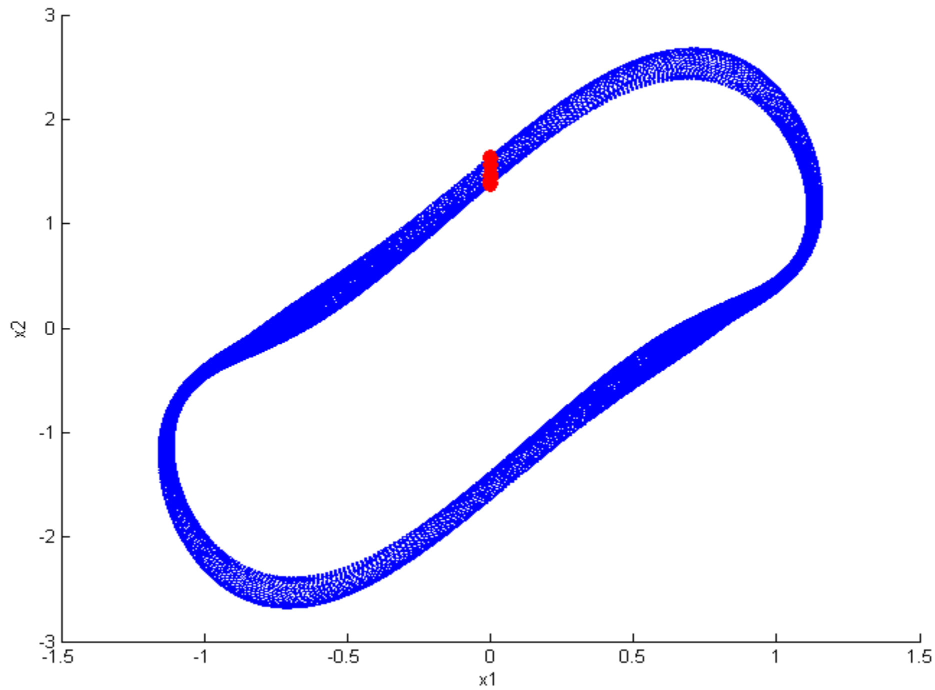

Fig. 4.7 The phase portrait for replacing b by $k\cos x$ with $\alpha = \beta = 0.7$, $a = 2.5$, $c = 35$.

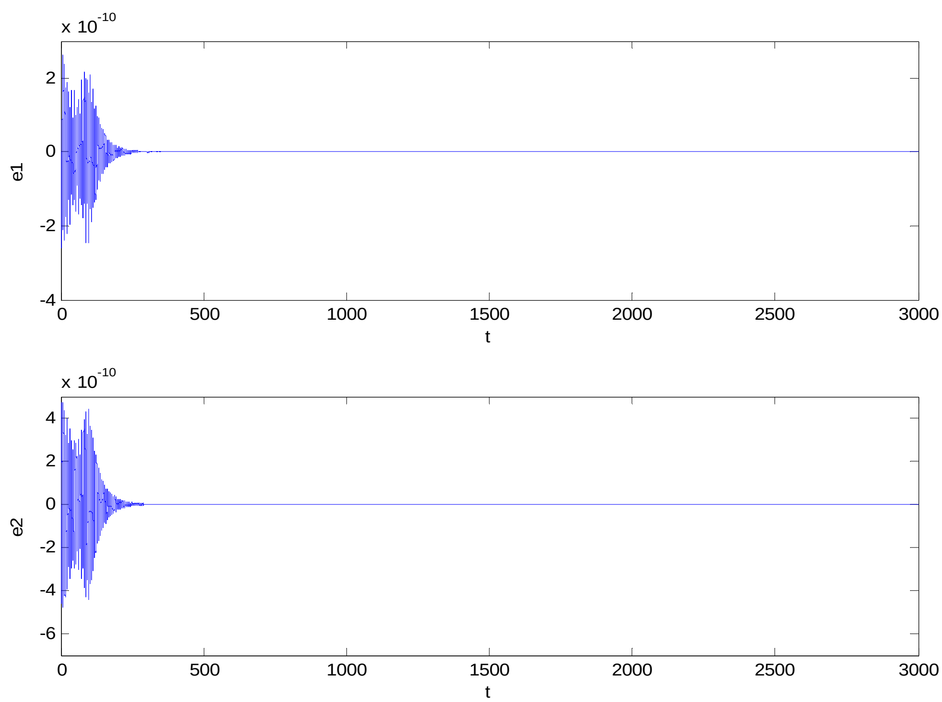

Fig. 4.8 Error dynamics for Case 4.

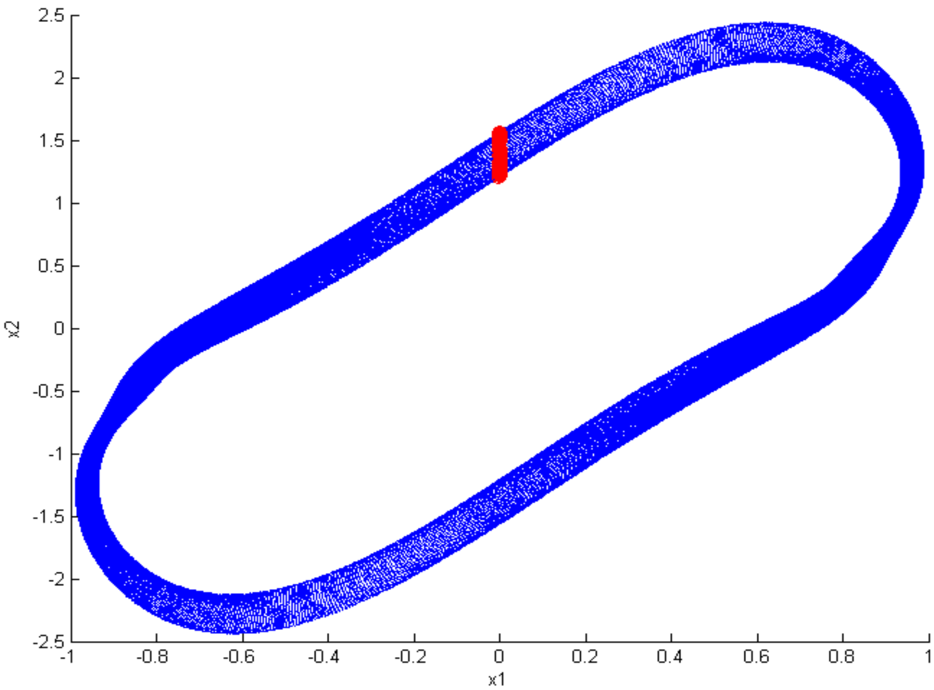

Fig. 4.9 The phase portrait for replacing b by $kcosx$ with $\alpha = \beta = 0.6$, a = 2.5, c= 50.

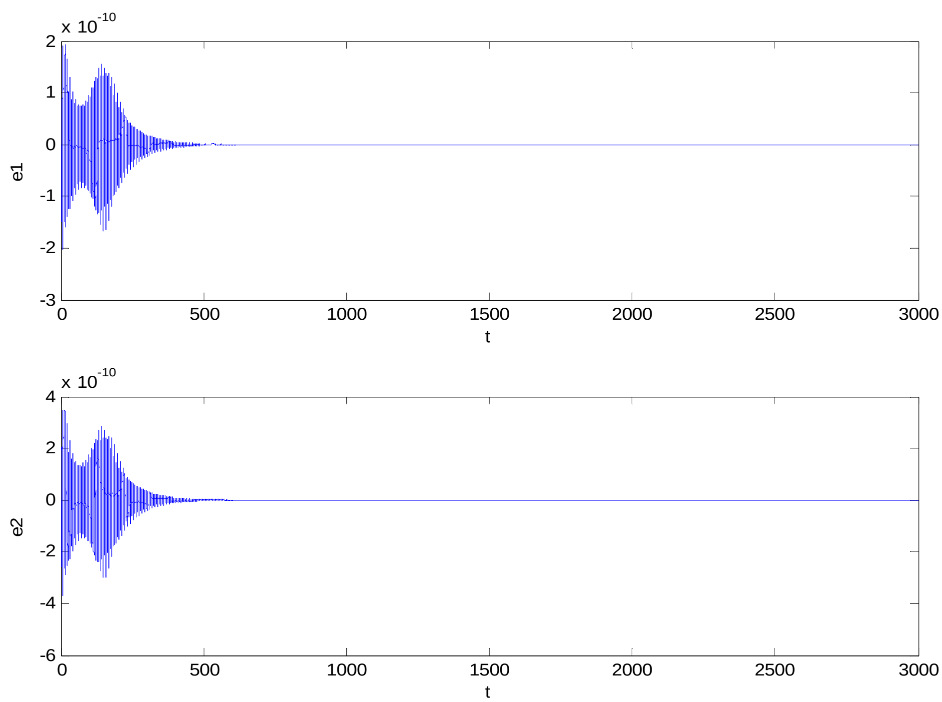

Fig. 4.10 Error dynamics for Case 5.

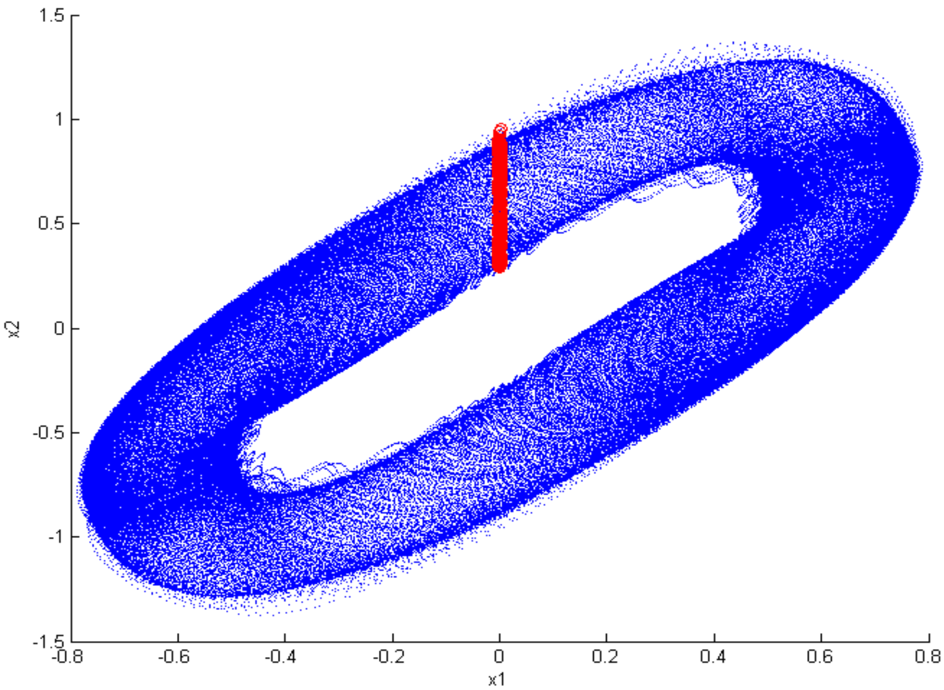

Fig. 4.11 The phase portrait for replacing b by $k\cos x$ with $\alpha = \beta = 0.5$, $a = 2$, $c = 35$.

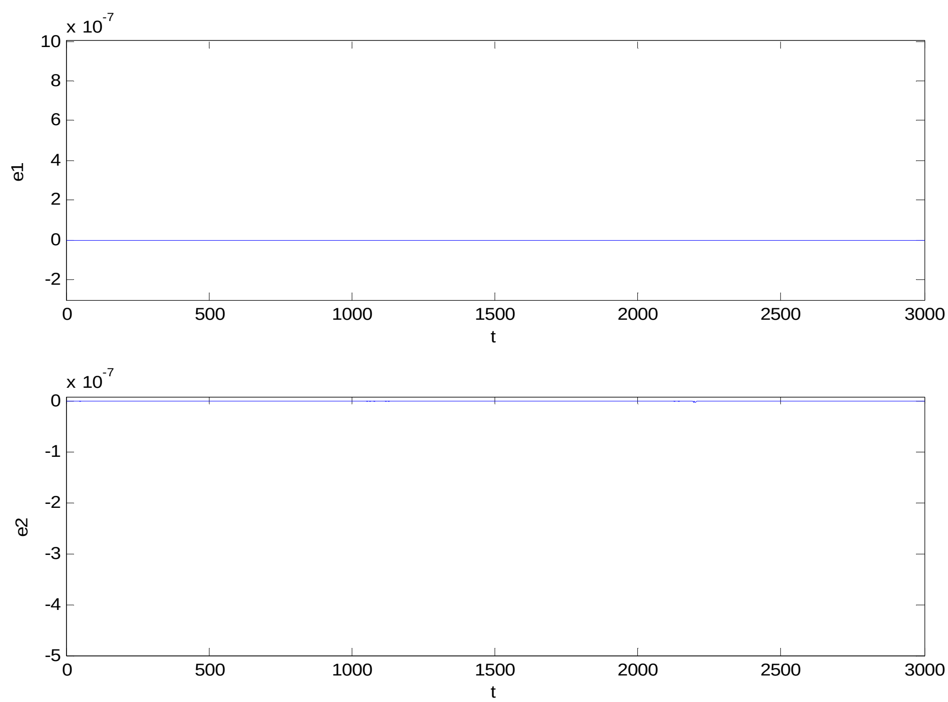

Fig. 4.12 Error dynamics for Case 6.

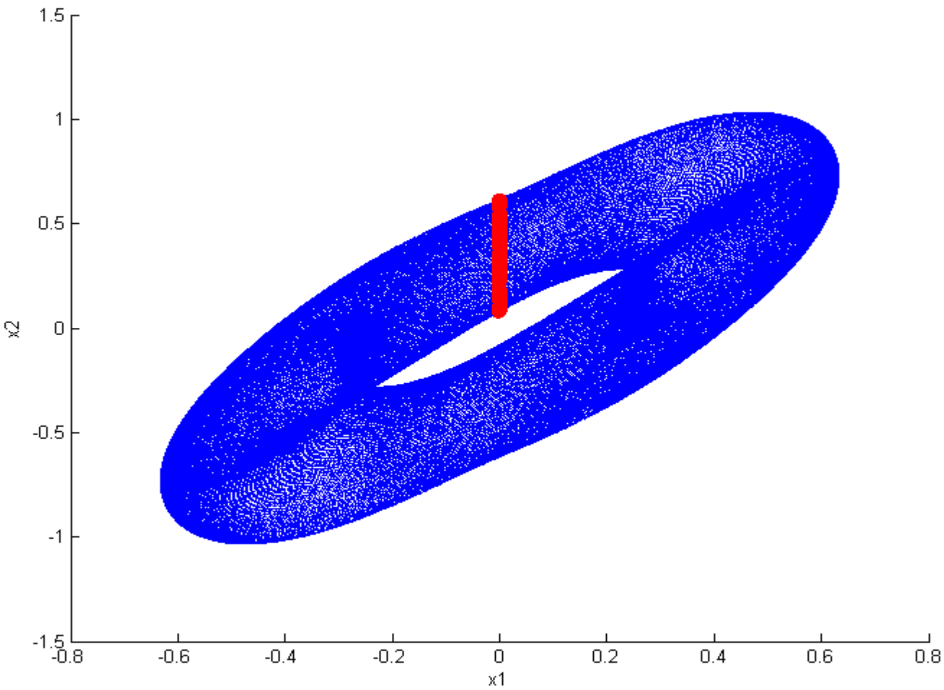

Fig. 4.13 The phase portrait for replacing b by $k\cos x$ with $\alpha = \beta = 0.4$, $a = 2$, $c = 65$.

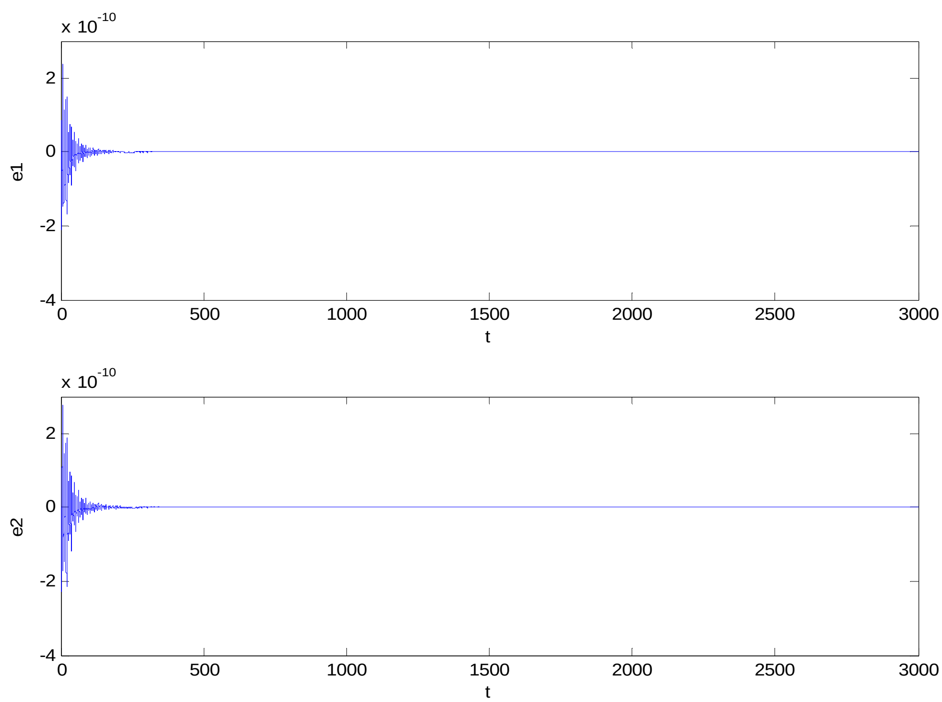

Fig. 4.14 Error dynamics for Case 7.

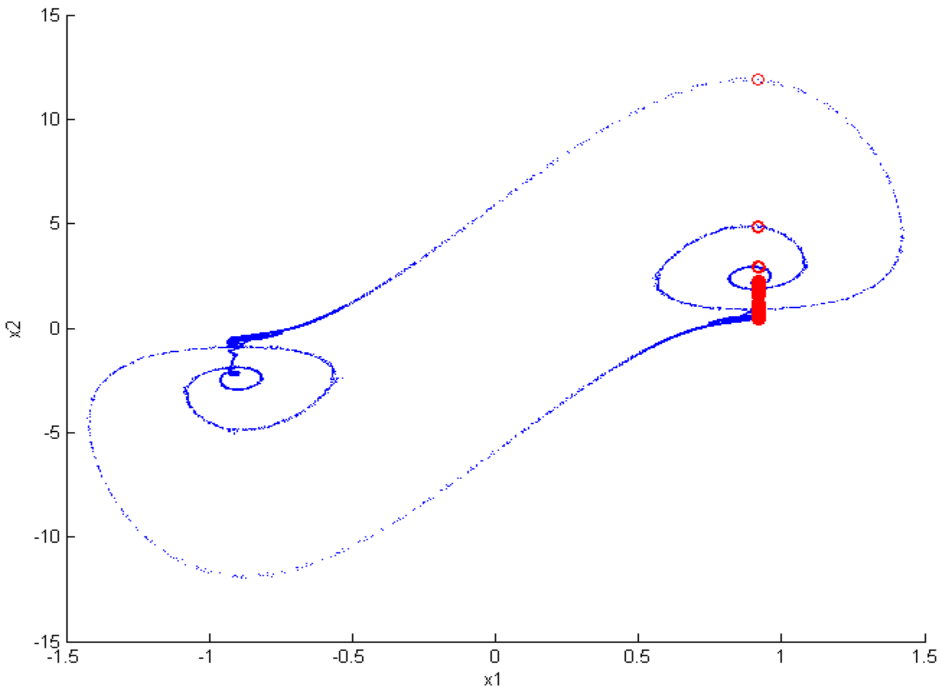

Fig. 4.15 The phase portrait for replacing b by $k\cos x$ with $\alpha = \beta = 0.3$, $a = 10$, $c = 65$.

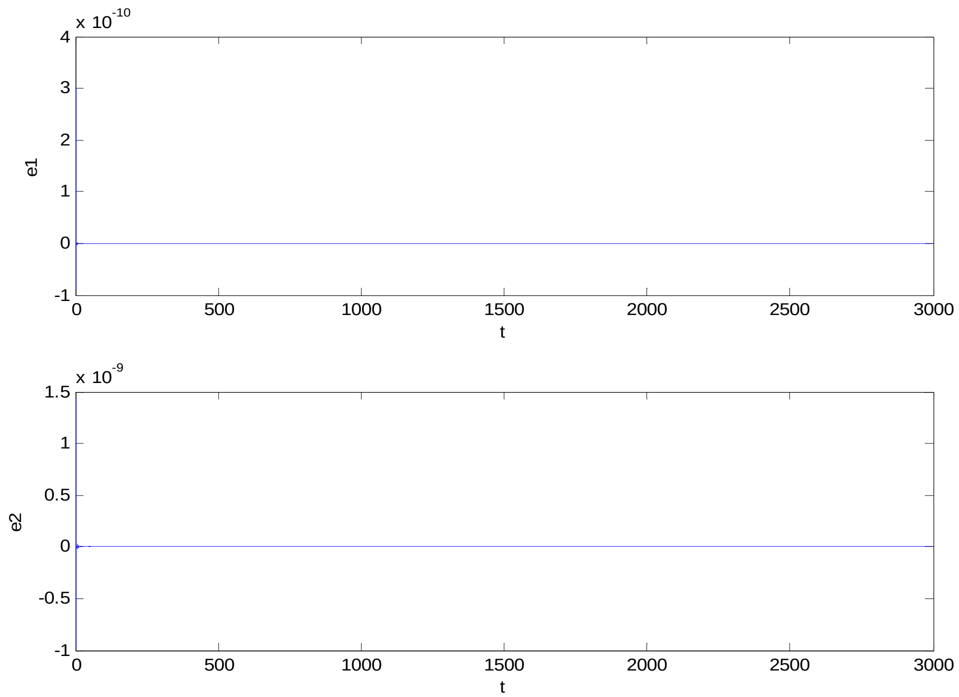

Fig. 4.16 Error dynamics for Case 8.

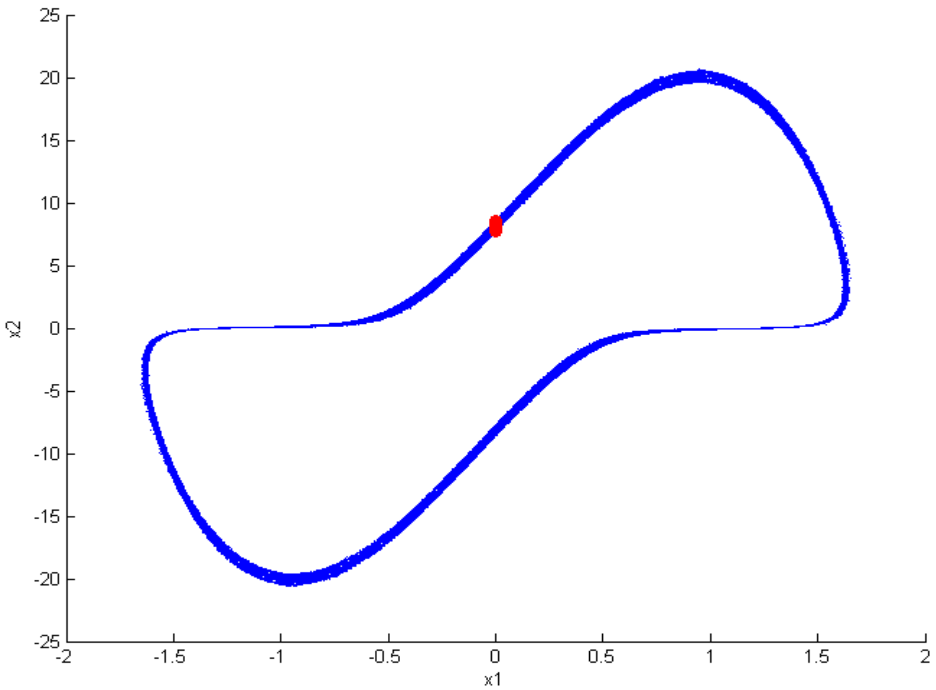

Fig. 4.17 The phase portrait for replacing b by $kcosx$ with $\alpha = \beta = 0.2$, a = 20, c = 55.

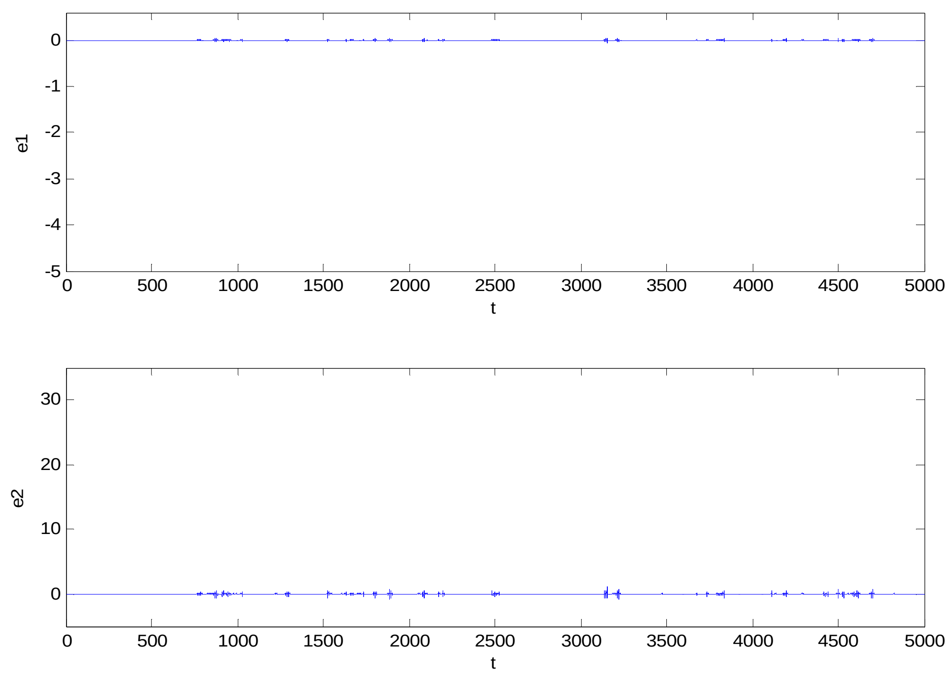

Fig. 4.18 Error dynamics for Case 9.

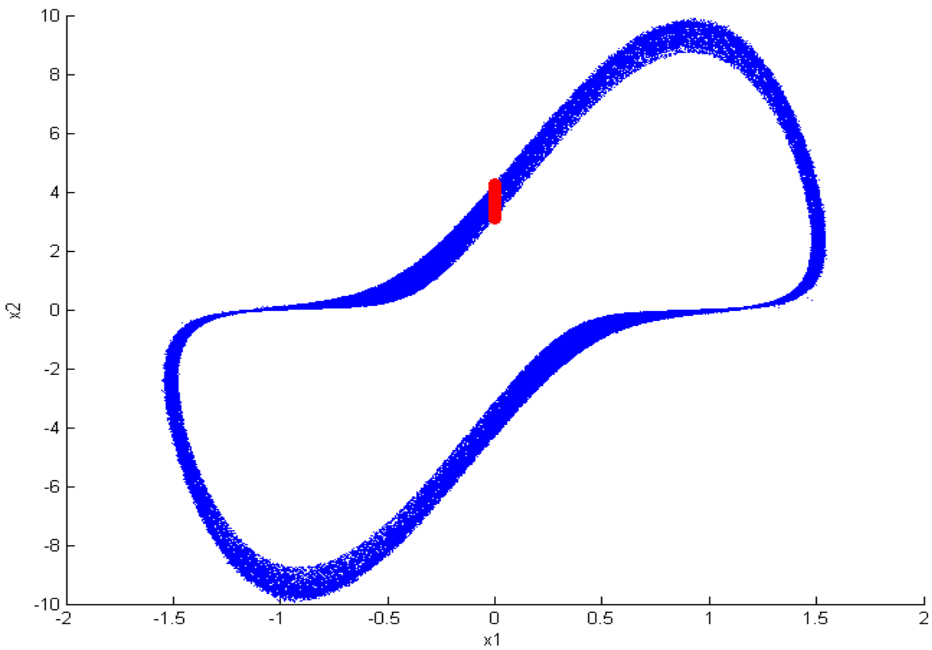

Fig. 4.19 The phase portrait for replacing b by $kcosx$ with $\alpha = \beta = 0.1$, $a = 10$, $c = 0.5$.

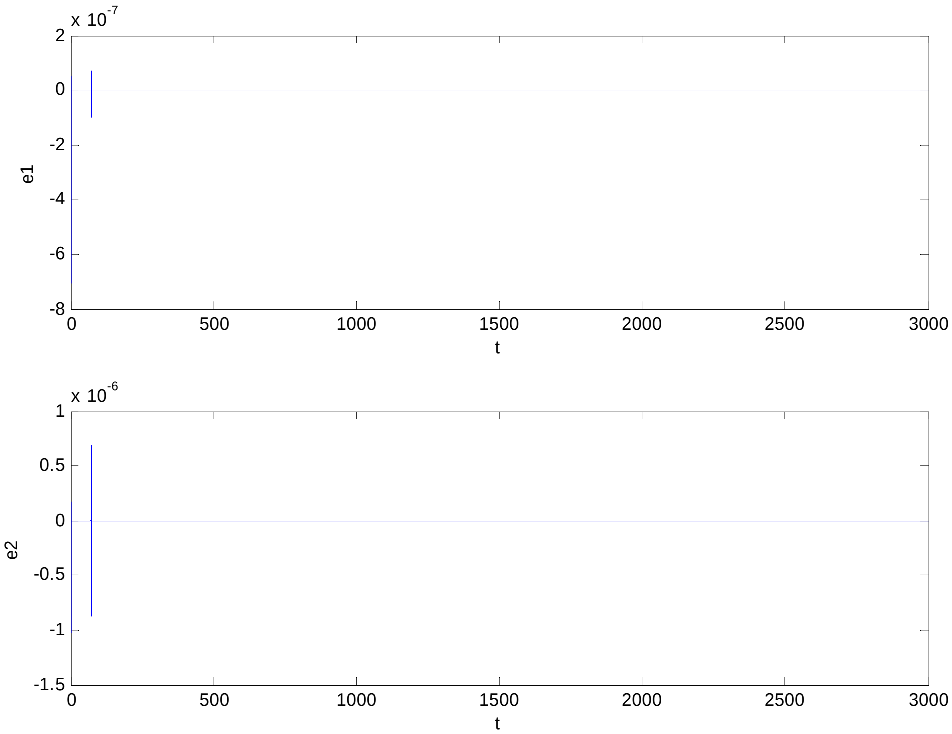

Fig. 4.20 Error dynamics for Case 10.

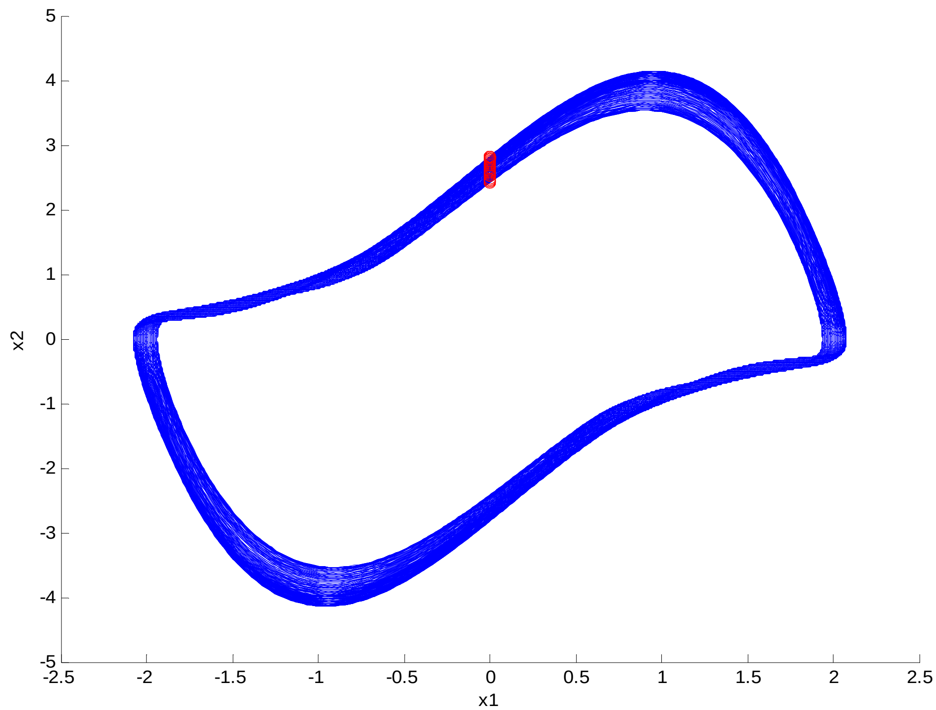

Fig. 4.21 The phase portrait for replacing *b* by *kcosy* with $\alpha = \beta = 1$, $a = 2$, $c = 10$.

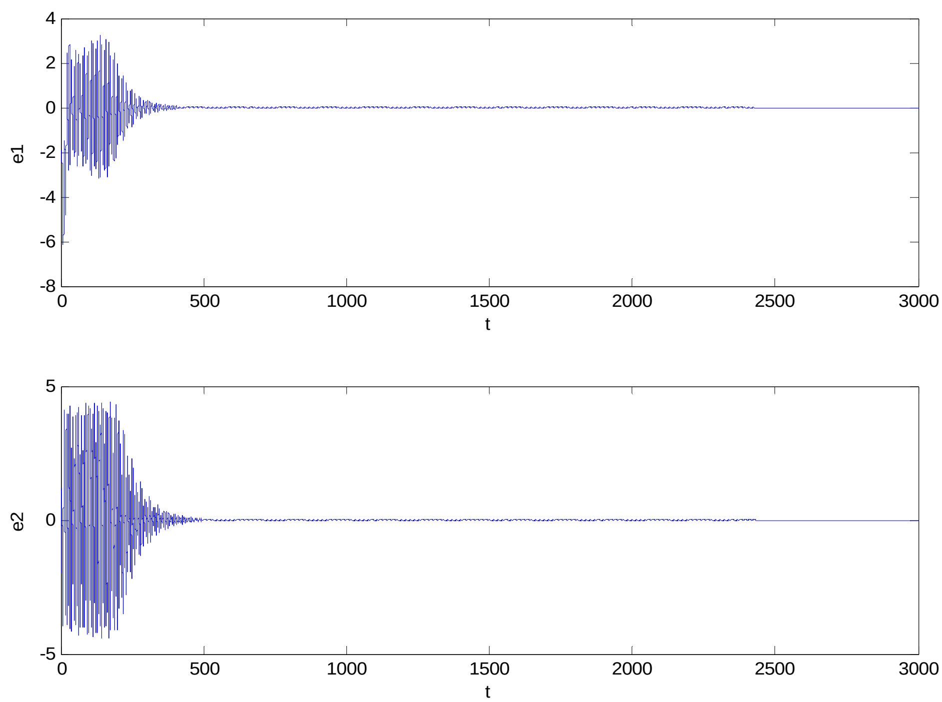

Fig. 4.22 Error dynamics for Case 1.

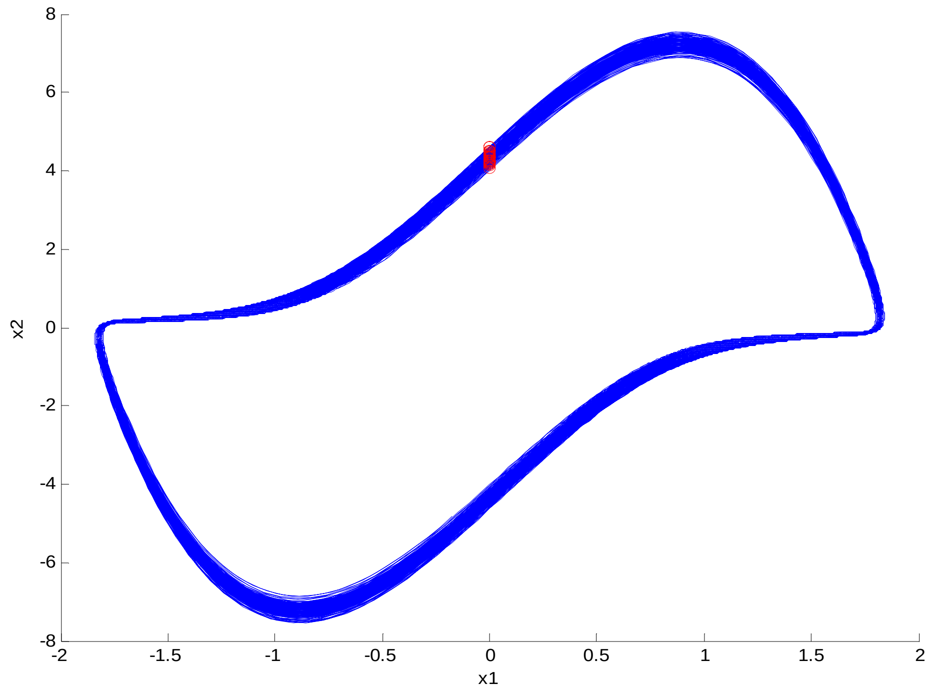

Fig. 4.23 The phase portrait for replacing b by $k\cos y$ with $\alpha = \beta = 0.9$, $a = 5$, $c = 5$.

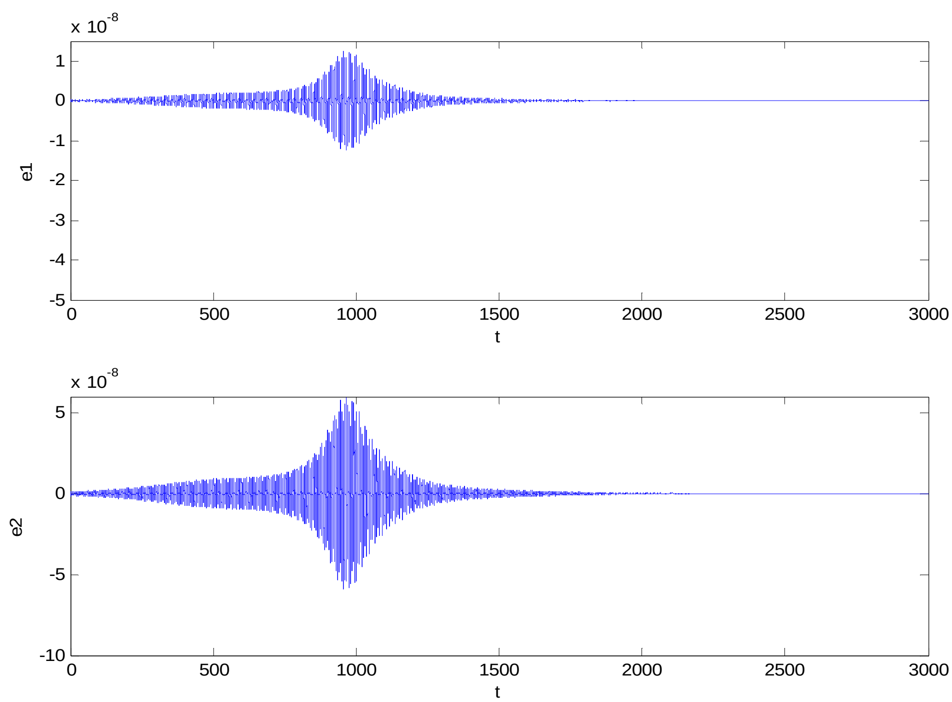

Fig. 4.24 Error dynamics for Case 2.

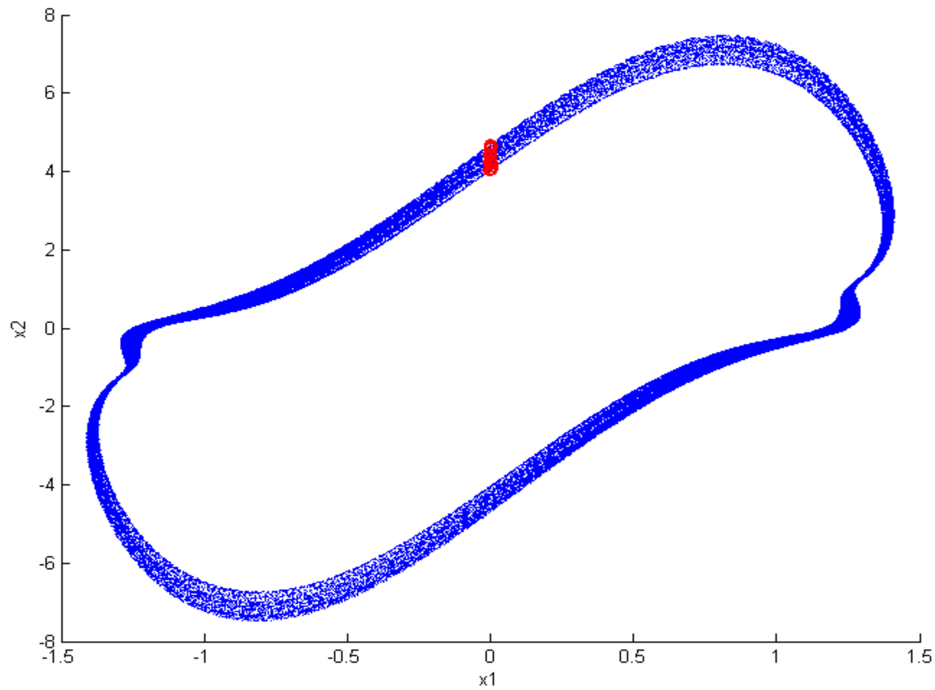

Fig. 4.25 The phase portrait for replacing b by $kcosy$ with $\alpha = \beta = 0.8$, a = 5, c = 5.

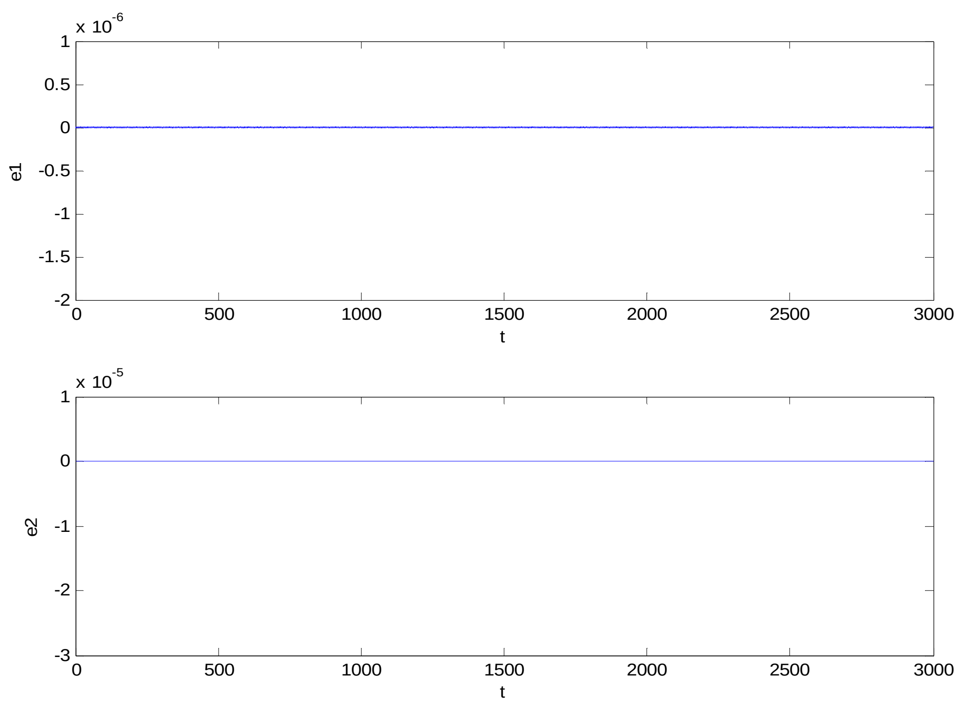

Fig. 4.26 Error dynamics for Case 3.

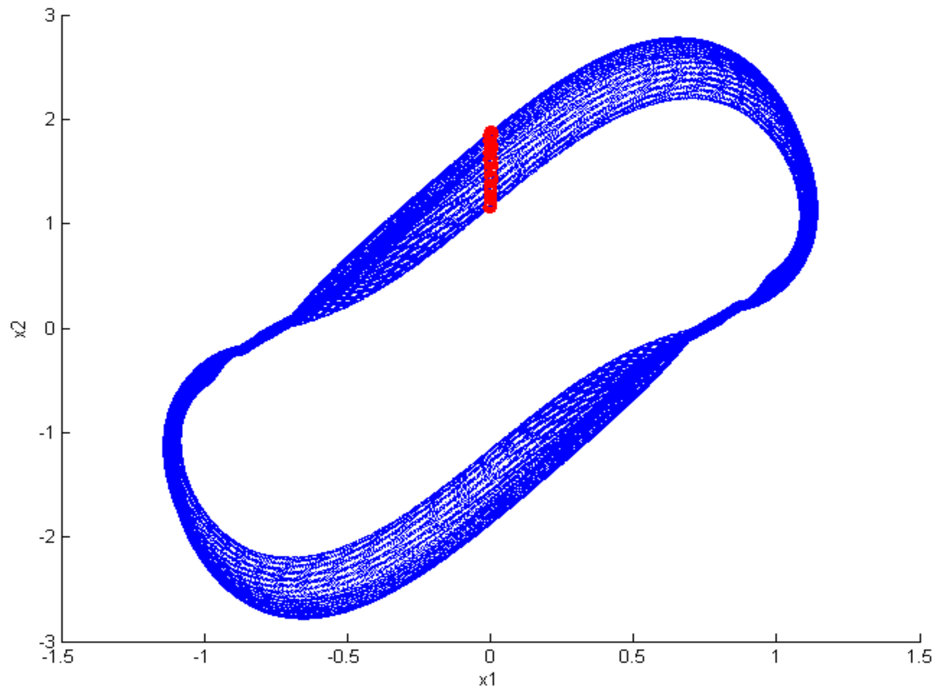

Fig. 4.27 The phase portrait for replacing *b* by *kcosy* with $\alpha = \beta = 0.7$, $a = 2.5$, $c = 35$.

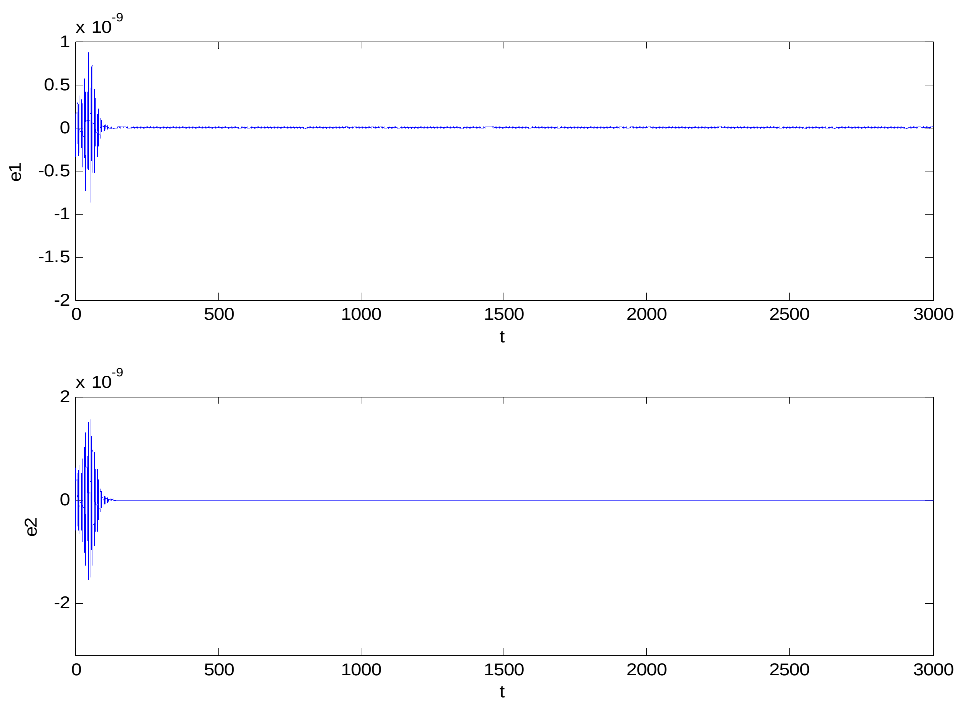

Fig. 4.28 Error dynamics for Case 4.

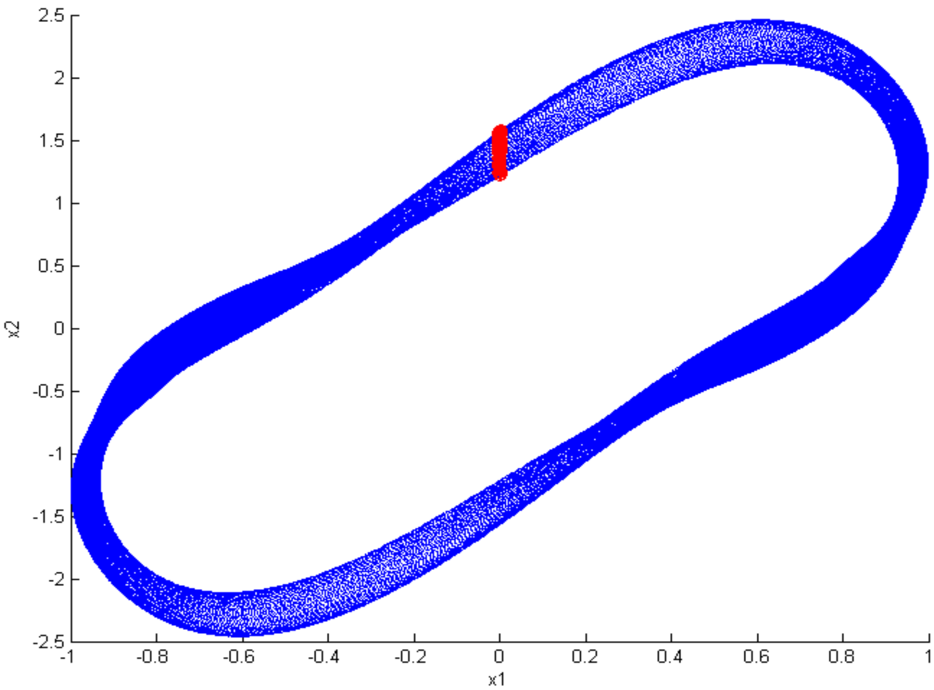

Fig. 4.29 The phase portrait for replacing b by $k\cos y$ with $\alpha = \beta = 0.6$, $a = 2.5$, $c = 50$.

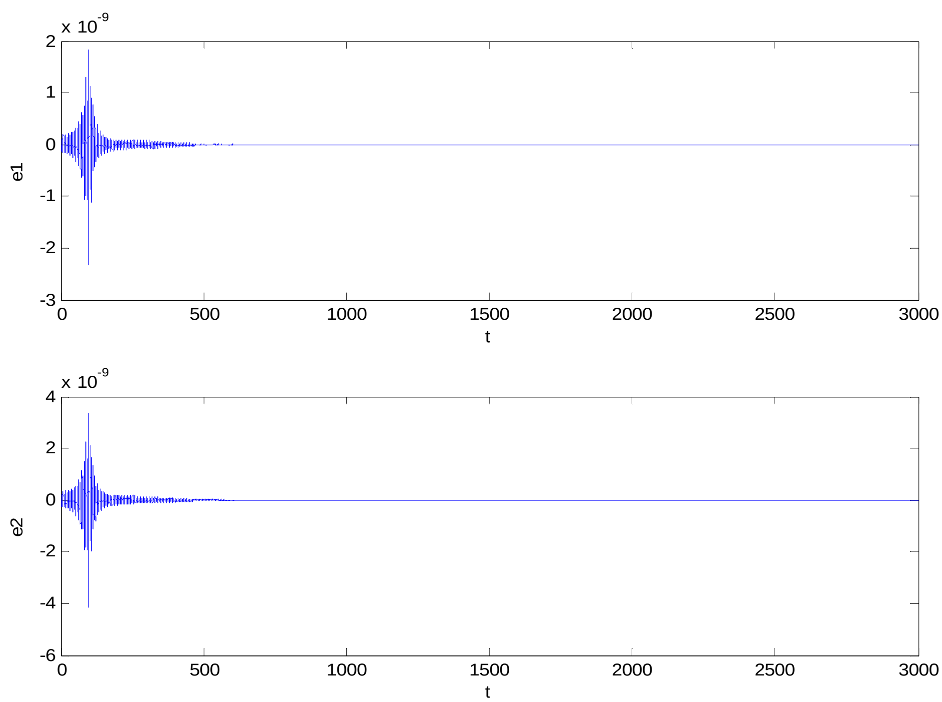

Fig. 4.30 Error dynamics for Case 5.

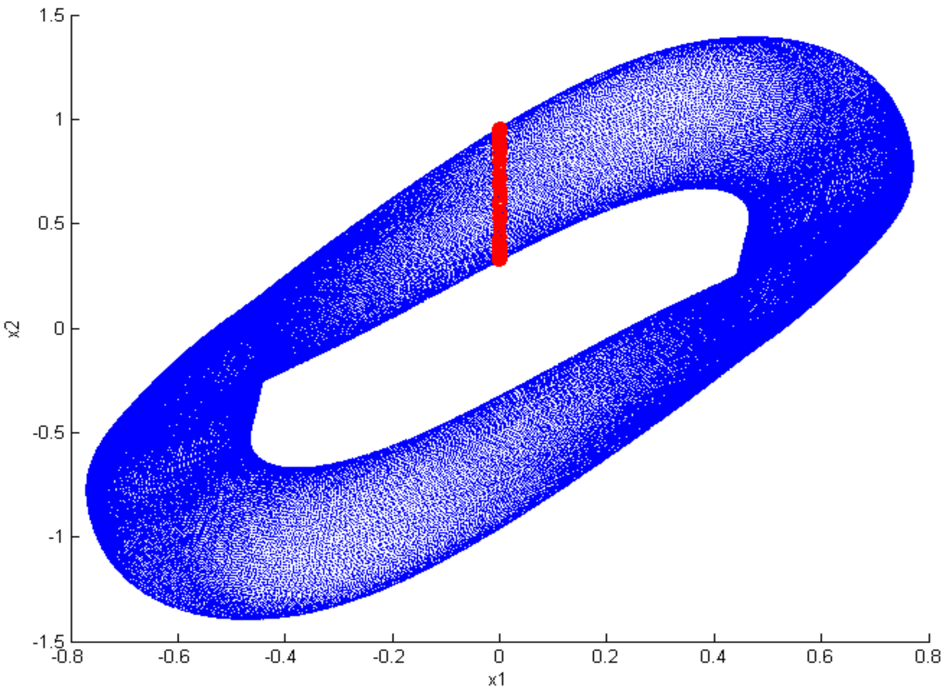

Fig. 4.31 The phase portrait for replacing *b* by *kcosy* with $\alpha = \beta = 0.5$, $a = 2$, $c = 35$.

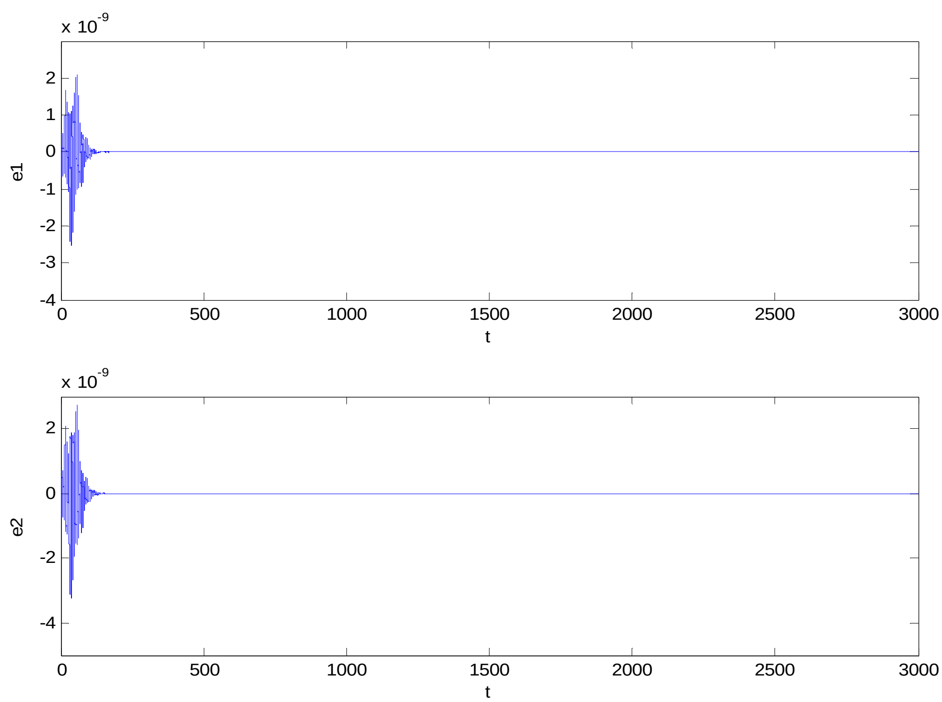

Fig. 4.32 Error dynamics for Case 6.

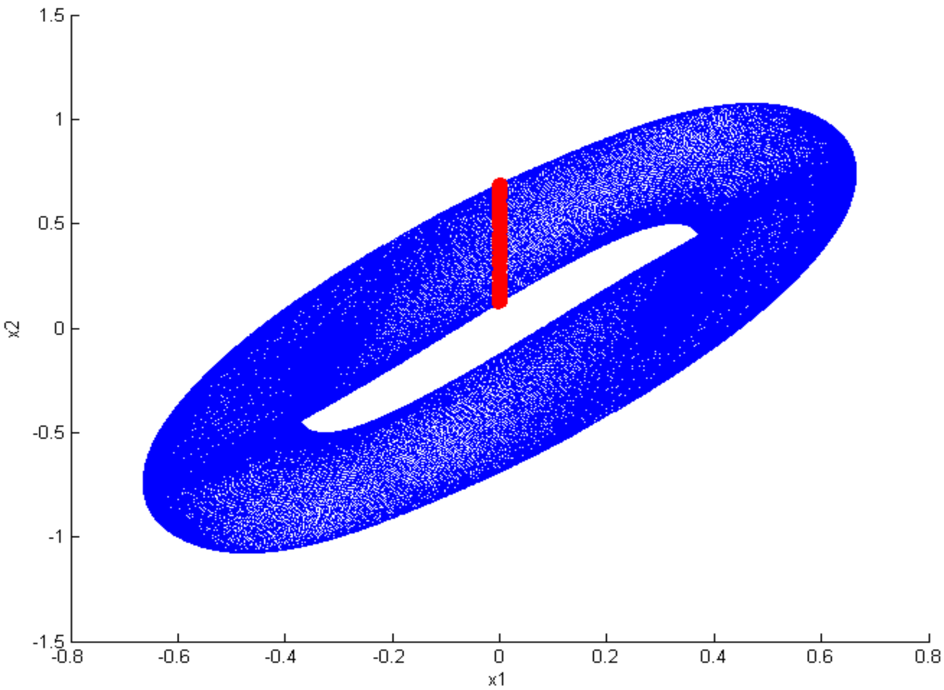

Fig. 4.33 The phase portrait for replacing *b* by *kcosy* with $\alpha = \beta = 0.4$, a = 2, c = 65.

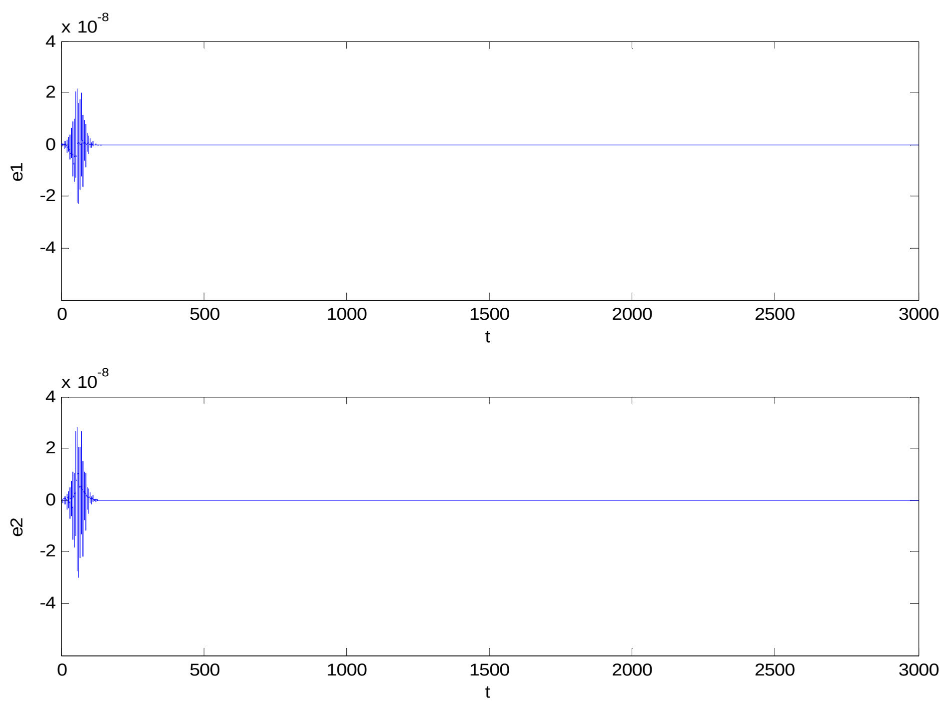

Fig. 4.34 Error dynamics for Case 7.

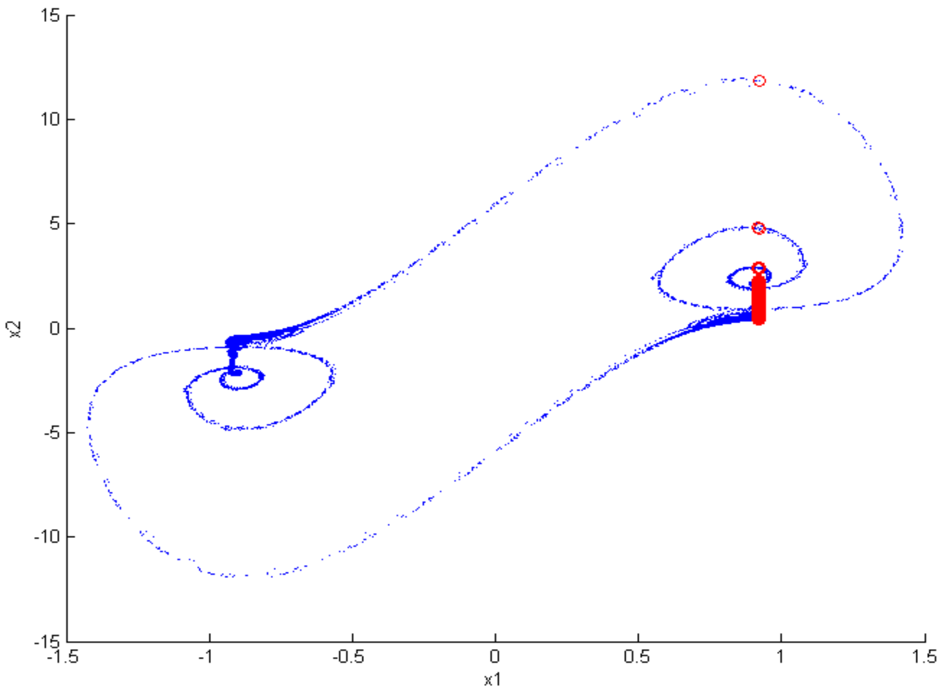

Fig. 4.35 The phase portrait for replacing b by $k\cos y$ with $\alpha = \beta = 0.3$, $a = 10$, $c = 65$.

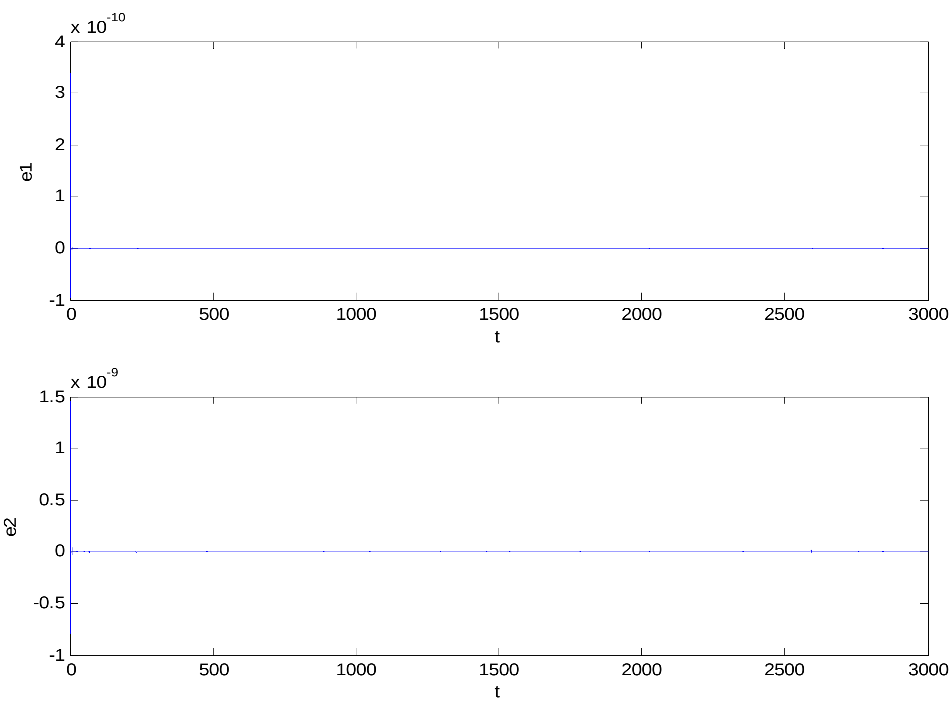

Fig. 4.36 Error dynamics for Case 8.

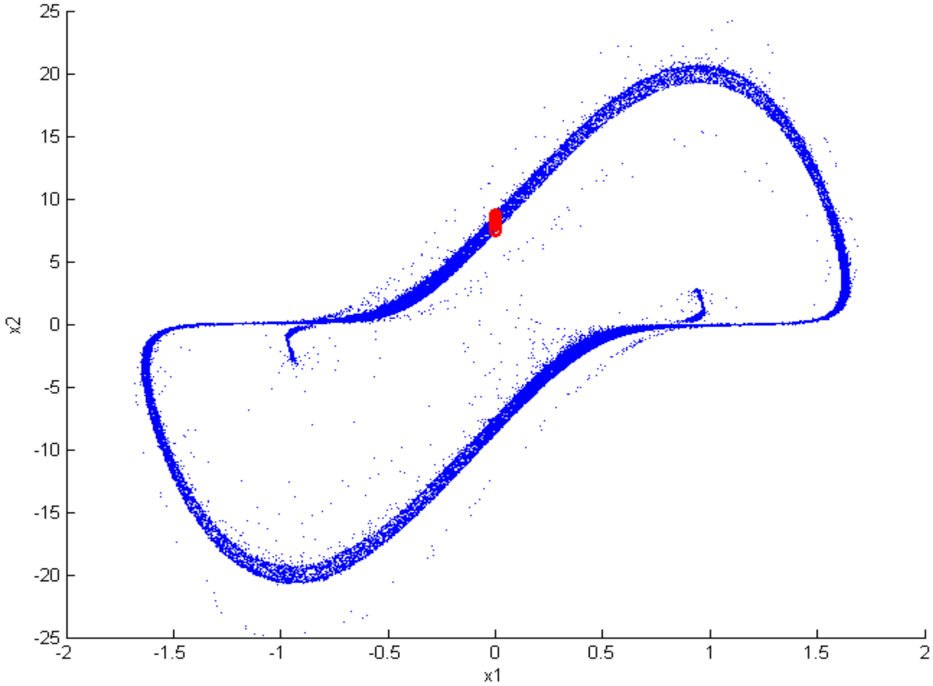

Fig. 4.37 The phase portrait for replacing b by $k\cos y$ with $\alpha = \beta = 0.2$, $a = 2$, $c = 1$.

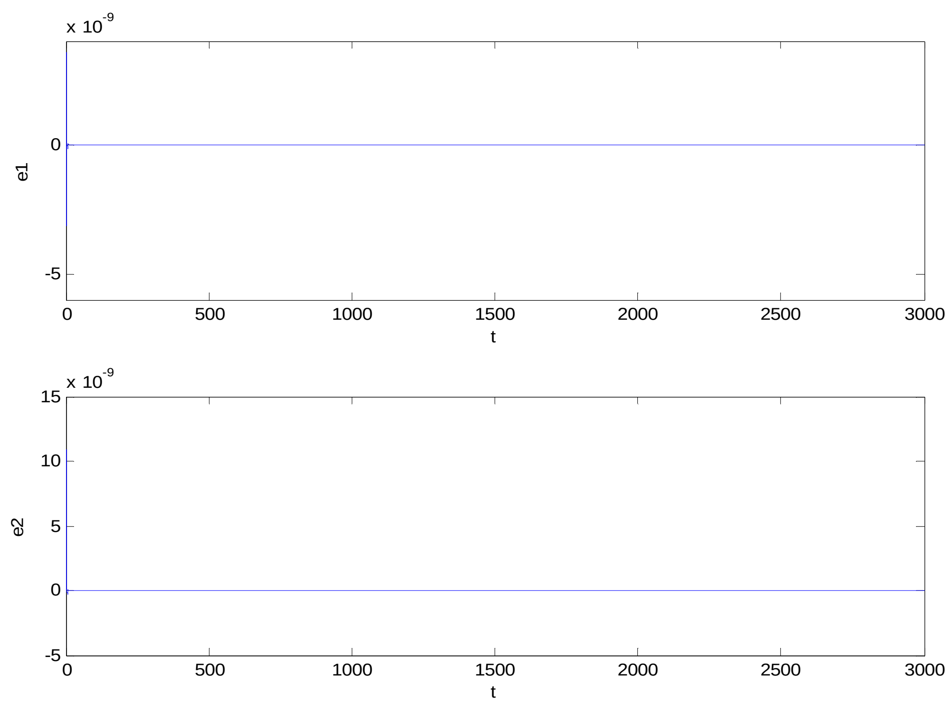

Fig. 4.38 Error dynamics for Case 9.

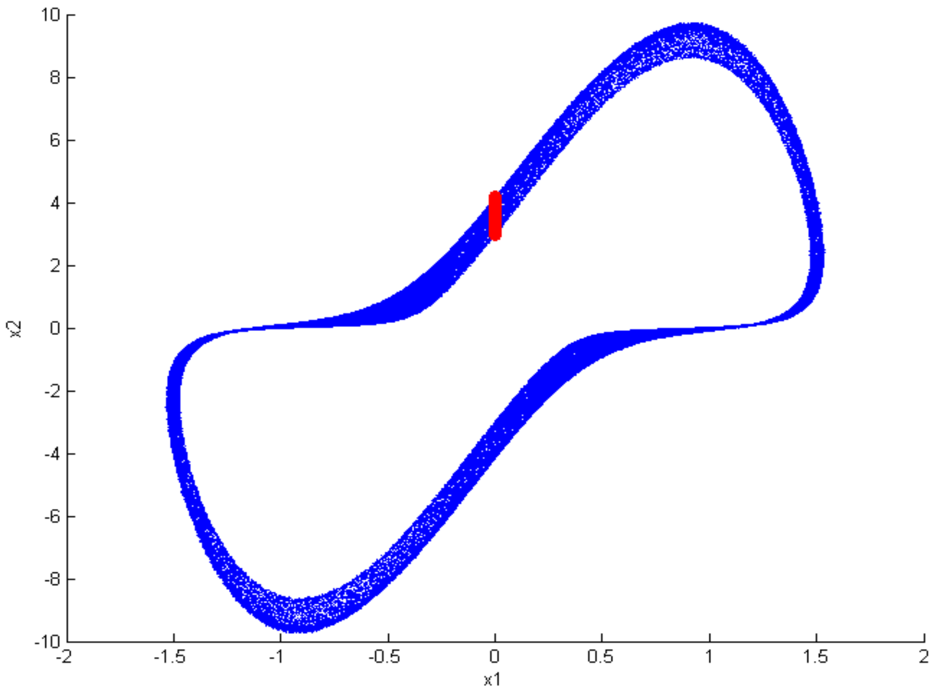

Fig. 4.39 The phase portrait for replacing b by $k\cos y$ with $\alpha = \beta = 0.1$, $a = 10$, $c = 1$.

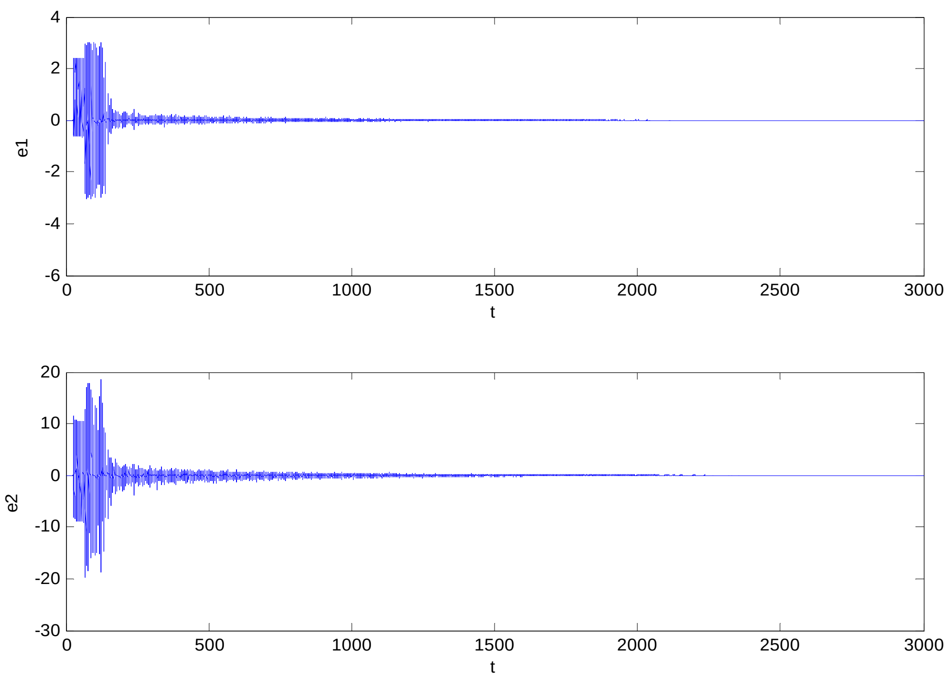

Fig. 4.40 Error dynamics for Case 10.

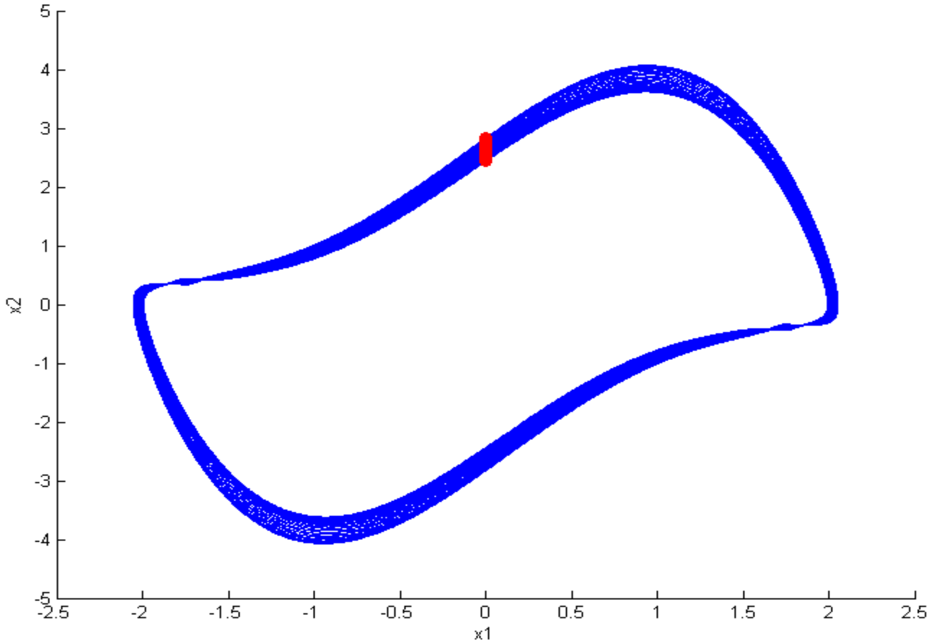

Fig. 4.41 The phase portrait for replacing *b* by *kcosxcosy* with $\alpha = \beta = 1$, a = 2, c = 10.

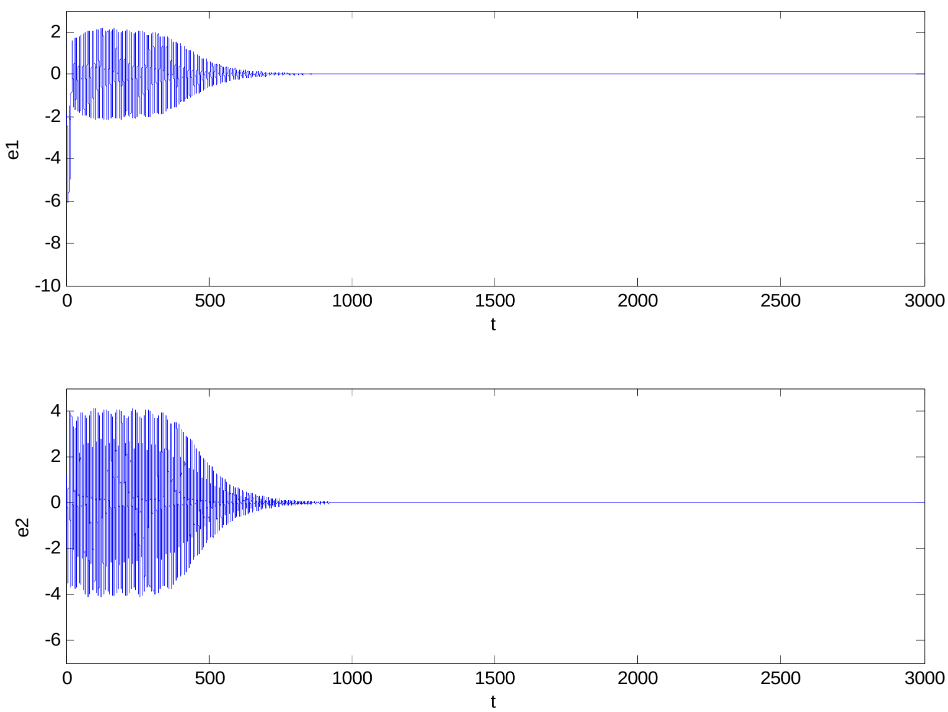

Fig. 4.42 Error dynamics for Case 1.

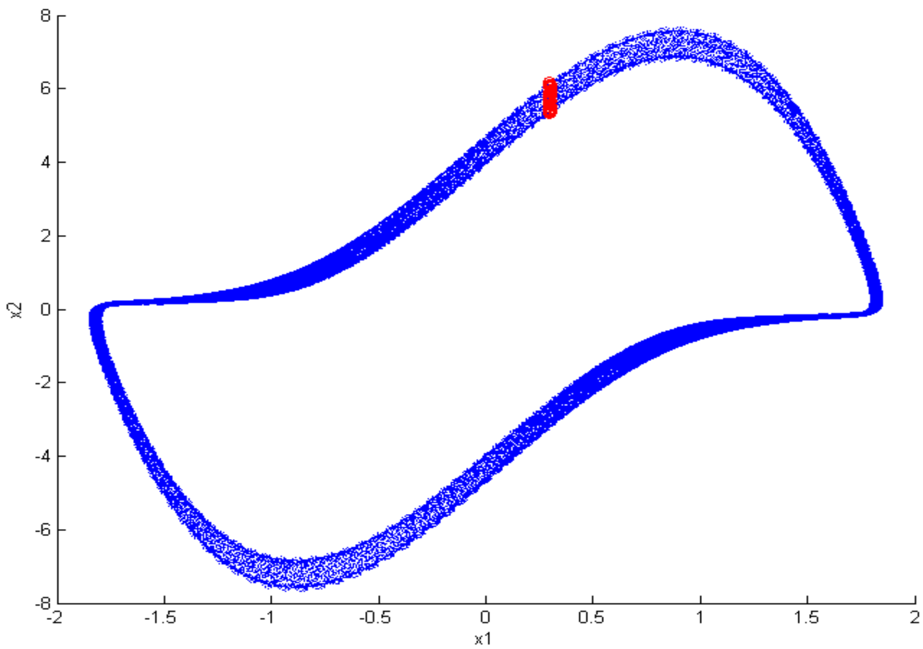

Fig. 4.43 The phase portrait for replacing *b* by *kcosxcosy* with $\alpha = \beta = 0.9$, *a* = 5, *c* = 5.

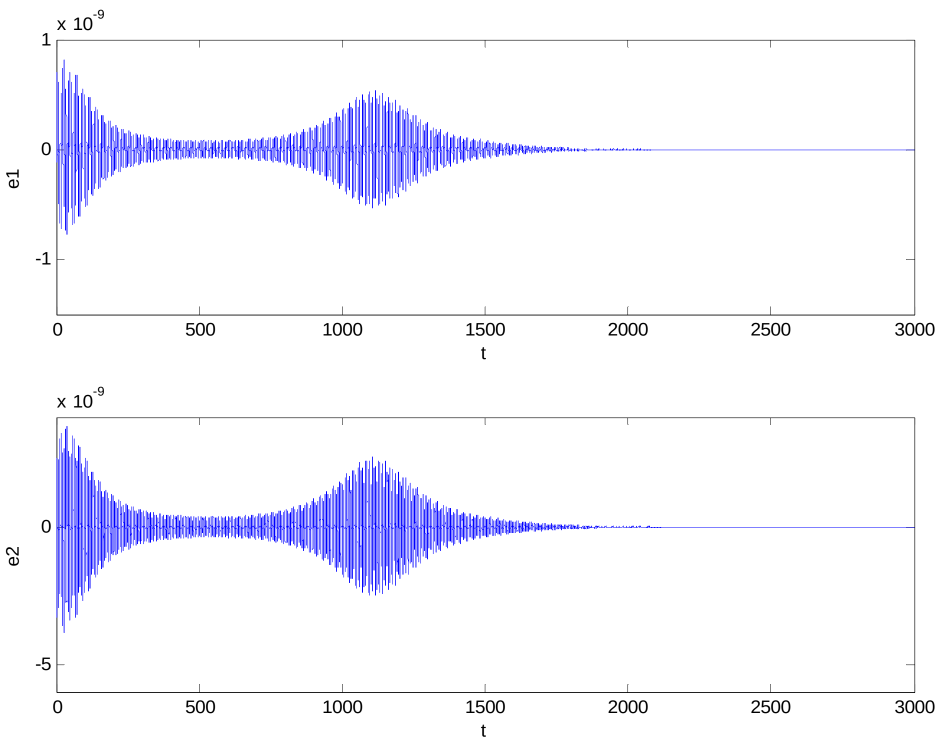

Fig. 4.44 Error dynamics for Case 2.

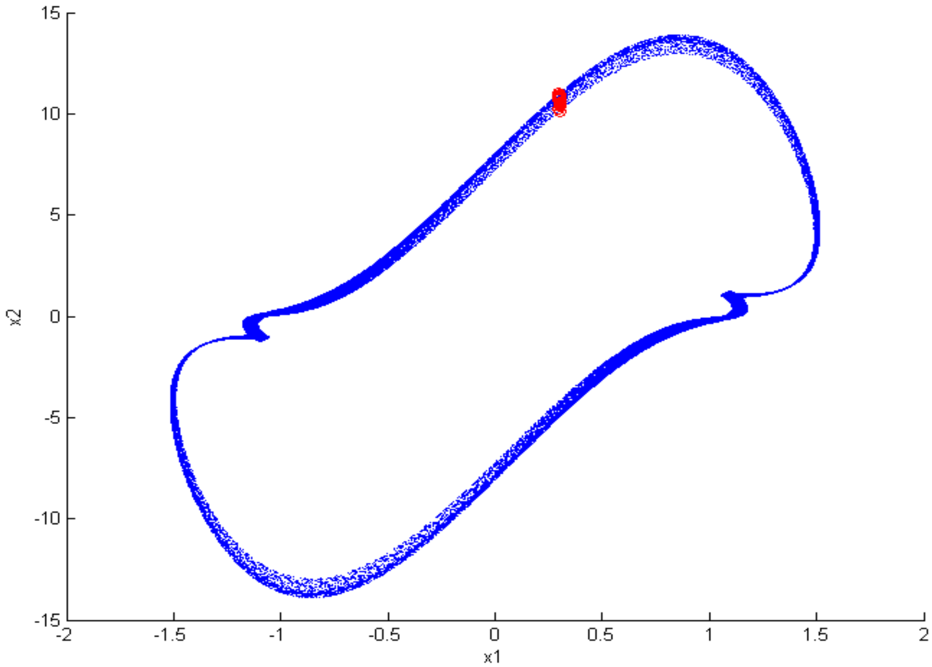

Fig. 4.45 The phase portrait for replacing b by $k\cos x\cos y$ with $\alpha = \beta = 0.8$, $a = 10$, $c = 5$.

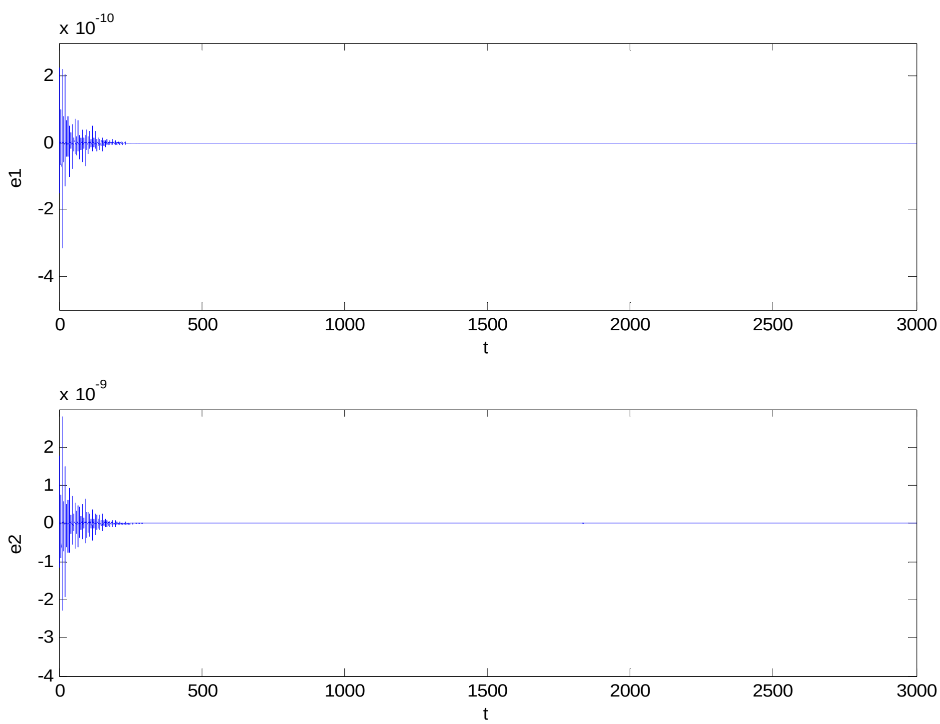

Fig. 4.46 Error dynamics for Case 3.

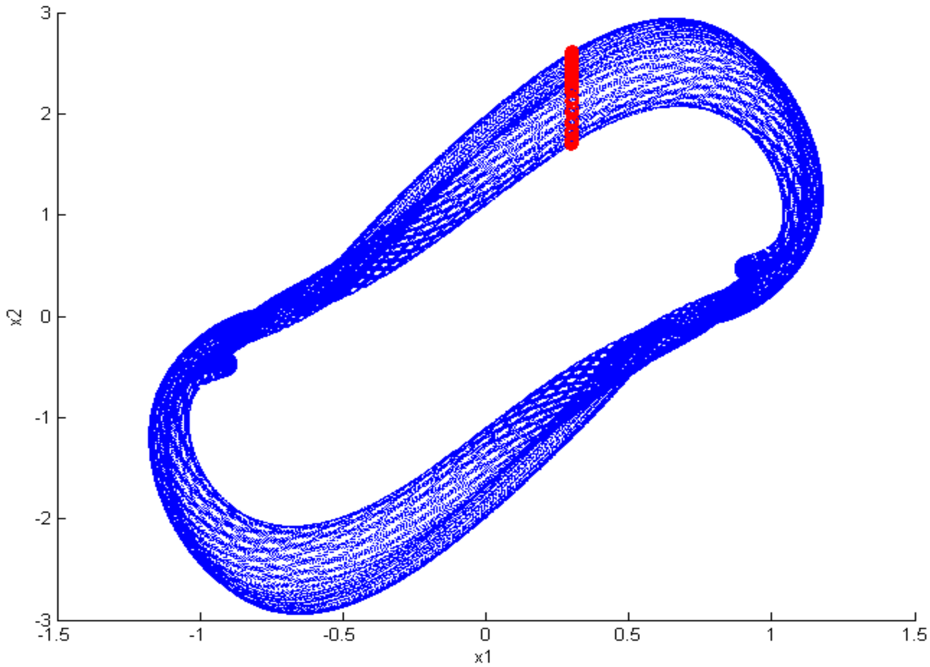

Fig. 4.47 The phase portrait for replacing b by $kcosxcosy$ with $\alpha = \beta = 0.7$, $a = 2.5$, $c = 35$.

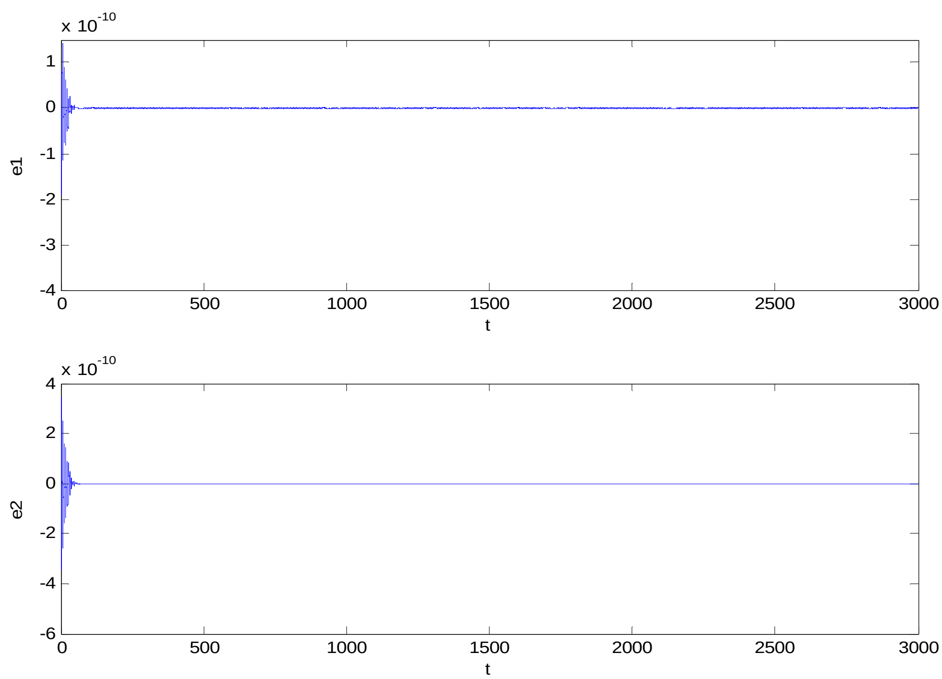

Fig. 4.48 Error dynamics for Case 4.

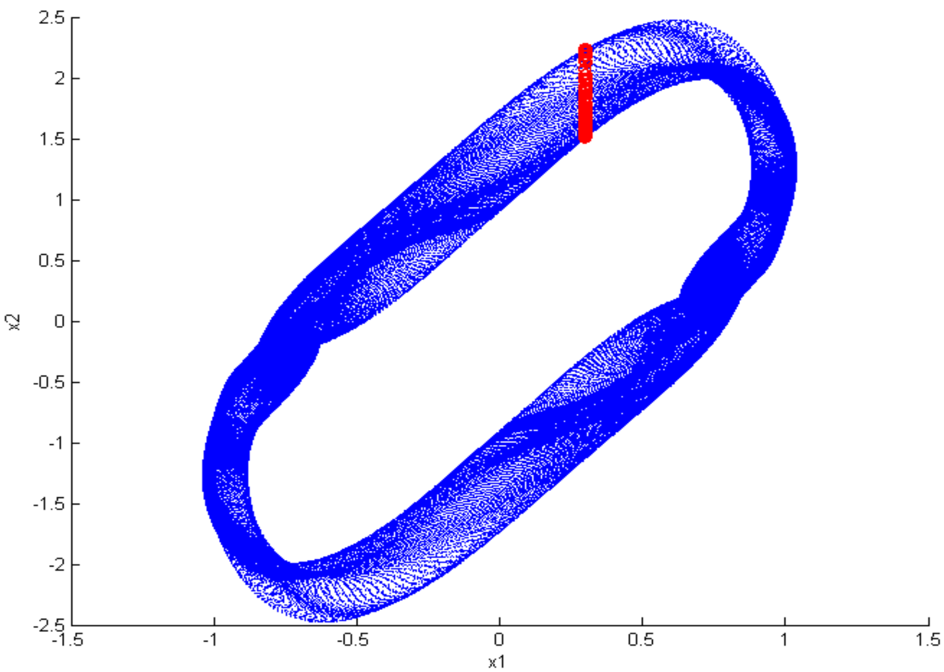

Fig. 4.49 The phase portrait for replacing *b* by *kcosxcosy* with $\alpha = \beta = 0.6$, $a = 2.5$, $c = 50$.

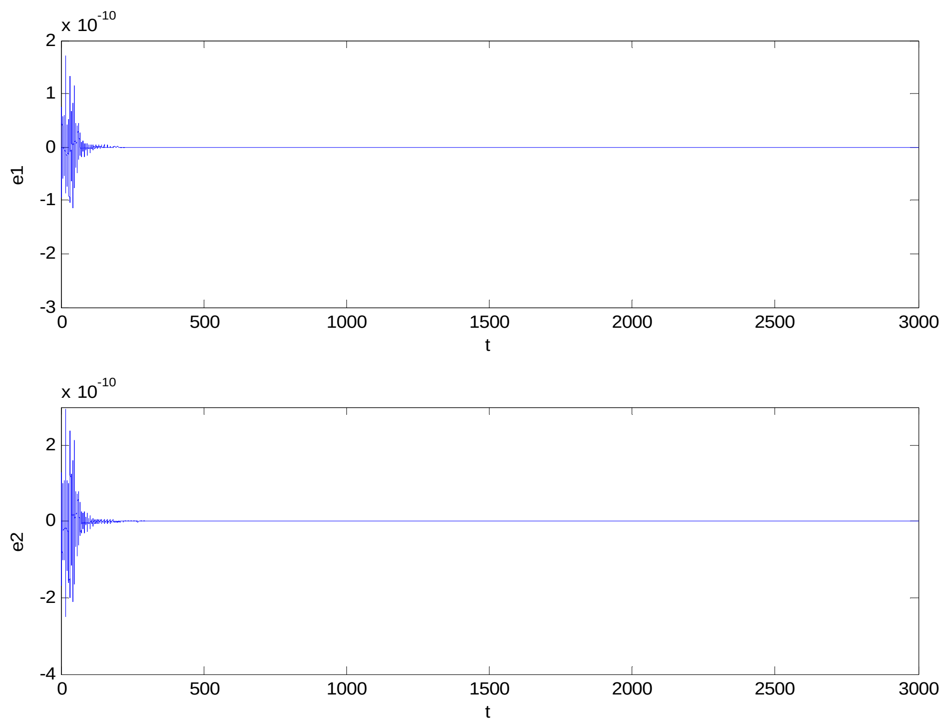

Fig. 4.50 Error dynamics for Case 5.

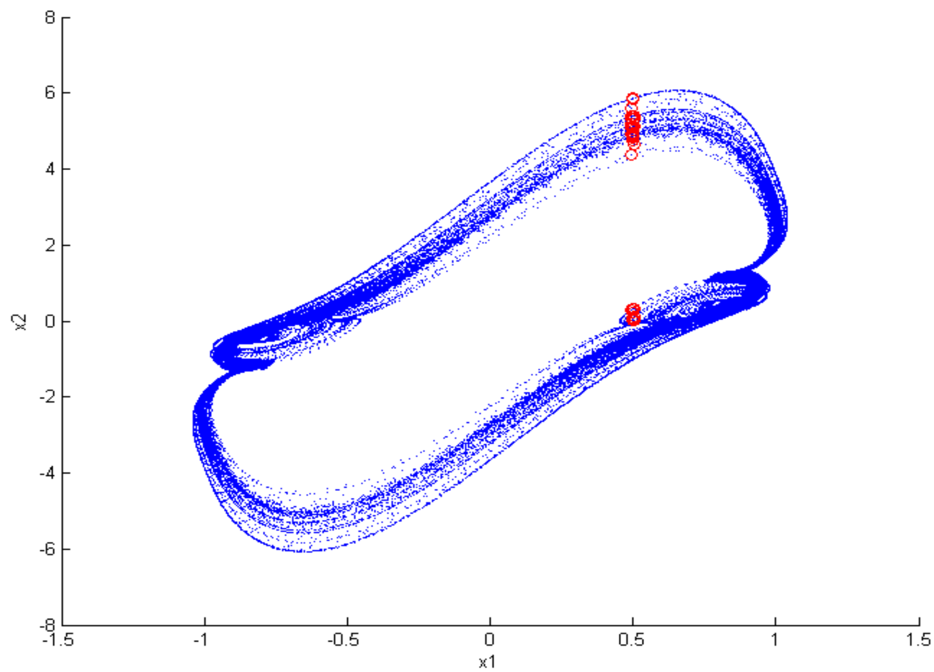

Fig. 4.51 The phase portrait for replacing *b* by *kcosxcosy* with $\alpha = \beta = 0.5$, a = 5.5, c = 45.

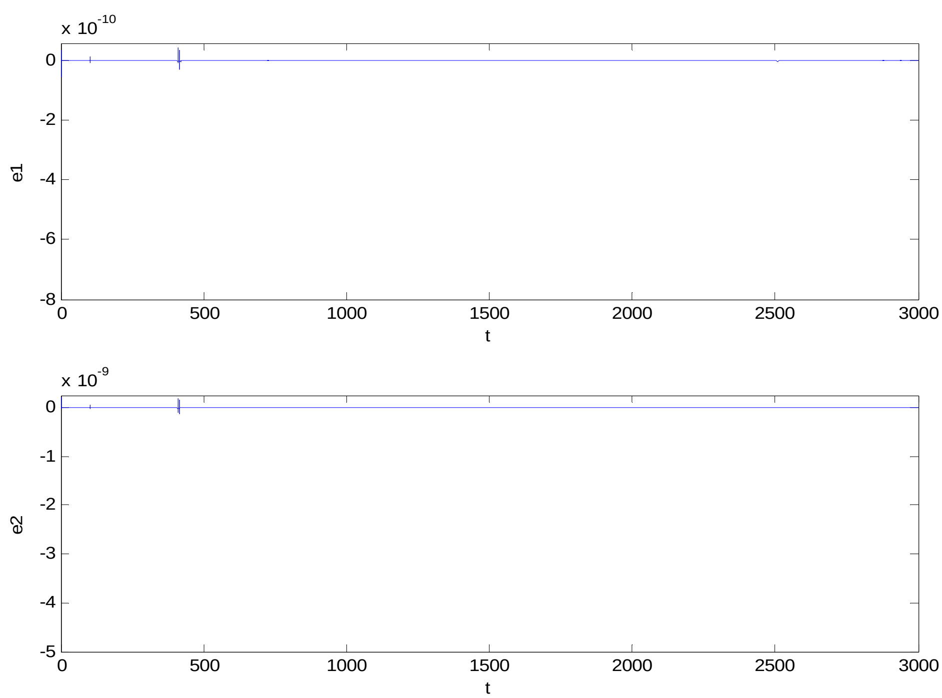

Fig. 4.52 Error dynamics for Case 6.

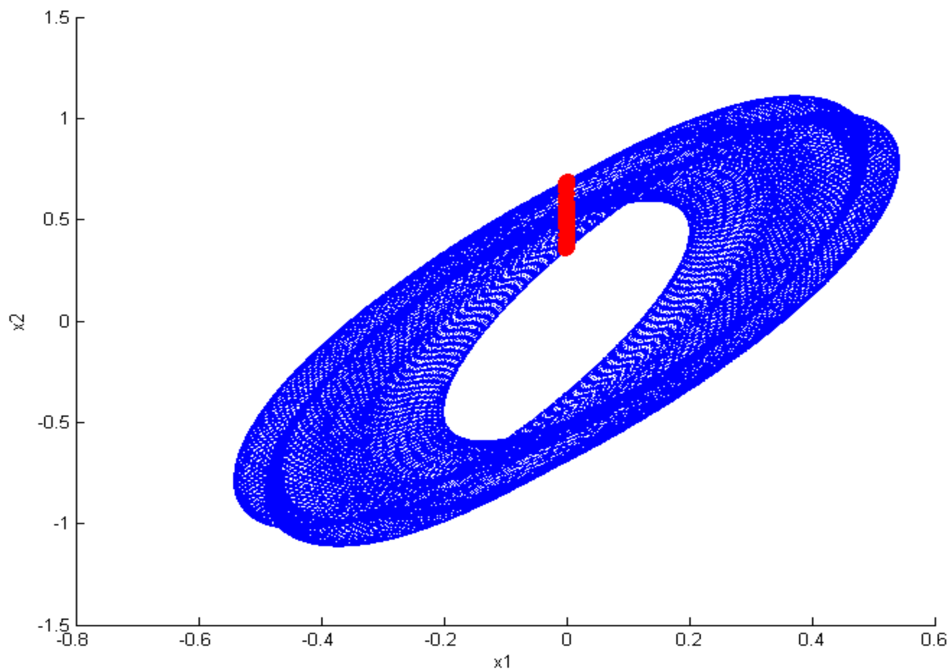

Fig. 4.53 The phase portrait for replacing *b* by *kcosxcosy* with $\alpha = \beta = 0.4$, a = 2, c = 65.

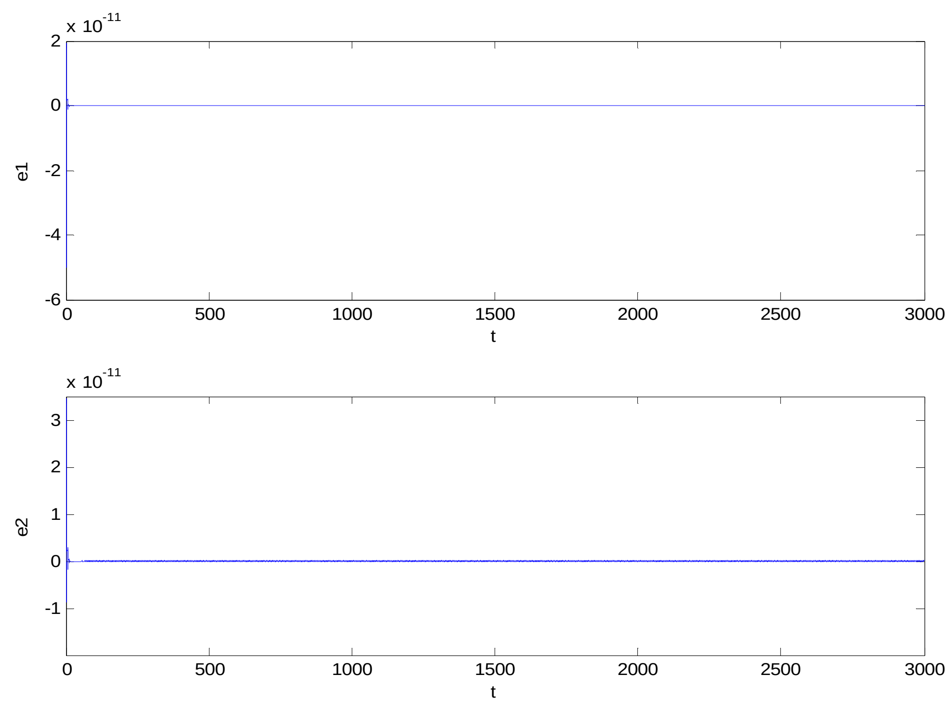

Fig. 4.54 Error dynamics for Case 7.

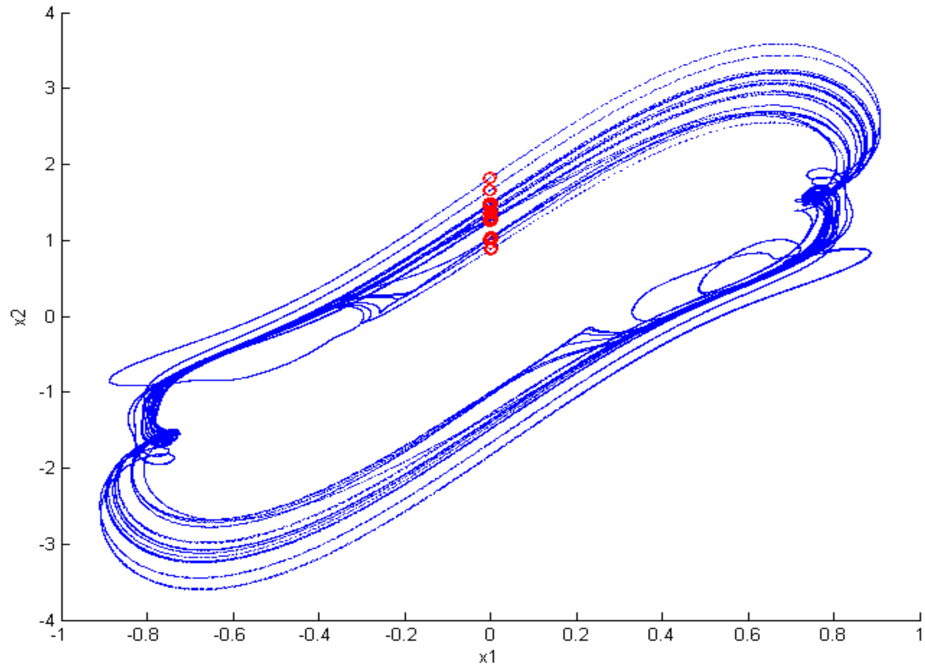

Fig. 4.55 The phase portrait for replacing *b* by *kcosxcosy* with $\alpha = \beta = 0.3$, *a* = 4, *c* = 35.

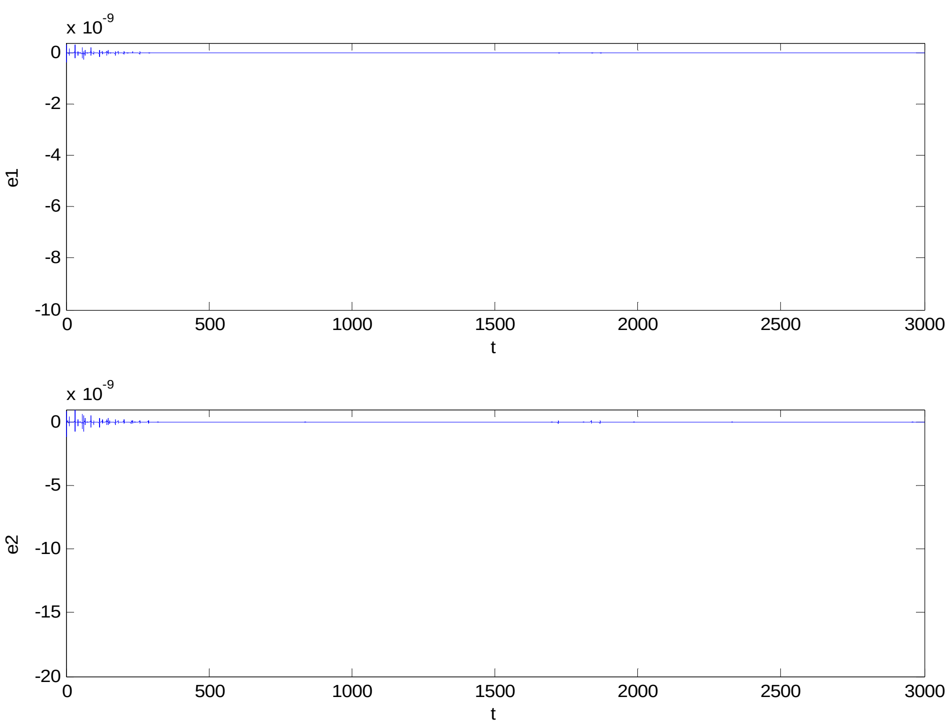

Fig. 4.56 Error dynamics for Case 8.

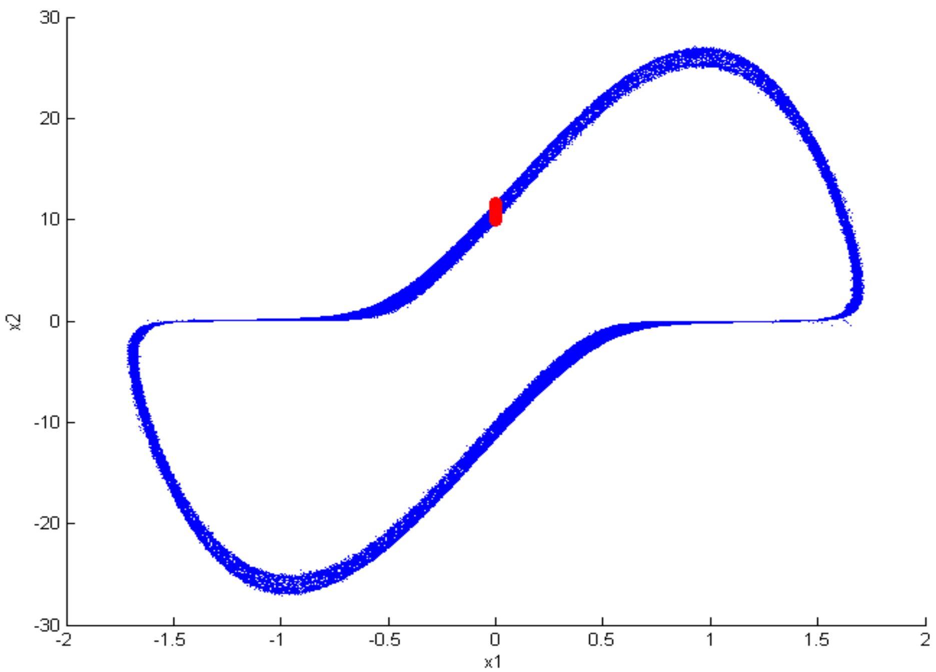

Fig. 4.57 The phase portrait for replacing *b* by *kcosxcosy* with $\alpha = \beta = 0.2$, $a = 2$, $c = 1$.

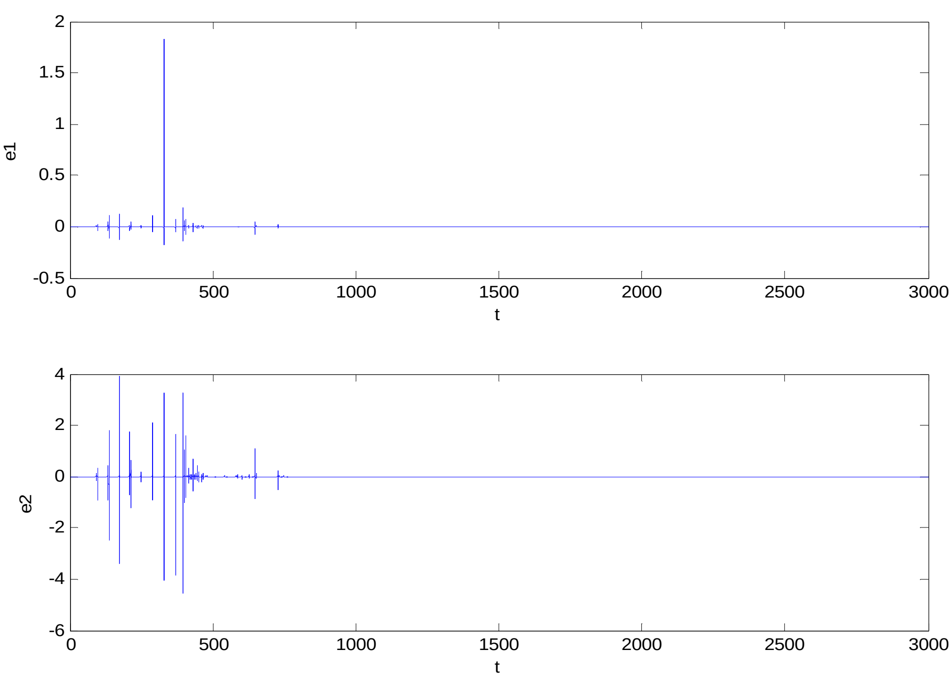

Fig. 4.58 Error dynamics for Case 9.

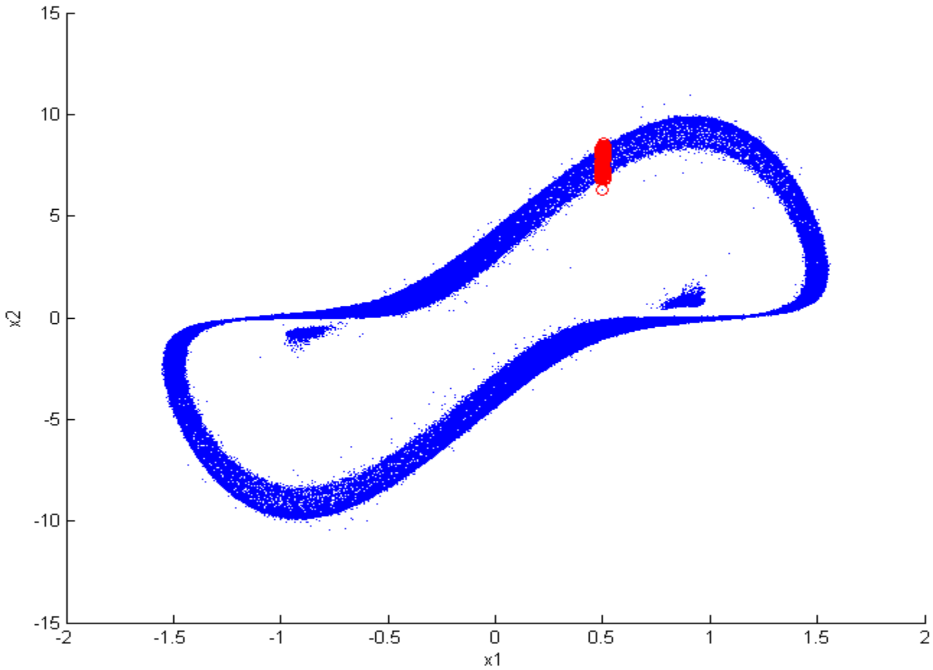

Fig. 4.59 The phase portrait for replacing b by $kcosxcosy$ with $\alpha = \beta = 0.1$, $a = 2$, $c = 10$.

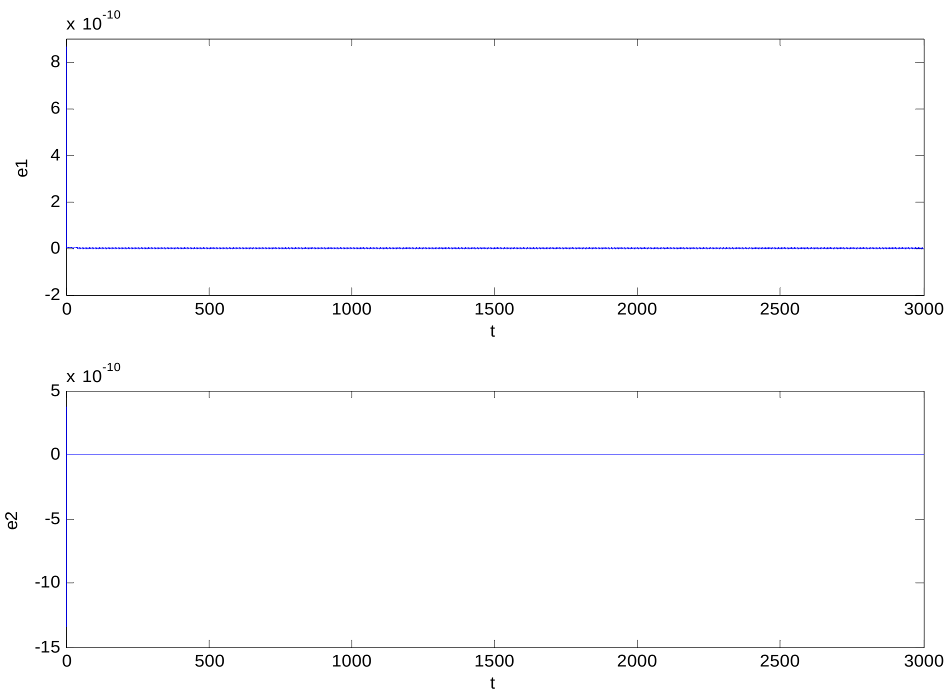

Fig. 4.60 Error dynamics for Case 10.

Chapter 5
Anticontrol of Chaos of the Fractional Order Modified Heartbeat Systems

Anticontrol of chaos of fractional order modified heartbeat systems is studied. Anticontrol of chaos is making a non-chaotic dynamical system chaotic, i.e., the regular behavior will be destroyed and replaced by chaotic behavior. Addition of a constant term and addition of $k|x|\sin x$ term where x is a state of the system are used to anticontrol the system effectively. By applying numerical results, phase portrait, Poincaré maps and bifurcation diagrams a variety of the phenomena of the chaotic motion can be presented.

5.1 Anticontrol of chaos by addition of a constant term

We add a constant term k in the second equation of system (2.6) and it become:

$$\begin{cases} \dfrac{d^{\alpha}x}{dt^{\alpha}} = y \\ \dfrac{d^{\beta}y}{dt^{\beta}} = -x + a(1-x^2)y + bz + k \\ \dot{z} = w \\ \dot{w} = -cz - dz^3 \end{cases} \tag{5.1}$$

In system (5.1), the parameter b is adjusted to achieve periodic motion for different α and β when k = 0. a, c, d are fixed and they are chosen as a= 5, c = 0.01, d = 0.001.

Case 1 Let $\alpha = \beta = 0.9$, b = 2.5, and $k \in [0.9, 1.2]$. Fig 5.1(a) shows the bifurcation diagram of the 1.8 order system. Fig 5.1(b) ~ 5.1(d) are the phase portraits with k = 0, 1.05, 1.1.

Case 2 Let $\alpha = \beta = 0.8$, b = 1.5, and $k \in [0.6, 1.2]$. Fig 5.2(a) shows the bifurcation diagram of the 1.6 order system. Fig 5.2(b) ~ 5.2(d) are the phase portraits with k = 0, 0.87, 1.05.

Case 3 Let $\alpha = \beta = 0.7$, b = 1.3, and $k \in [0.1, 1.6]$. Fig 5.3(a) shows the bifurcation diagram of the 1.4 order system. Fig 5.3(b) ~ 5.3(d) are the phase portraits with k = 0, 1.5, 1.6.

Case 4 Let $\alpha = \beta = 0.6$, b = 1, and $k \in [1.282, 1.312]$. Fig 5.4(a) shows the bifurcation diagram of the 1.2 order system. Fig 5.4(b) ~ 5.4(d) are the phase portraits with k = 0, 1.291, 1.298.

Case 5 Let $\alpha = \beta = 0.5$, b = 1, and $k \in [1.32, 1.42]$. Fig 5.5(a) shows the bifurcation diagram of the 1.0 order system. Fig 5.5(b) ~ 5.5(d) are the phase portraits with k = 0, 1.35, 1.38.

Case 6 Let $\alpha = \beta = 0.4$, b = 1.5, and $k \in [1.88, 1.94]$. Fig 5.6(a) shows the bifurcation diagram of the 0.8 order system. Fig 5.6(b) ~ 5.6(d) are the phase portraits with k = 0, 1.915, 1.93.

Case 7 Let $\alpha = \beta = 0.3$, b = 1.5, and $k \in [1.89, 1.98]$. Fig 5.7(a) shows the bifurcation diagram of the 0.6 order system. Fig 5.7(b) ~ 5.7(d) are the phase portraits with k = 0, 1.9, 1.94.

5.2 Anticontrol of chaos by addition of a nonlinear term

We add a non-linear term $k|x|sinx$ in the second equation of system (2.6) and it become:

$$\begin{cases} \dfrac{d^\alpha x}{dt^\alpha} = y \\ \dfrac{d^\beta y}{dt^\beta} = -x + a(1-x^2)y + bz + \mathrm{k}\,|\,\mathrm{x}\,|\,\mathrm{sinx} \\ \dot{z} = w \\ \dot{w} = -cz - dz^3 \end{cases} \tag{5.2}$$

In system (5.2), the parameter b is also adjusted to achieve periodic motion for different α and β when k = 0. a, c, d are fixed as 5.1.

Case 1 Let $\alpha = \beta = 0.9$, b = 2.5, and $k \in [0.2, 0.4]$. Fig 5.8(a) shows the bifurcation diagram of the 1.8 order system. Fig 5.8(b) ~ 5.8(d) are the phase portraits with k = 0, 0.35, 0.4.

Case 2 Let $\alpha = \beta = 0.8$, b = 2.5, and $k \in [1.0, 1.3]$. Fig 5.9(a) shows the bifurcation diagram of the 1.6 order system. Fig 5.9(b) ~ 5.9(d) are the phase portraits with k = 0, 1.03, 1.2.

Case 3 Let $\alpha = \beta = 0.7$, b = 0.5, and $k \in [1.19, 1.24]$. Fig 5.10(a) shows the bifurcation diagram of the 1.4 order system. Fig 5.10(b) ~ 5.10(d) are the phase portraits with k = 0, 1.205, 1.215.

Case 4 Let $\alpha = \beta = 0.6$, b = 1, and $k \in [0.8, 1.3]$. Fig 5.11(a) shows the bifurcation diagram of the 1.2 order system. Fig 5.11(b) ~ 5.11(d) are the phase portraits with k = 0, 0.95, 1.05.

Case 5 Let $\alpha = \beta = 0.5$, b = 0.5, and $k \in [0.1, 0.7]$. Fig 5.12(a) shows the bifurcation diagram of the 1.0 order system. Fig 5.12(b) ~ 5.12(d) are the phase portraits with k = 0, 0.4, 0.6.

Case 6 Let $\alpha = \beta = 0.4$, b = 1, and $k \in [1.16, 1.37]$. Fig 5.13(a) shows the bifurcation diagram of the 0.8 order system. Fig 5.13(b) ~ 5.13(d) are the phase portraits with k = 0, 1.25, 1.3.

Anticontrol of chaos in the fractional order systems of a modified van der Pol system are studied in the chapter. An efficient way to transform a non-chaotic dynamical system into a chaotic one is easily made by addition of a constant term or by addition of $k|x|\sin x$ term where x is a state variable of the system. It is found that chaos exists in the fractional order systems with order from 1.8 down to 0.6 for the addition of constant term, and from 1.8 down to 0.8 for the addition of $k|x|\sin x$ term.

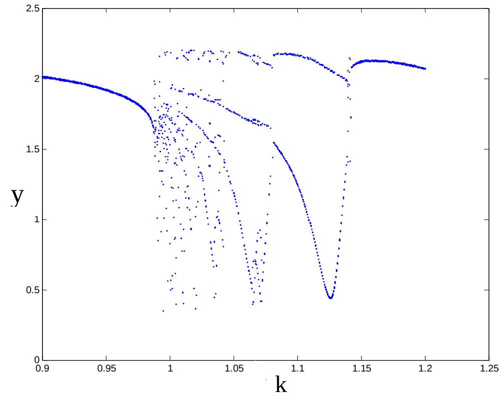

(a)

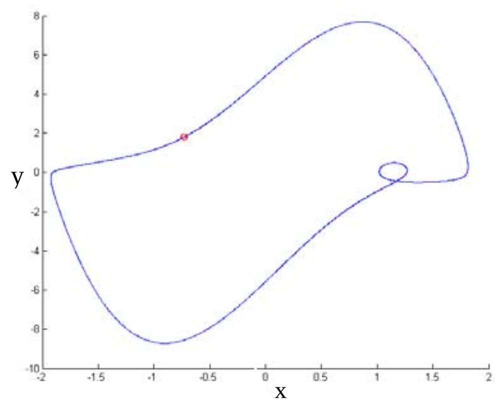

(b) $k = 0$

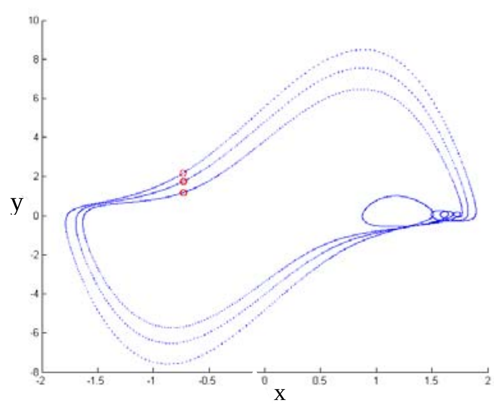

(c) $k = 1.05$

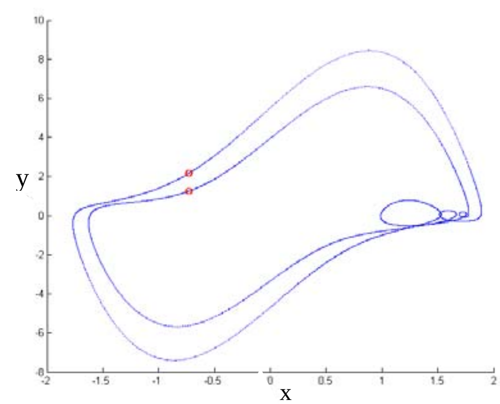

(d) $k = 1.1$

Fig 5.1 The bifurcation diagram for $\alpha = \beta = 0.9$ and phase portrait for $\alpha = \beta = 0.9$ with $k = 0$, $k = 1.05$, $k = 1.1$ respectively.

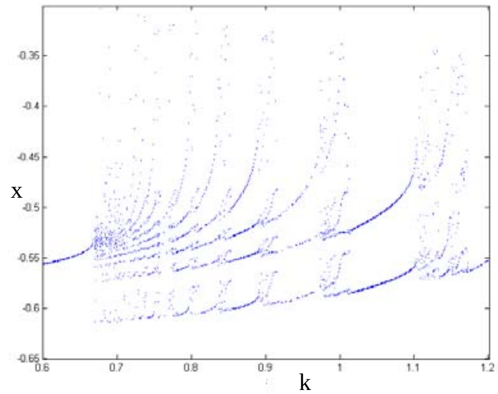

(a)

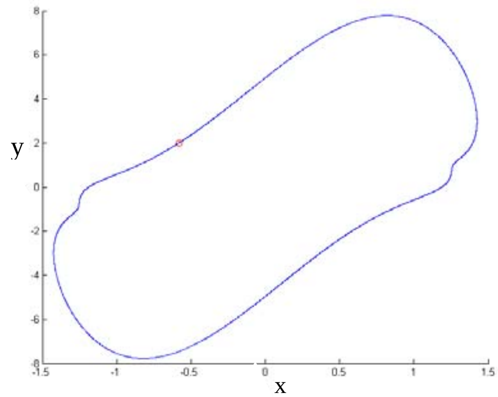

(b) k = 0

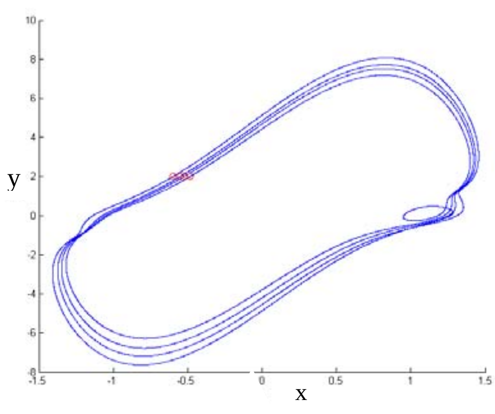

(c) k = 0.87

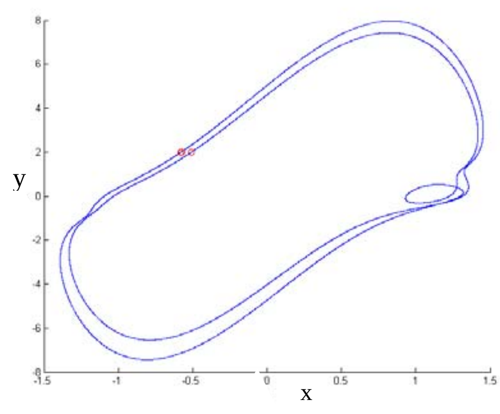

(d) k = 1.05

Fig 5.2 The bifurcation diagram for $\alpha = \beta = 0.8$ and phase portrait for $\alpha = \beta = 0.8$ with k = 0, 0.87, 1.05, respectively.

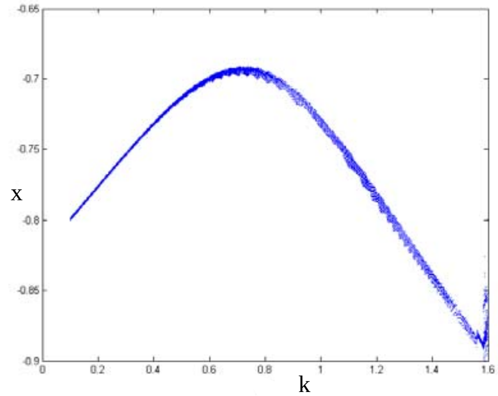

(a)

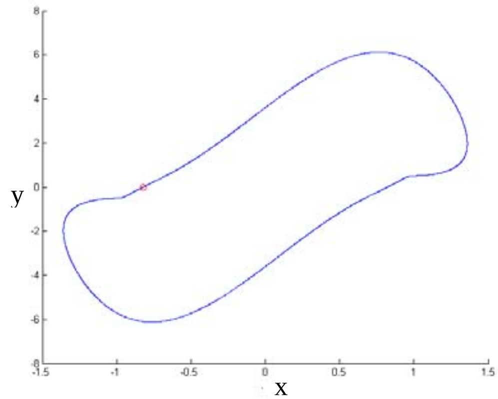

(b) $k = 0$

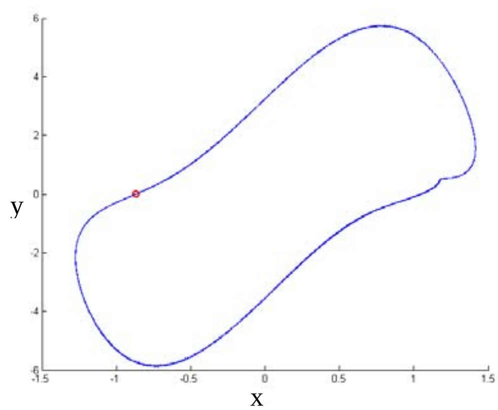

(c) $k = 1.5$

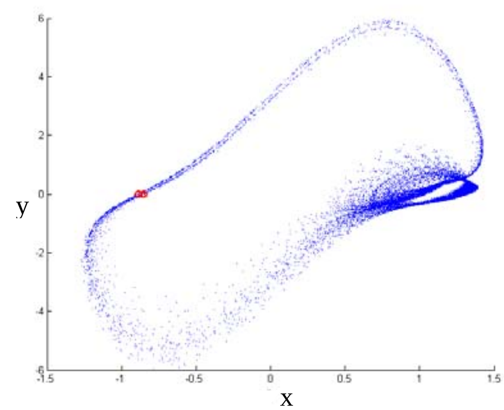

(d) $k = 1.6$

Fig 5.3 The bifurcation diagram for $\alpha = \beta = 0.7$ and phase portrait for $\alpha = \beta = 0.7$ with $k = 0$, 1.5, 1.6, respectively.

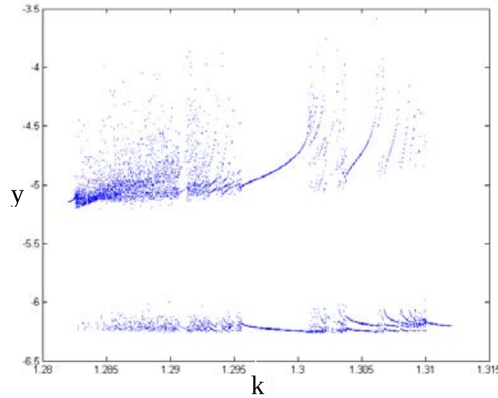

(a)

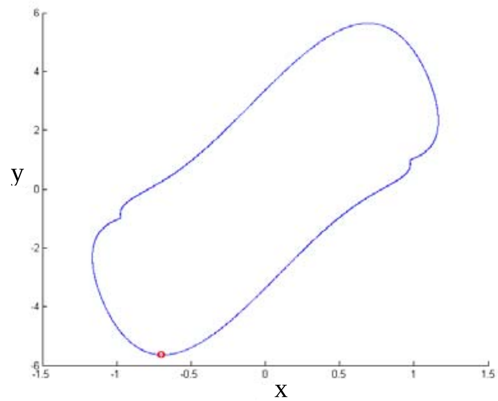

(b) $k = 0$

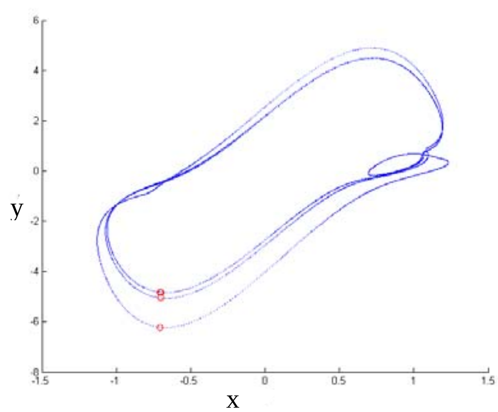

(c) $k = 1.291$

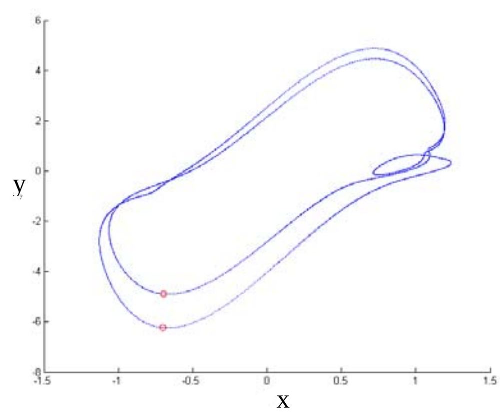

(d) $k = 1.298$

Fig 5.4 The bifurcation diagram for $\alpha = \beta = 0.6$ and phase portrait for $\alpha = \beta = 0.6$ with $k = 0$, 1.291, 1.298, respectively.

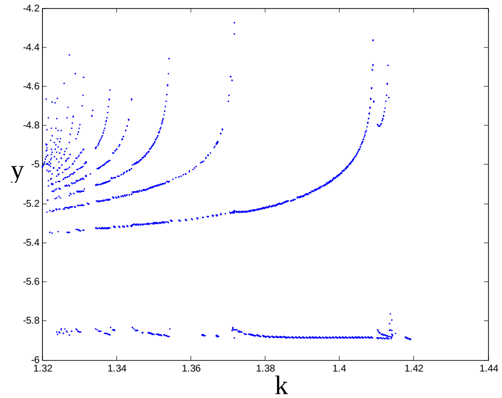

(a)

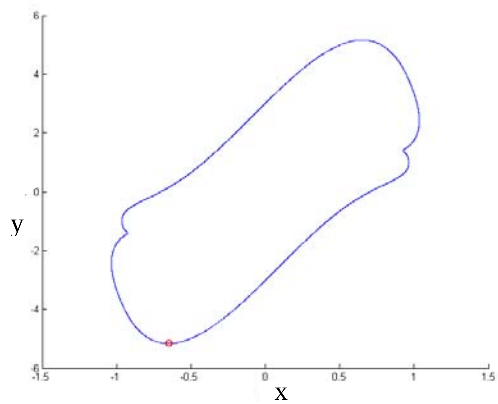

(b) $k = 0$

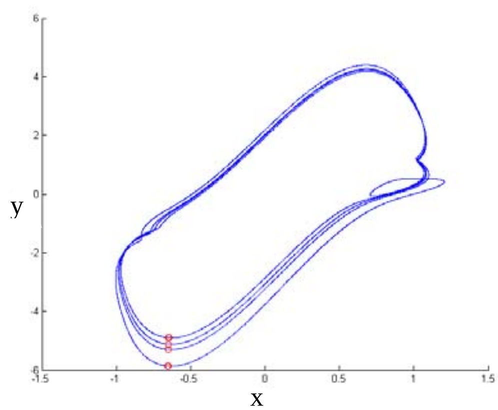

(c) $k = 1.35$

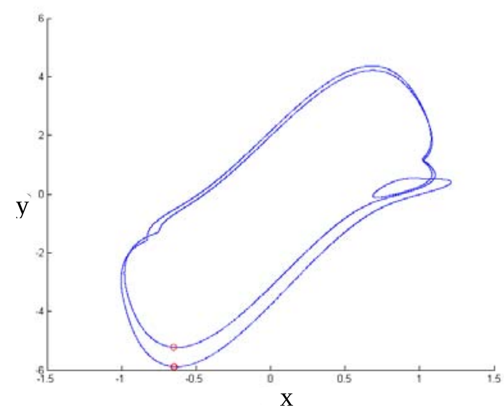

(d) $k = 1.38$

Fig 5.5 The bifurcation diagram for $\alpha = \beta = 0.5$ and phase portrait for $\alpha = \beta = 0.5$ with $k = 0$, 1.35, 1.38, respectively.

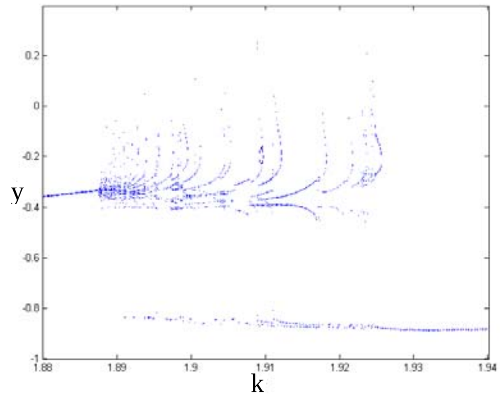

(a)

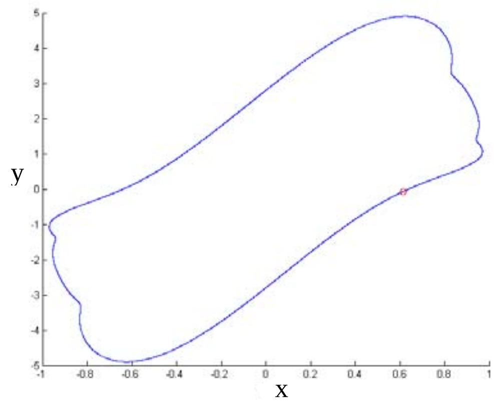

(b) $k = 0$

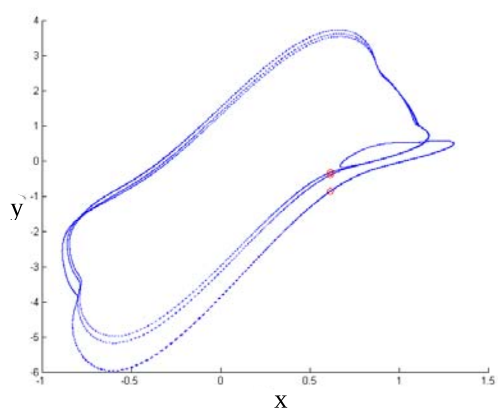

(c) $k = 1.915$

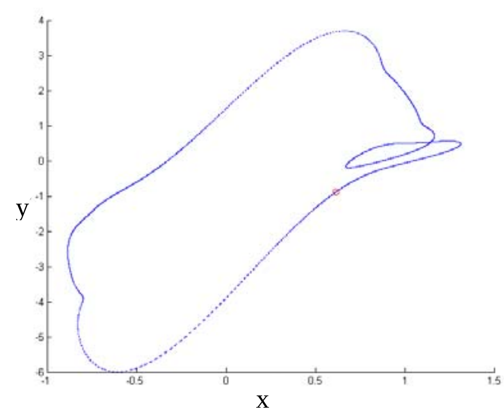

(d) $k = 1.93$

Fig 5.6 The bifurcation diagram for $\alpha = \beta = 0.4$ and phase portrait for $\alpha = \beta = 0.4$ with $k = 0$, 1.915, 1.93, respectively.

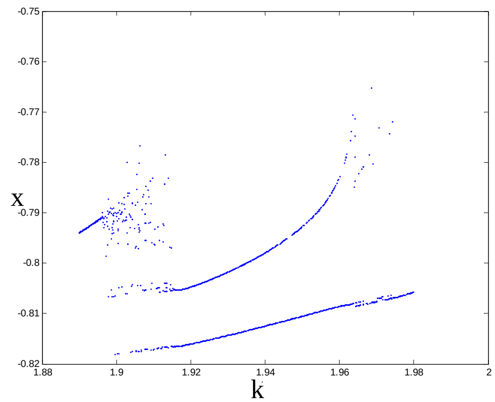

(a)

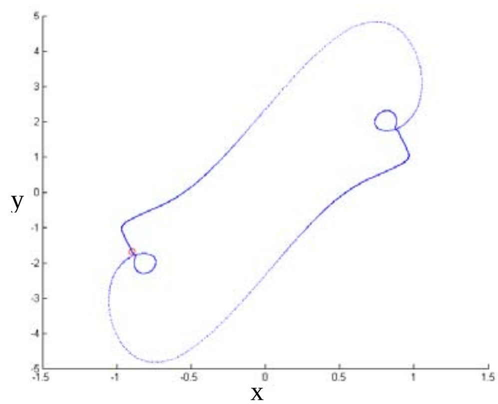

(b) $k = 0$

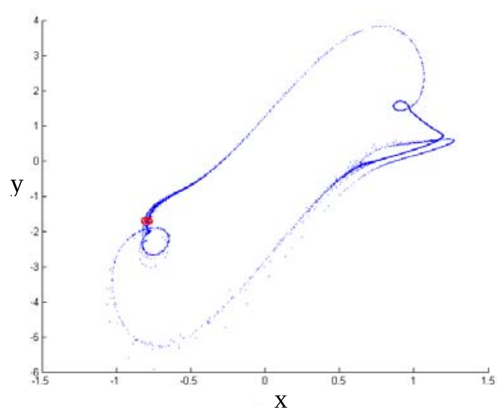

(c) $k = 1.9$

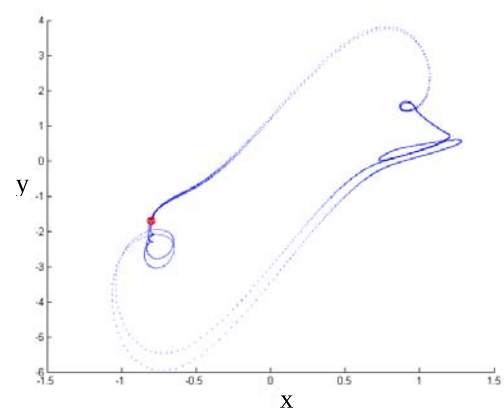

(d) $k = 1.94$

Fig 5.7 The bifurcation diagram for $\alpha = \beta = 0.3$ and phase portrait for $\alpha = \beta = 0.3$ with $k = 0$, 1.9, 1.94, respectively.

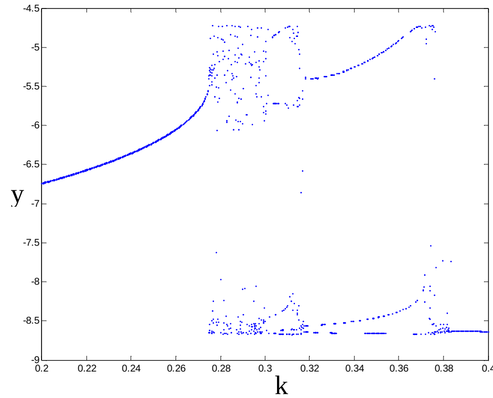

(a)

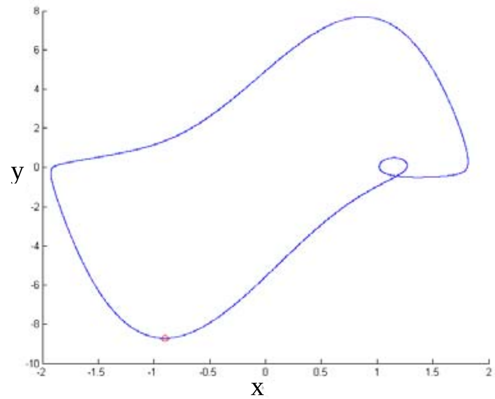

(b) $k = 0$

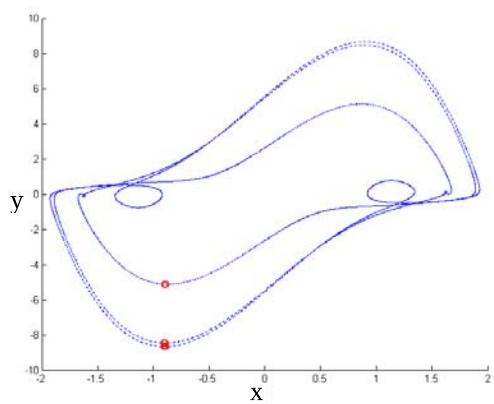

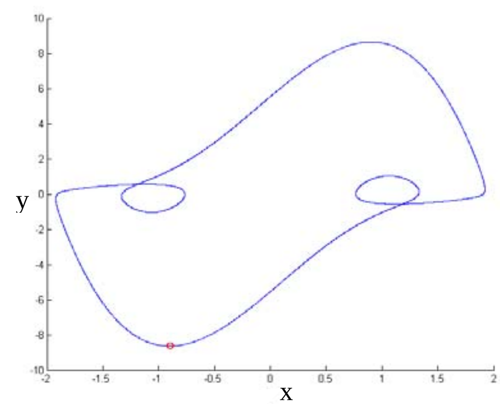

(c) $k = 0.35$

(d) $k = 0.4$

Fig 5.8 The bifurcation diagram for $\alpha = \beta = 0.9$ and phase portrait for $\alpha = \beta = 0.9$ with $k = 0$, 0.35, 0.4, respectively.

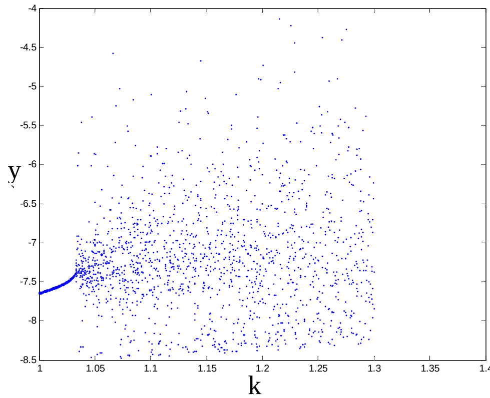

(a)

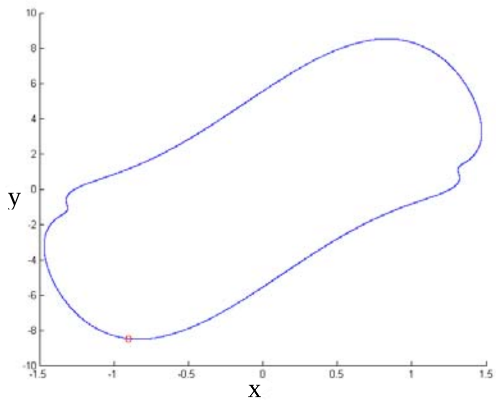

(b) $k = 0$

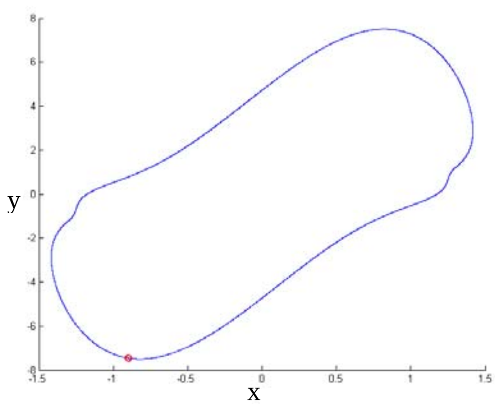

(c) $k = 1.03$

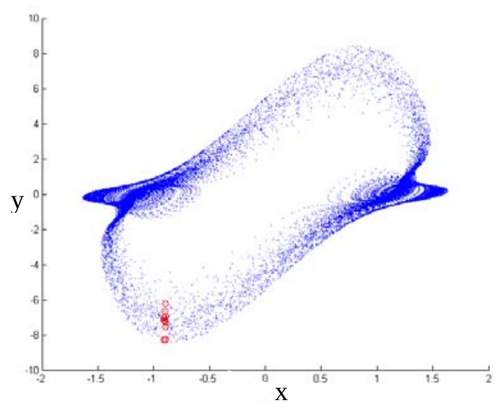

(d) $k = 1.2$

Fig 5.9 The bifurcation diagram for $\alpha = \beta = 0.8$ and phase portrait for $\alpha = \beta = 0.8$ with $k = 0$, 1.03, 1.2, respectively.

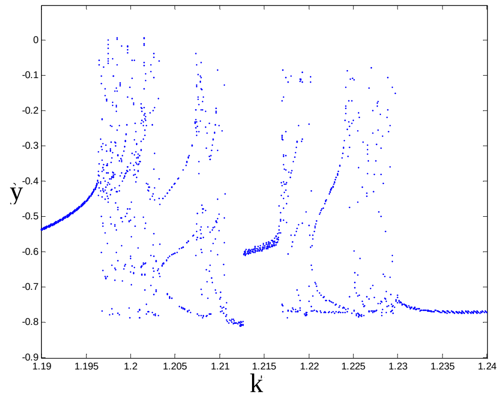

(a)

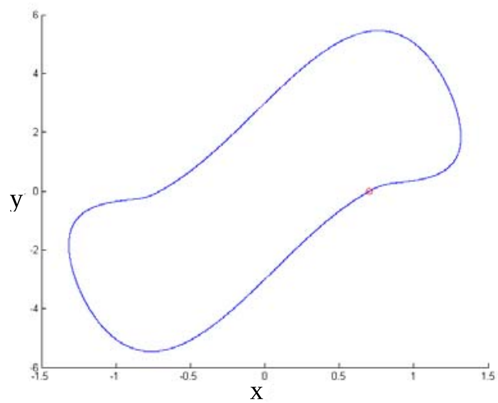

(b) $k = 0$

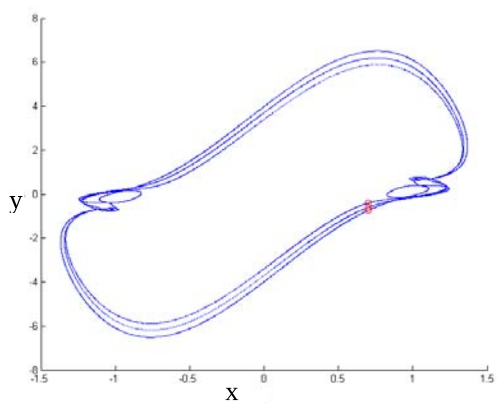

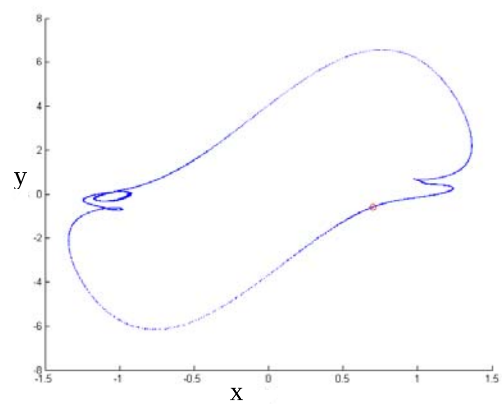

(c) $k = 1.205$ (d) $k = 1.215$

Fig 5.10 The bifurcation diagram for $\alpha = \beta = 0.7$ and The phase portrait for $\alpha = \beta = 0.7$ with k = 0, 1.205, 1.215, respectively.

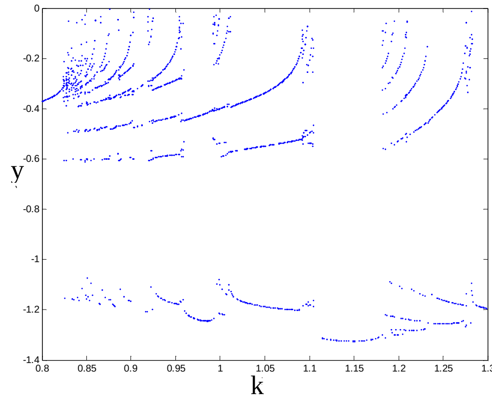

(a)

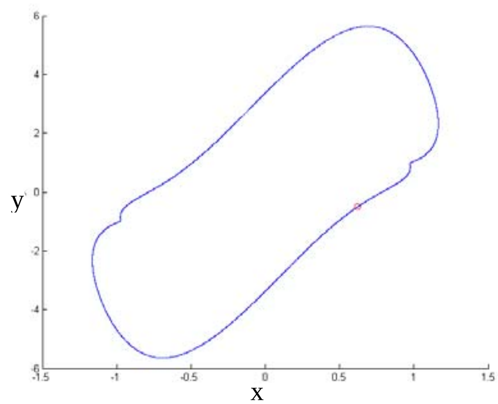

(b) $k = 0$

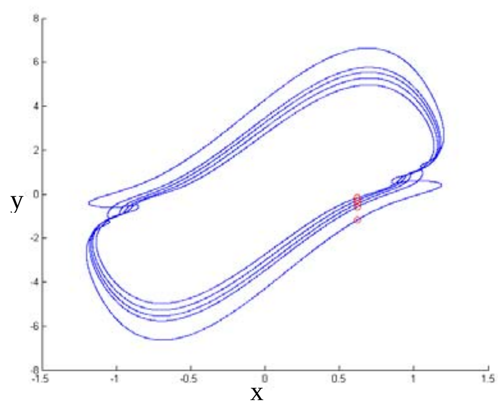

(c) $k = 0.95$

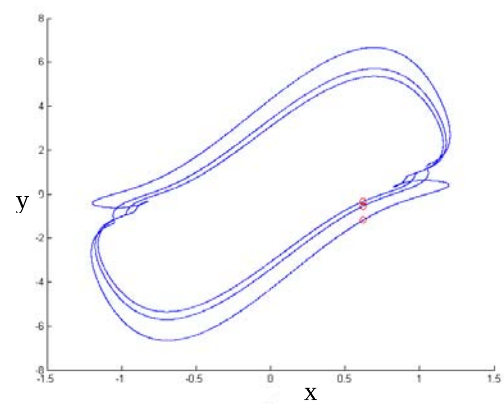

(d) $k = 1.05$

Fig 5.11 The bifurcation diagram for $\alpha = \beta = 0.6$ and phase portrait for $\alpha = \beta = 0.6$ with $k = 0$, 0.95, 1.05, respectively.

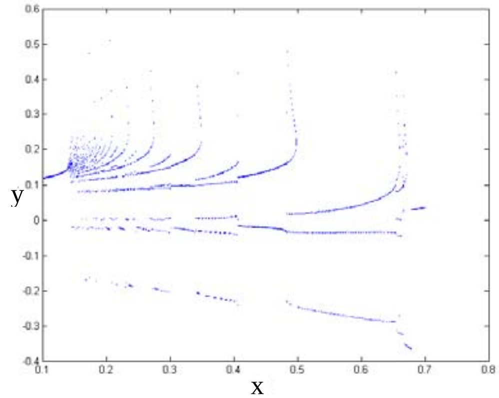

(a)

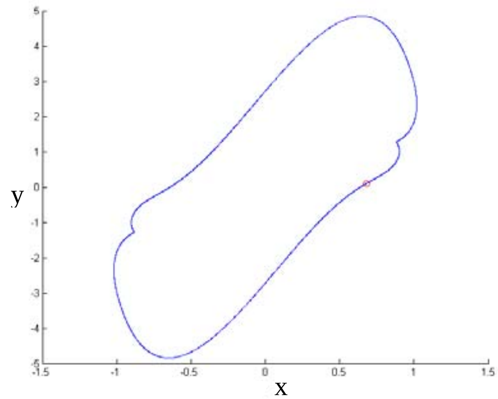

(b) $k = 0$

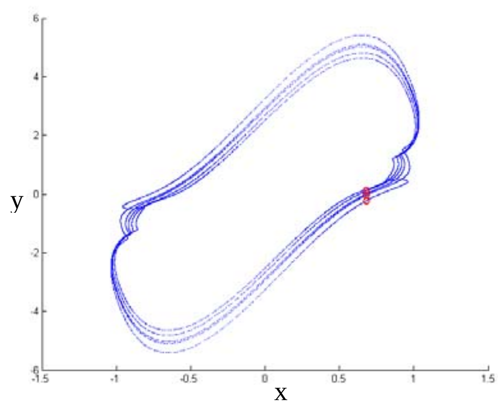

(c) $k = 0.4$

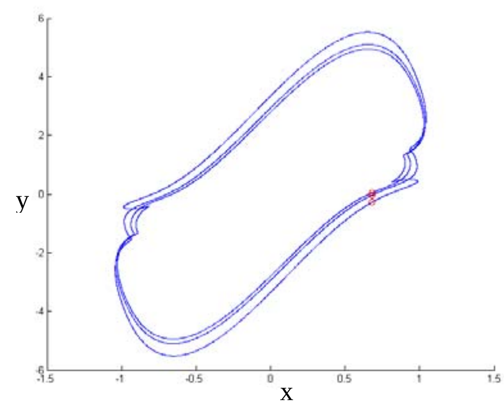

(d) $k = 0.6$

Fig 5.12 The bifurcation diagram for $\alpha = \beta = 0.5$ and phase portrait for $\alpha = \beta = 0.5$ with k = 0, 0.4, 0.6, respectively.

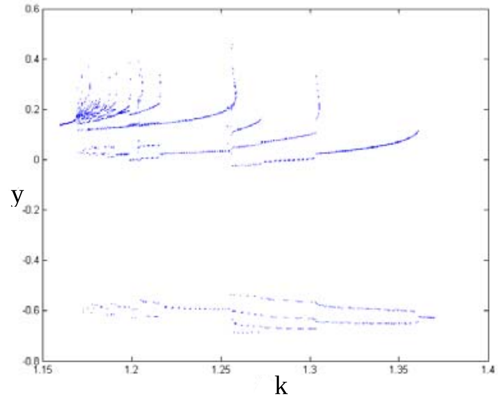

(a)

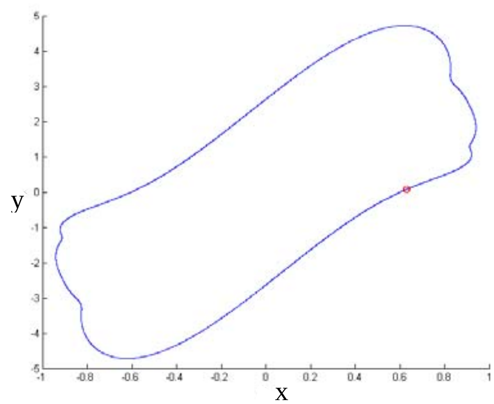

(b) k = 0

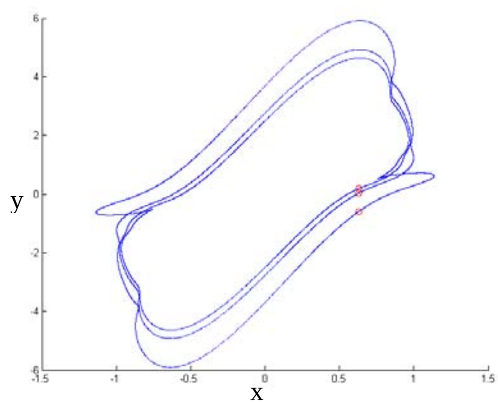

(c) k = 1.25

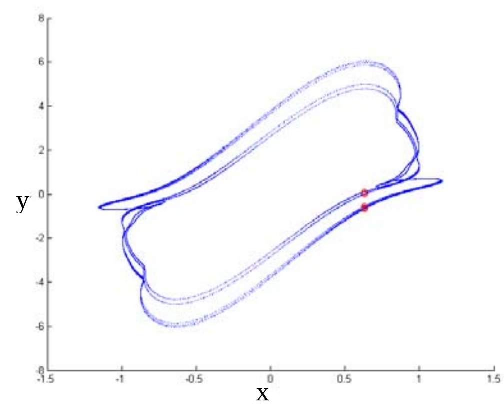

(d) k = 1.3

Fig 5.13 The bifurcation diagram for $\alpha = \beta = 0.4$ and phase portrait for $\alpha = \beta = 0.4$ with k = 0, 1.25, 1.3, respectively.

Chapter 6

Parameter Excited Chaotization of Integral and Fractional Order Modified Heartbeat Systems

Chaotization of integral and fractional order modified heartbeat systems by replacing the parameter of modified heartbeat system by the function of the chaotic state variables of a second chaotic nano resonator system is studied. It is named parameter excited chaotization which can be successfully obtained for very low total fractional order 0.2. By phase portraits, Poincaré maps and bifurcation diagrams, the simulation results of fractional order modified van der Pol systems are presented.

6.1 A nano resonator system and the chaotization scheme

Chaotization, i.e. anticontrol of chaos, is making a non-chaotic dynamical system chaotic. This means that the regular behavior will be destroyed and replaced by chaotic behavior.

Nano resonator system is a modified form of nonlinear damped Mathieu system which is obtained when the nano Mathieu oscillator has nonlinear time-dependent spring constant. The nonlinear damped Mathieu system is a nonautonomous system with two states *x* and *y*:

$$\begin{cases} \dfrac{dx}{dt} = y \\ \dfrac{dy}{dt} = -(e + f\sin\omega_1 t)x - (e + f\sin\omega_1 t)x^3 - gy + h\sin\omega_2 t \end{cases} \tag{6.1}$$

where *a*, *b*, *c*, *d* are constant parameters, and ω_1, ω_2 are circular frequencies. Let $\omega_1 = \omega_2 = \omega$, and replace $sin\,\omega t$ by *z* which is the periodic time function solution of the nonlinear oscillator

$$\begin{cases} \dfrac{dz}{dt} = w \\ \dfrac{dw}{dt} = -iz - jz^3 \end{cases} \tag{6.2}$$

where *i*, *j* are constants. Then we have the modified nonlinear damped Mathieu system, i.e. the nano resonator system:

$$\begin{cases} \dfrac{dx}{dt} = y \\ \dfrac{dy}{dt} = -(e+fz)x - (e+fz)x^3 - gy + hz \\ \dfrac{dz}{dt} = w \\ \dfrac{dw}{dt} = -iz - jz^3 \end{cases} \tag{6.3}$$

It becomes an autonomous system with four states where *e*, *f*, *g*, *h*, *i* and *j* are constants of the system. In our numerical simulations, six parameters $e = 0.2$, $f = 0.2$, $g = 0.4$, $h = 50$, $i = 1$ and $j = 0.3$ are chosen to make the states *x* and *y* of system (6.3) be a chaotic [74].

Next, let the parameter *b* of system (2.6) be replaced by *ksiny* where *k* is a constant and *y* is a chaotic state variable of system (6.3). We study the parameter excited chaotization of system (2.6) for various α, β.

6.2 Chaotization by parameter excited method

The parameter k is adjusted to achieve chaos for different α and β. $a = 5$, $c = 4$, $i = 0.0001$ are fixed and $k \in [0,5]$.

6.2.1 Chaotization of a integral order modified heartbeat system

Let $\alpha = \beta = 1$. Fig 6.1(a) shows the bifurcation diagram of the 2 order system. Fig 6.1(b) is the nonchaotic phase portrait of the system (2.6) with $b = 2.5$. Fig 6.1(c) shows chaotic phase portrait when $k = 4$.

6.2.2 Chaotization of a fraction order modified van der Pol system

Case 1 Let $\alpha = \beta = 0.9$. Fig 6.2(a) shows the bifurcation diagram of the 1.8 order system. Fig 6.2(b) is the nonchaotic phase portrait of the system (2.6) with $b = 2.5$. Fig 6.2(c) shows chaotic phase portrait when $k = 4$.

Case 2 Let $\alpha = \beta = 0.8$. Fig 6.3(a) shows the bifurcation diagram of the 1.6 order system. Fig 6.3(b) is the nonchaotic phase portrait of the system (2.6) with $b = 1.5$. Fig 6.3(c) shows chaotic phase portrait when $k = 3$.

Case 3 Let $\alpha = \beta = 0.7$. Fig 6.4(a) shows the bifurcation diagram of the 1.4 order system. Fig 6.4(b) is the nonchaotic phase portrait of the system (2.6) with $b = 1.3$. Fig 6.4(c) shows chaotic phase portrait when $k = 3.5$.

Case 4 Let $\alpha = \beta = 0.6$. Fig 6.5(a) shows the bifurcation diagram of the 1.2 order system. Fig 6.5(b) is the nonchaotic phase portrait of the system (2.6) with $b = 1$. Fig 6.5(c) shows chaotic phase portrait when $k = 3.5$.

Case 5 Let $\alpha = \beta = 0.5$. Fig 6.6(a) shows the bifurcation diagram of the 1.0 order system. Fig 6.6(b) is the nonchaotic phase portrait of the system (2.6) with $b = 1$. Fig 6.6(c) shows chaotic phase portrait when $k = 3$.

Case 6 Let $\alpha = \beta = 0.4$. Fig 6.7(a) shows the bifurcation diagram of the 0.8 order system. Fig 6.7(b) is the nonchaotic phase portrait of the system (2.6) with $b = 1.5$. Fig 6.7(c) shows chaotic phase portrait when $k = 2.5$.

Case 7 Let $\alpha = \beta = 0.3$. Fig 6.8(a) shows the bifurcation diagram of the 0.6

order system. Fig 6.8(b) is the nonchaotic phase portrait of the system (2.6) with $b = 1.5$. Fig 6.8(c) shows chaotic phase portrait when $k = 3.5$.

Case 8 Let $\alpha = \beta = 0.2$. Fig 6.9(a) shows the bifurcation diagram of the 0.4 order system. Fig 6.9(b) is the nonchaotic phase portrait of the system (2.6) with $b = 5$. Fig 6.9(c) shows chaotic phase portrait when $k = 1$.

Case 9 Let $\alpha = \beta = 0.1$. Fig 6.10(a) shows the bifurcation diagram of the 0.2 order system. Fig 6.10(b) is the nonchaotic phase portrait of the system (2.6) with $b = 8$. Fig 6.10(c) shows chaotic phase portrait when $k = 0.5$.

Chaotizations in the integral and fractional order systems of a modified van der Pol systems are studied in the chapter. An efficient way to transform a non-chaotic dynamics of the system into a chaotic one is easily made by replacing a parameter of the system by *ksiny* where *k* is a adjustable constant and *y* is a chaotic state variable of a second system, a modified nano resonator system. It is found that chaos exists in the integral and fractional order systems with total order from 2 down to 0.2.

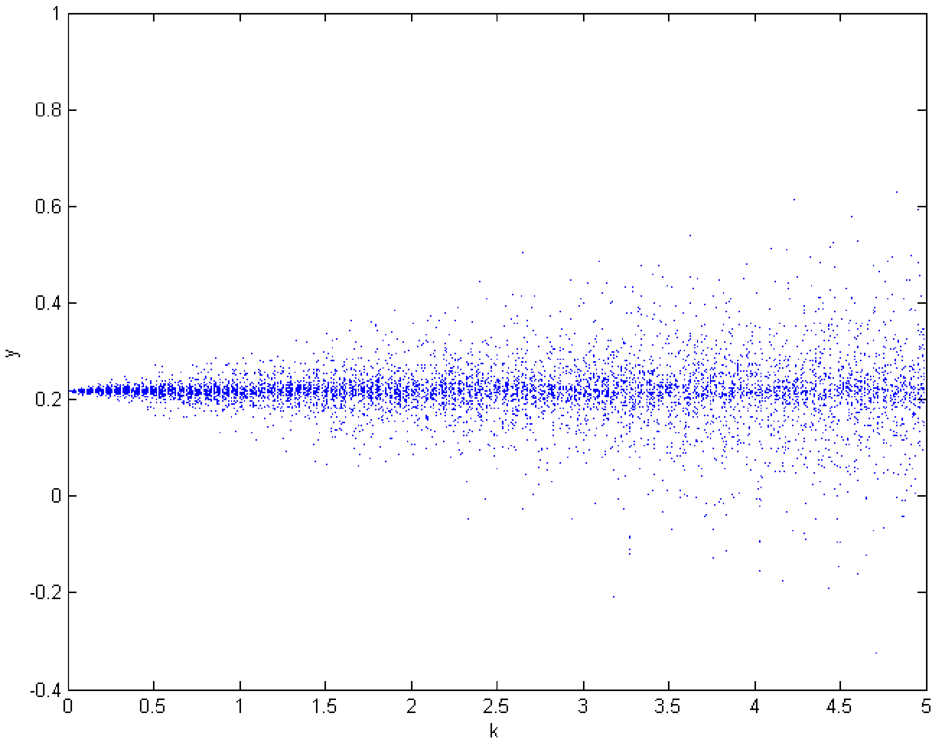

(a)

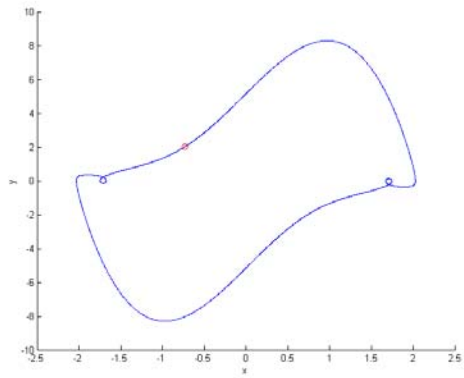

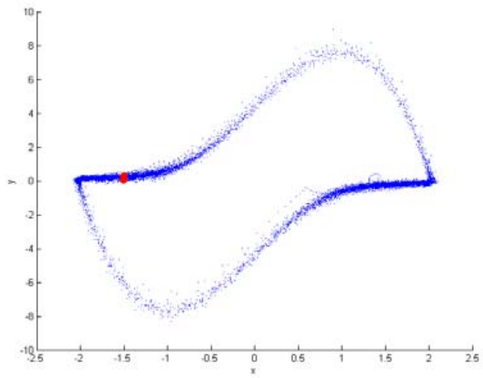

(b) (c)

Fig 6.1(a) The bifurcation diagram for $\alpha = \beta = 1$. (b) The phase portrait for $\alpha = \beta = 1$, $b = 2.5$. (c) The phase portrait for $\alpha = \beta = 1$, $k = 4$.

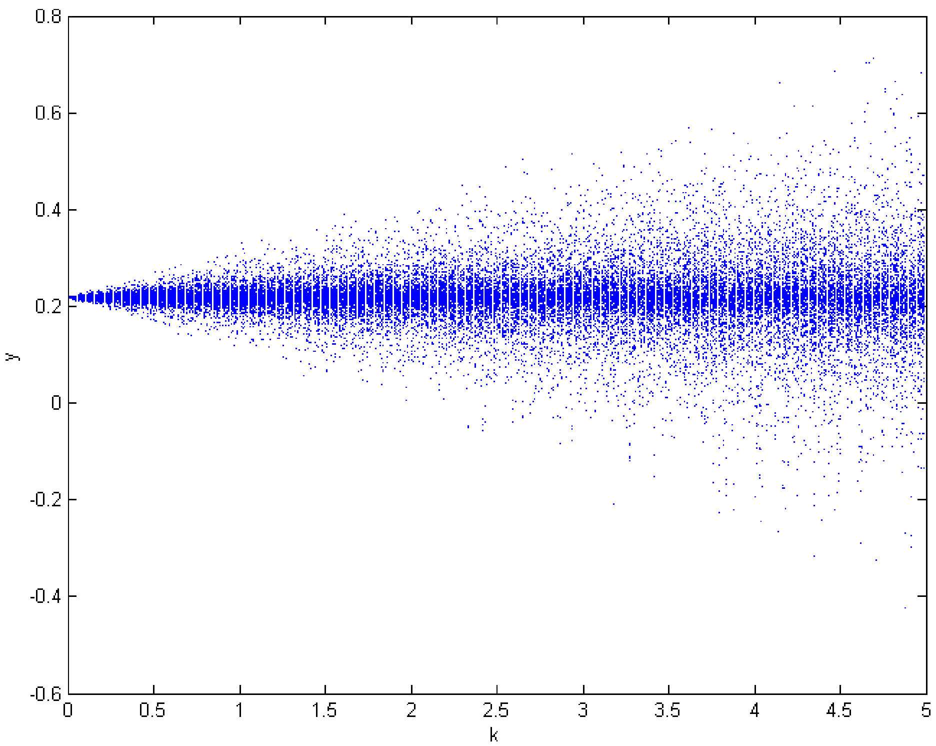

(a)

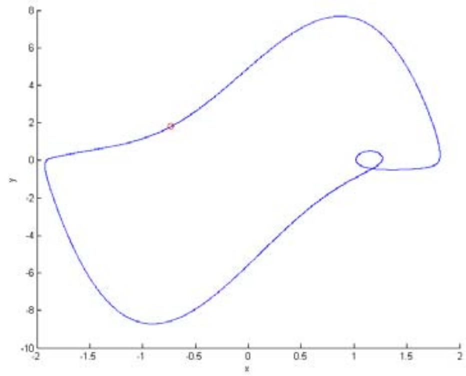

(b)

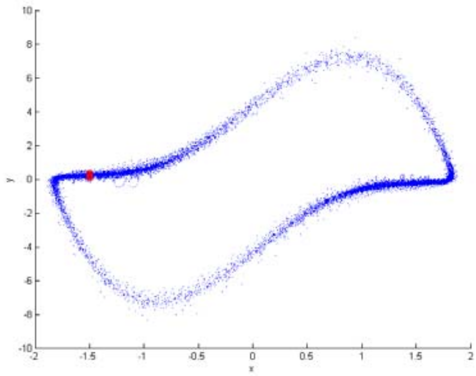

(c)

Fig 6.2(a) The bifurcation diagram for $\alpha = \beta = 0.9$. (b) The phase portrait for $\alpha = \beta = 0.9$, b = 2.5. (c) The phase portrait for $\alpha = \beta = 0.9$, k = 4.

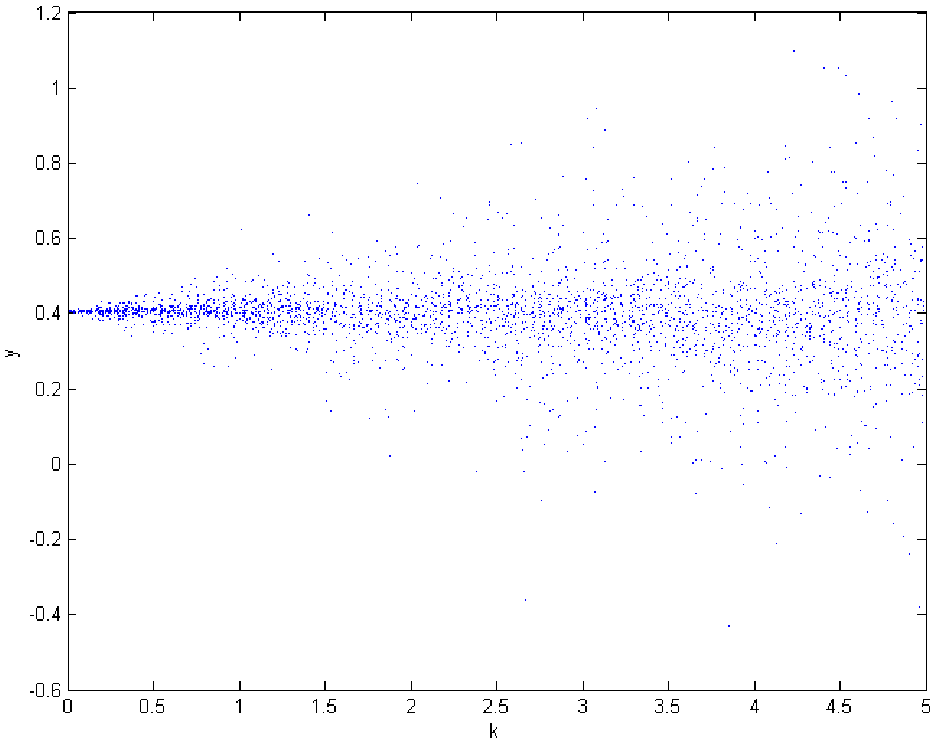

(a)

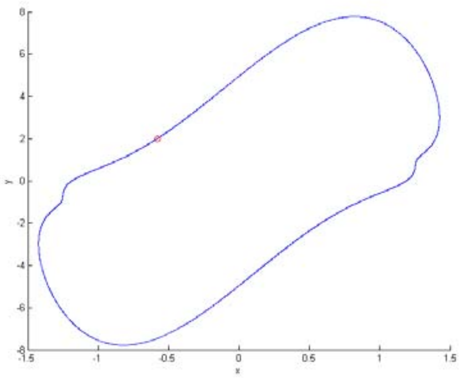

(b)

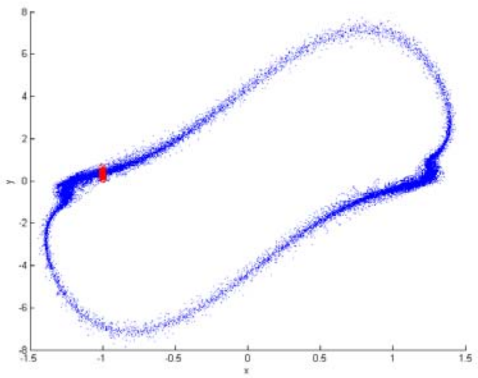

(c)

Fig 6.3(a) The bifurcation diagram for $\alpha = \beta = 0.8$. (b) The phase portrait for $\alpha = \beta = 0.8$, $b = 1.5$. (c) The phase portrait for $\alpha = \beta = 0.8$, $k = 3$.

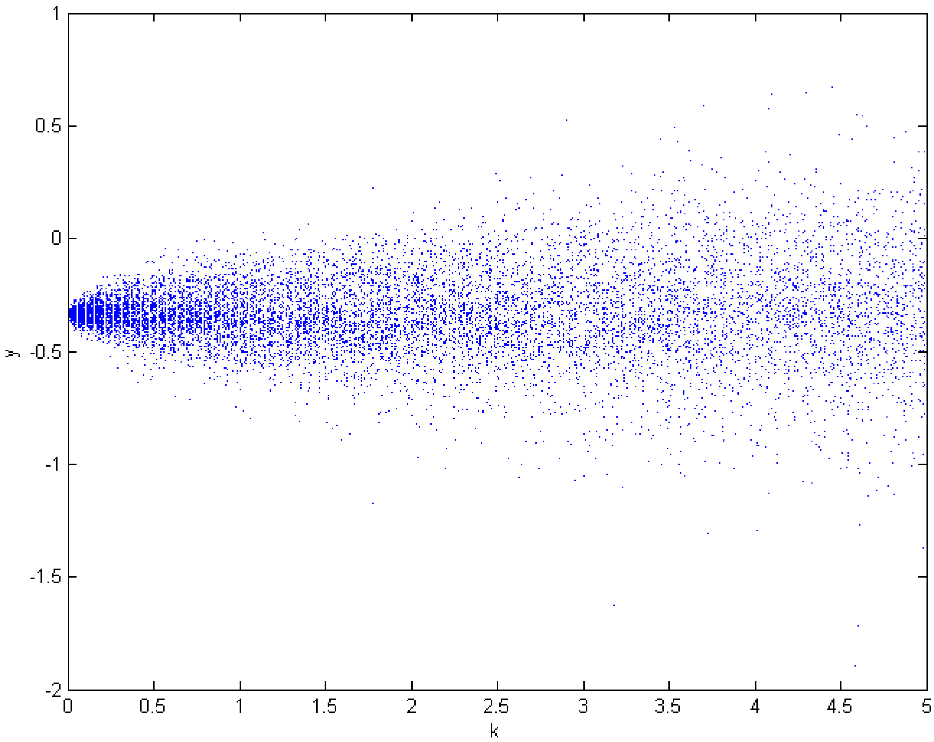

(a)

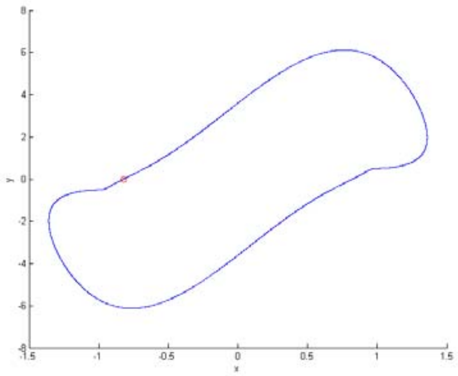

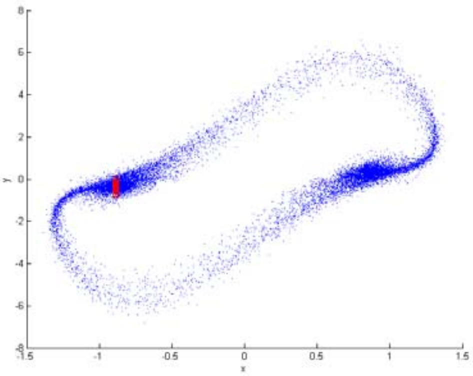

(b) (c)

Fig 6.4(a) The bifurcation diagram for $\alpha = \beta = 0.7$. (b) The phase portrait for $\alpha = \beta = 0.7$, b = 1.3. (c) The phase portrait for $\alpha = \beta = 0.7$, k = 3.5.

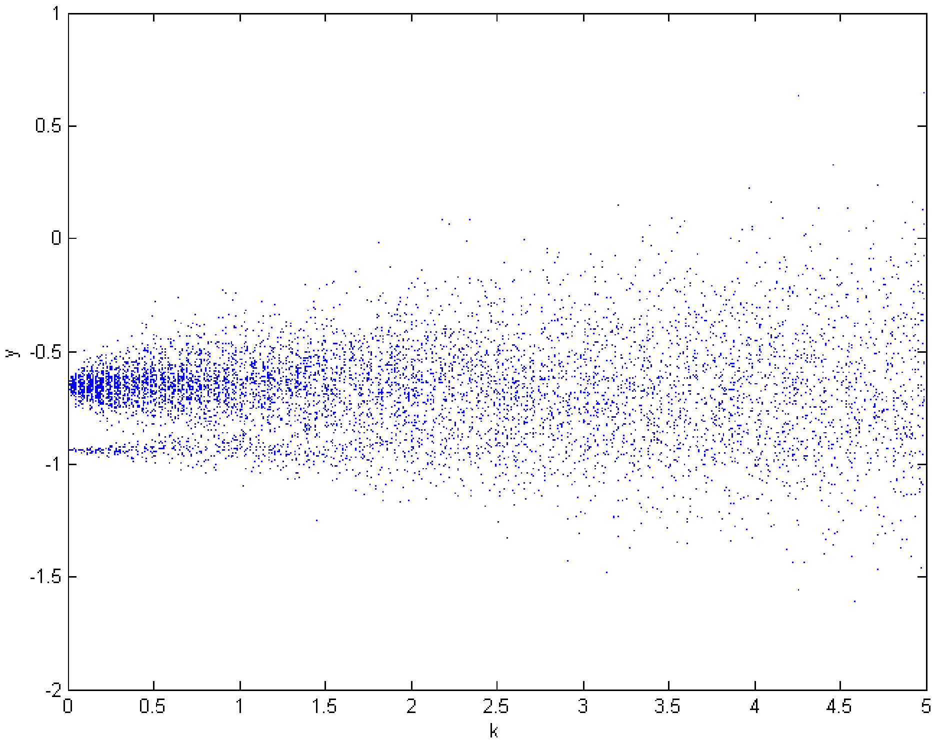

(a)

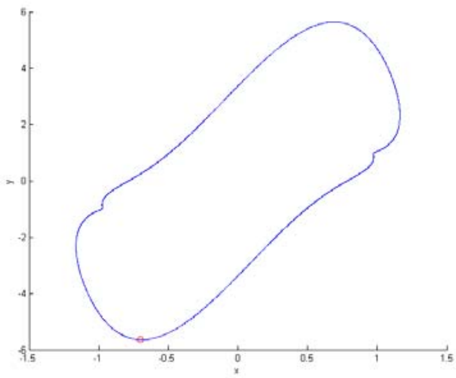

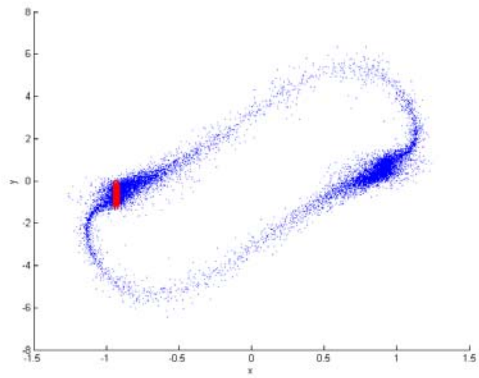

(b) (c)

Fig 6.5(a) The bifurcation diagram for $\alpha = \beta = 0.6$. (b) The phase portrait for $\alpha = \beta = 0.6$, $b = 1$. (c) The phase portrait for $\alpha = \beta = 0.6$, $k = 3.5$.

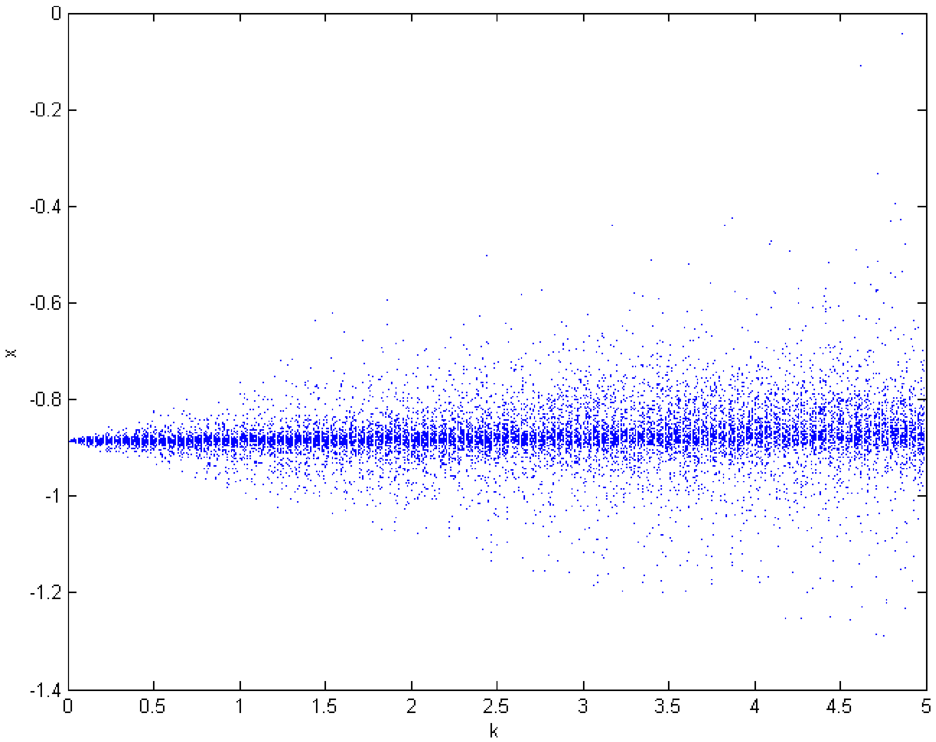

(a)

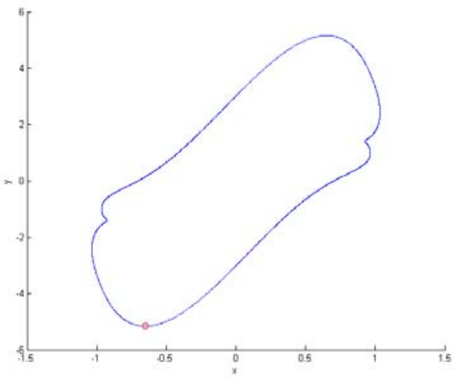

(b)

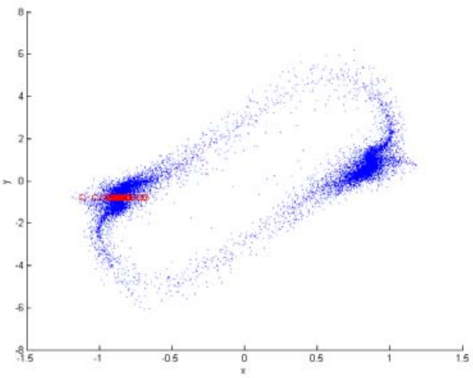

(c)

Fig 6.6(a) The bifurcation diagram for $\alpha = \beta = 0.5$. (b) The phase portrait for $\alpha = \beta = 0.5$, b = 1. (c) The phase portrait for $\alpha = \beta = 0.5$, k = 3.

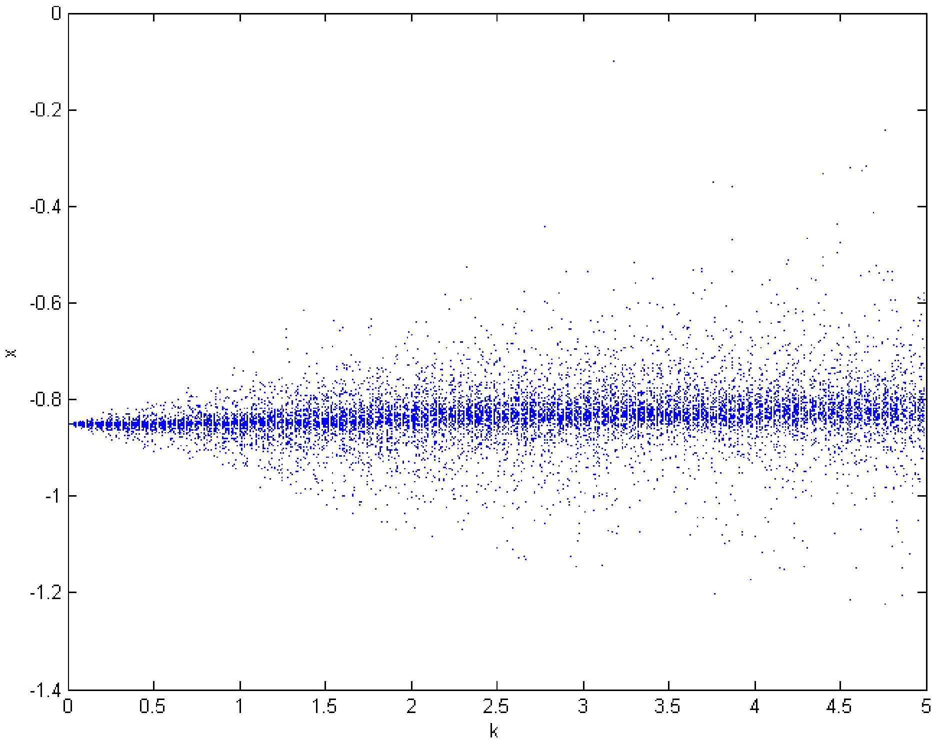

(a)

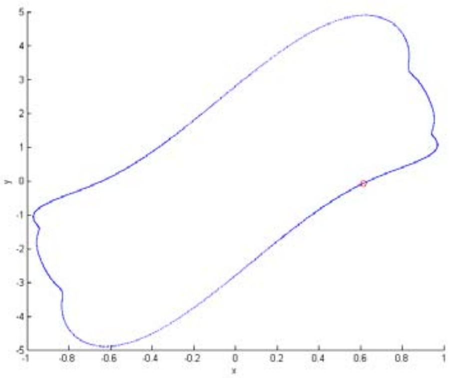

(b)

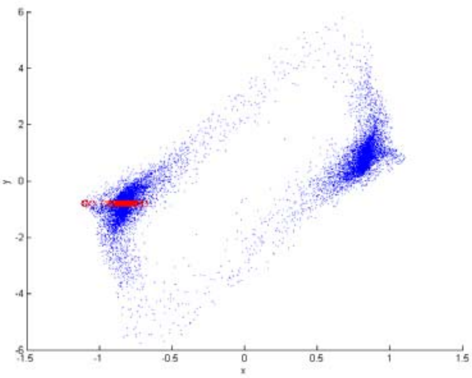

(c)

Fig 6.7(a) The bifurcation diagram for $\alpha = \beta = 0.4$. (b) The phase portrait for $\alpha = \beta = 0.4$, $b = 1.5$. (c) The phase portrait for $\alpha = \beta = 0.4$, $k = 2.5$.

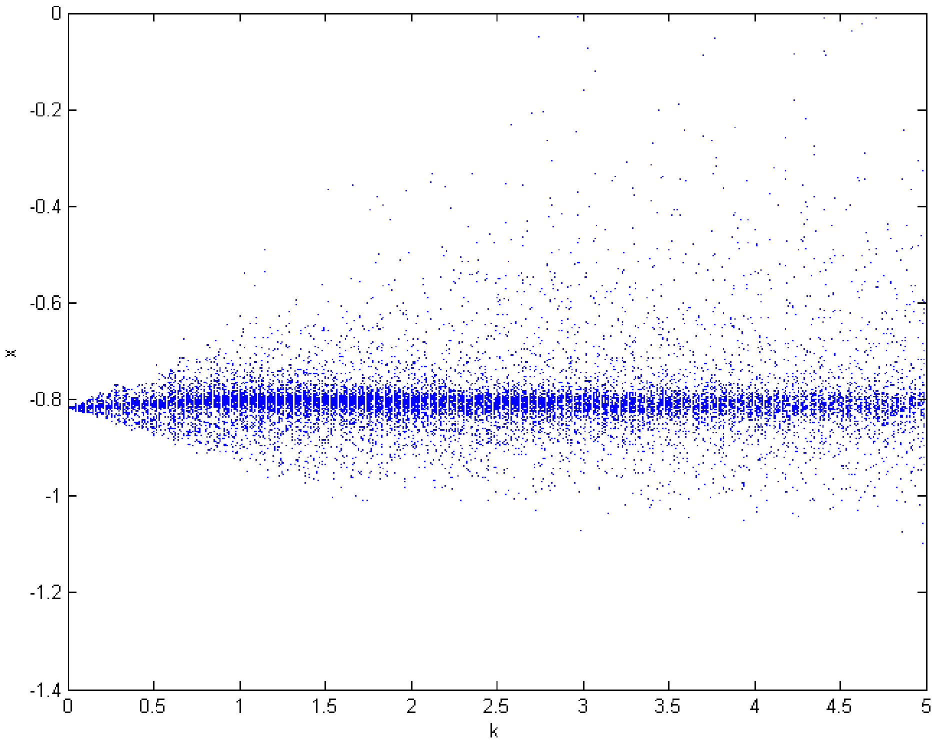

(a)

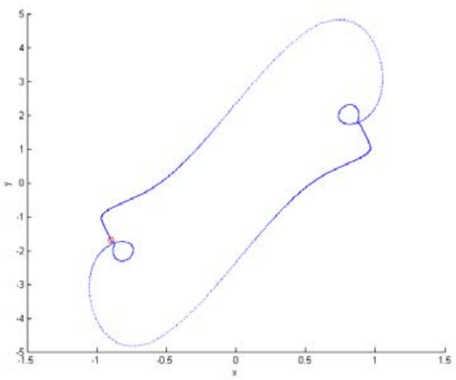

(b)

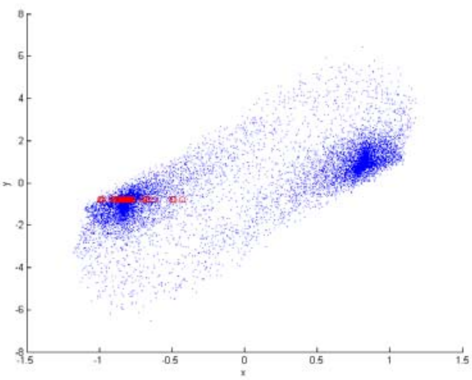

(c)

Fig 6.8(a) The bifurcation diagram for $\alpha = \beta = 0.3$. (b) The phase portrait for $\alpha = \beta = 0.3$, $b = 1.5$. (c) The phase portrait for $\alpha = \beta = 0.3$, $k = 3.5$.

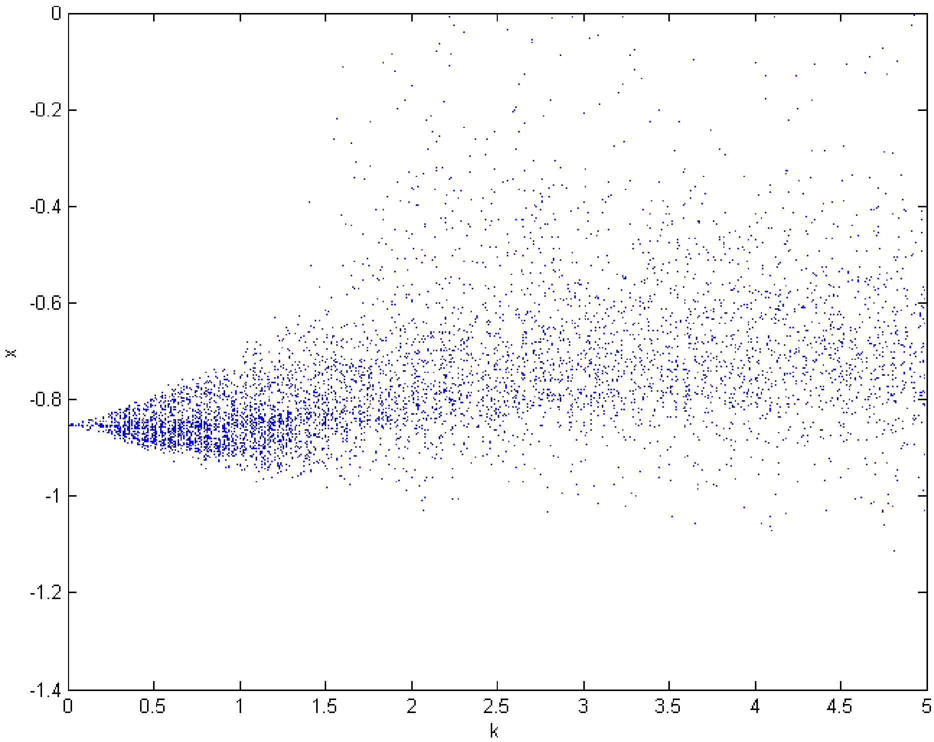

(a)

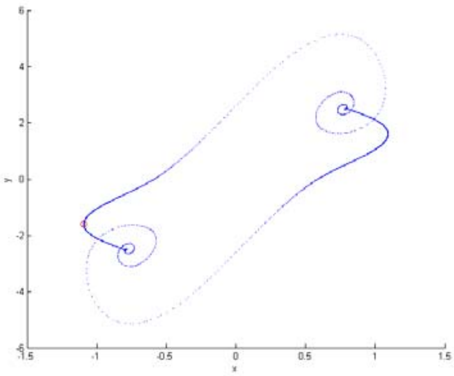

(b)

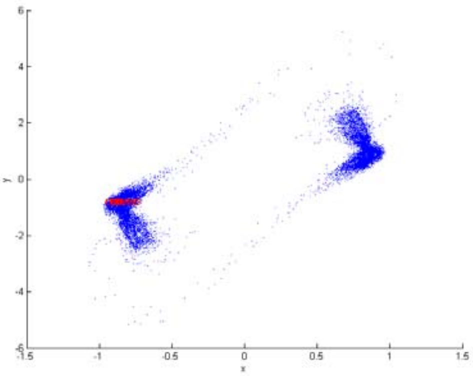

(c)

Fig 6.9(a) The bifurcation diagram for $\alpha = \beta = 0.2$. (b) The phase portrait for $\alpha = \beta = 0.2$, $b = 5$. (c) The phase portrait for $\alpha = \beta = 0.2$, $k = 1$.

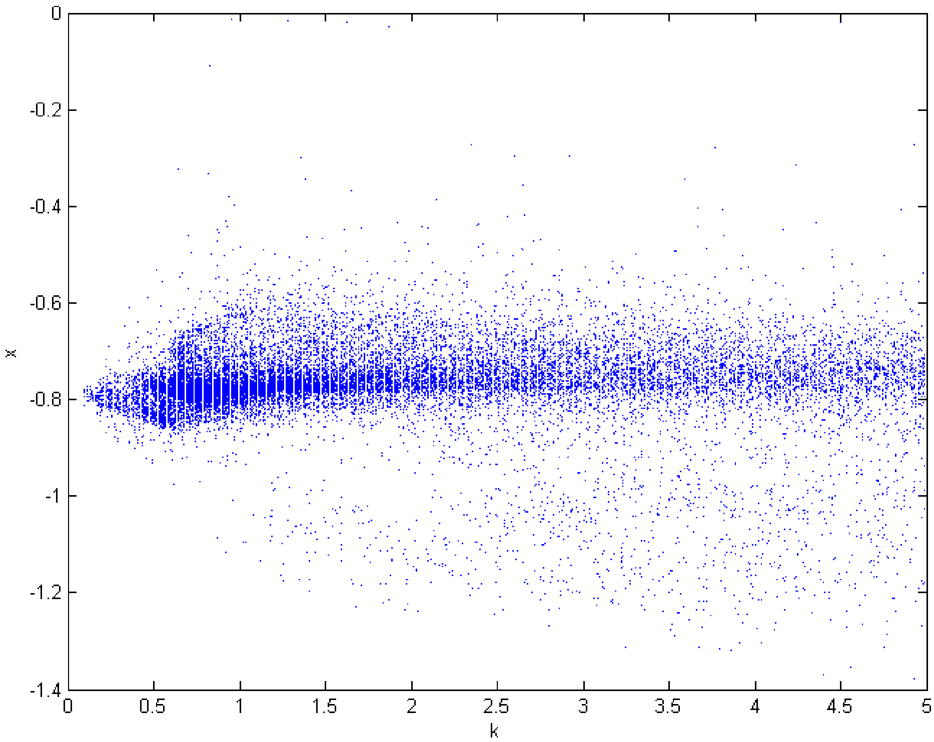

(a)

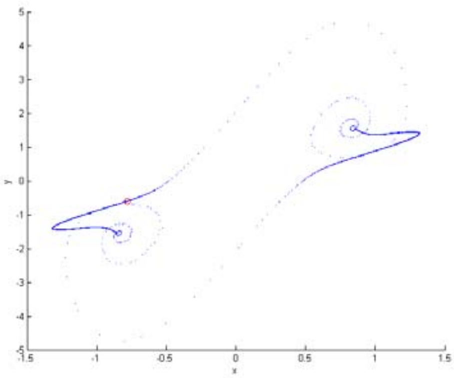

(b)

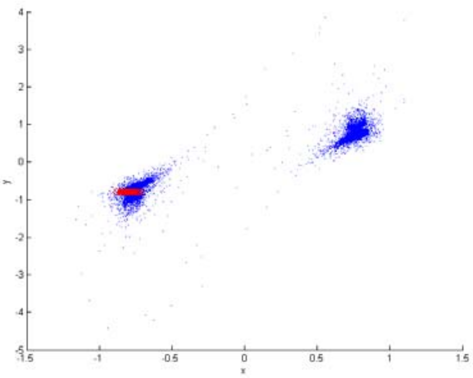

(c)

Fig 6.10(a) The bifurcation diagram for $\alpha = \beta = 0.1$. (b) The phase portrait for $\alpha = \beta = 0.1$, b = 8. (c) The phase portrait for $\alpha = \beta = 0.1$, k = 0.5.

Chapter 7

Conclusions

Chaos is desirable under certain circumstances and chaotic phenomena are quite useful in many applications such as fluid mixing, human brain, and heart beat regulation, etc. Thus, this motivates us to investigate anticontrol of chaos. Recently many scientists in various fields have been attracted to investigate chaos synchronization due to its application in a variety of fields such as secure communications, chemical, physical, and biological systems, neural networks, etc. Many scholars have investigated the control and dynamics of the fractional order dynamical systems. The results have been shown that nonlinear chaotic systems still have chaotic behavior and chaos synchronization can be achieved when their models become fractional.

In this thesis, integral and fractional order modified van der Pol systems are investigated. Chapter 2 contains a fractional derivative and the model of modified van der Pol system.

In Chapter 3, the dynamics of integral and fractional order modified van der Pol systems are investigated. The chaotic phenomena exist for $0.8 \le (\alpha + \beta) \le 2.0$ and the range of the chaos gradually decreases as the total order number $\alpha + \beta$ decreases. The numerical results of periodic and chaotic phenomena are presented by phase portraits, Poincaré maps and bifurcation diagrams.

The synchronizations of two uncoupled integral and fractional order chaotic modified van der Pol systems are achieved by parameter excited synchronization in Chapter 4. It is found that this approach is very effective even for very low total fractional order 0.2.

Anticontrol of chaos of fractional order modified van der Pol systems by addition of a constant term and addition of k|x|sinx term are discussed in Chapter 5. The results show that chaos exists in the fractional order systems with total order from 1.8 down to 0.6 for the addition of constant term, and from 1.8 down to 0.8 for the addition of k|x|sinx term.

Finally, the parameter excited chaotization of integral and fractional order modified van der Pol systems is studied in Chapter 6. It is found that chaotization can be successfully obtained in the integral and fractional order systems with total order from 2 down to 0.2.

REFERENCES

[1] Ottino JM et al. Chaos, symmetry, and self-similarity: exploiting order and disorder in mixing process. Science 1992; 257: 754–60.

[2] Schiff SJ et al. Controlling chaos in the brain. Nature 1994; 370: 615–20.

[3] Brandt ME, Chen G. Bifurcation control of two nonlinear models of cardiac activity. IEEE Trans Circ Syst 1997; 44: 1031–4.

[4] Chen H.-K. "Synchronization of two different chaotic systems: a new system and each of the dynamical systems Lorenz, Chen and *Lü*", Chaos, Solitons and Fractals Vol. 25; 1049-56, 2005.

[5] Chen H.-K., Lin T-N "Synchronization of chaotic symmetric gyros by one-way coupling conditions", ImechE Part C: Journal of Mechanical Engineering Science Vol. 217; 331-40, 2003.

[6] Chen H.-K. "Chaos and chaos synchronization of a symmetric gyro with linear-plus-cubic damping", Journal of Sound & Vibration, Vol. 255; 719-40,2002.

[7] Ge Z.-M., Yu T.-C., and Chen Y.-S. "Chaos synchronization of a horizontal platform system", Journal of Sound and Vibration 731-49, 2003.

[8] Ge Z.-M., Lin T.-N. "Chaos, chaos control and synchronization of electro-mechanical gyrostat system", Journal of Sound and Vibration Vol. 259; No.3, 2003.

[9] Ge Z.-M., Chen Y.-S. "Synchronization of unidirectional coupled chaotic systems via partial stability", Chaos, Solitons and Fractals Vol. 21; 101-11, 2004.

[10] Ge Z.-M., Chen C.-C. "Phase synchronization of coupled chaotic multiple time scales systems", Chaos, Solitons and Fractals Vol. 20; 639-47, 2004.

[11] Ge Z.-M., Lin C.-C. and Chen Y.-S. "Chaos, chaos control and synchronization of vibromrter system", Journal of Mechanical Engineering Science Vol. 218;

1001-20, 2004.

[12] Chen H.-K., Lin T.-N. and Chen J.-H. “The stability of chaos synchronization of the Japanese attractors and its application”, Japanese Journal of Applied Physics Vol. 42; No. 12, 7603-10, 2003.

[13] Ge Z.-M. and Shiue “Non-linear dynamics and control of chaos for Tachometer”, Journal of Sound and Vibration Vol. 253; No4, 2002.

[14] Ge Z.-M. and Lee C.-I. “Non-linear dynamics and control of chaos for a rotational machine with a hexagonal centrifugal governor with a spring”, Journal of Sound and Vibration Vol. 262; 845-64, 2003.

[15] Ge Z.-M., Hsiao C.-M. and Chen Y.-S. “Non-linear dynamics and chaos control for a time delay Duffing system”, Int. J. of Nonlinear Sciences and Numerical Vol. 6; No. 2, 187-199, 2005.

[16] Liao T.L., Huang N.S. “Control and synchronization of discrete-time chaotic systems via variable structure control technique”, Phys Lett A 262–68 1997.

[17] Yang, Yu; Ma, Xi-Kui; Zhang, Hao “Synchronization and parameter identification of high-dimensional discrete chaotic systems via parametric adaptive control “, Chaos, Solitons and Fractals 28; 244-251, 2006.

[18] Ge Z.-M., Tzen P.-C. and LeeS.-C. “Parametric analysis and fractal-like basins of attraction by modified interpolates cell mapping”, Journal of Sound and Vibration Vol. 253; No. 3, 2002.

[19] Ge Z.-M. and Lee S.-C. “Parameter used and accuracies obtain in MICM global analyses”, Journal of Sound and Vibration Vol. 272; 1079-85, 2004.

[20] Ge Z.-M. and Leu W.-Y. “Chaos synchronization and parameter identification for loudspeaker system” Chaos, Solitons and Fractals Vol. 21; 1231-47, 2004.

[21] Ge Z.-M. and Chang C.-M. “Chaos synchronization and parameter identification for single time scale brushless DC motor”, Chaos, Solitons and Fractals Vol. 20;

889-903, 2004.

[22] Ge Z.-M. and Lee J.-K. “Chaos synchronization and parameter identification for gyroscope system”, Applied Mathematics and Computation, Vol. 63; 667-82, 2004.

[23] Ge Z.-M. and Cheng J.-W. “Chaos synchronization and parameter identification of three time scales brushless DC motor”, Chaos, Solitons and Fractals Vol. 24; 597-616, 2005.

[24] Ge Z.-M. and Chen Y.-S. “Adaptive synchronization of unidirectional and mutual coupled chaotic systems”, Chaos, Solitons and Fractals Vol. 26; 881-88, 2005.

[25] Edouard, D.; Dufour, P.; Hammouri, H. “Observer based multivariable control of a catalytic reverse flow reactor: comparison between LQR and MPC approaches “, Computers and Chemical Engineering 29; 851-865, 2005.

[26] Ho, H.F.; Wong, Y.K.; Rad, A.B.; Lo, W.L. “State observer based indirect adaptive fuzzy tracking control”, Simulation Modelling Practice and Theory 13; 646-63, 2005.

[27] Bai E-W, Lonngren K.E. “Synchronization and Control of Chaotic Systems”, Chaos, Solitons & Fractals 9; 1571-75, 1999.

[28] Bai E-W, Lonngren K.E. “Sequential synchronization of two Lorenz systems using active control”, Chaos, Solitons & Fractals 7;1041-44, 2000.

[29] Agiza H.N., Yassen M.T. “Synchronization of Rossler and Chen chaotic dynamical systems using active control “, Phys Lett A 4; 191-97, 2001.

[30] Chen, Shihua; Lü, Jinhu “Parameters identification and synchronization of chaotic systems based upon adaptive control”, Phys Lett A 4; 353-58, 2002.

[31] Li Z., Han C.Z., Shi S.J. “Modification for synchronization of Rossler and Chen chaotic systems”, Phys Lett A 3-4; 224-30, 2002.

[32] Ho M.C., Hung Y.C., Chou C.H. “Phase and anti-phase synchronization of two

chaotic systems by using active control", Phys Lett A 1; 43-48, 2002.

[33] Ho M.C., Hung Y.C. "Synchronization of two different systems by using generalized active control", Phys Lett A 5-6; 424-28, 2002.

[34] Huang L.L., Feng R.P., Wang M. "Synchronization of chaotic systems via nonlinear control", Phys Lett A 4 271-75, 2004.

[35] Chen H.K. "Global chaos synchronization of new chaotic systems via nonlinear control", Chaos, Solitons & Fractals 4; 1245-51, 2005.

[36] R. Hilfer, editor, Applications of fractional calculus in physics, New Jersey, World Scientific, 2001.

[37] Ahmad W, Sprott JC "Chaos in fractional order system autonomous nonlinear systems", Chaos, Solitons & Fractals 16: 339-351, 2003.

[38] Oustaloup A., Levron F., Nanot F., Mathieu B. "Frequency band complex non integer differentiator: characterization and synthesis", IEEE Trans CAS-I 47: 25–40, 2000.

[39] Hartley T. T., Lorenzo C. F. "Dynamics and control of initialized fractional-order systems", Nonlinear Dyn 29: 201–33, 2002.

[40] Ahmad W., El-Khazali R., El-Wakil A. "Fractional-order Wien-bridge oscillator", Electr Lett 37: 1110–2, 2001.

[41] Li C., Liao X., Yu J. "Synchronization of fractional order chaotic systems", Phys Rev E 68: 067203, 2003.

[42] Arena P., Caponetto R., Fortuna L., Porto D. "Bifurcation and chaos in noninteger order cellular neural networks", Int J Bifur Chaos 7: 1527–39 1998.

[43] Arena P., Fortuna L., Porto D. "Chaotic behavior in noninteger-order cellular neural networks", Phys Rev E 61: 776–81.

[44] Arena P., Caponetto R., Fortuna L., Porto D. "Chaos in a fractional order Duffing system", In: Proc. ECCTD, Budapest 1259–62, 1997.

[45] Grigorenko I., Grigorenko E. "Chaotic dynamics of the fractional Lorenz system", Phys Rev Lett 91: 034101, 2003.

[46] Li C., Chen G. "Chaos and hyperchaos in fractional order Rössler equations", Physica A 341: 55-61, 2004.

[47] Ahmad W. M., Harb W. M. "On nonlinear control design for autonomous chaotic systems of integer and fractional orders", Chaos, Solitons & Fractals 18: 693–701, 2003.

[48] Wajdi M. Ahmad "Stabilization of generalized fractional order chaotic systems using state feedback control", Chaos, Solitons and Fractals 22, 141-150, 2004.

[49] Li C., Chen G. "Chaos in the fractional order Chen system and its control", Chaos, Solitons & Fractals 22, 549-554, 2004.

[50] Delbosco D., Rodino L. "Existence and uniqueness for a nonlinear fractional differential equation", J. Math. Anal. Appl. 204: 609–625, 1996.

[51] Diethelm K., Ford N.J. "Analysis of fractional differential equations", J. Math. Anal. Appl. 265: 229–248, 2002.

[52] Podlubny I. *Fractional Differential Equations*, Academic Press, New York, 1999.

[53] Samko S., Kilbas A., Marichev O. *Fractional Integrals and Derivatives*, Gordon and Breach, Yverdon, 1993.

[54] Chen H.-K. and Lee C.-I "Anti-control of chaos in rigid body motion", Chaos, Solitons and Fractals Vol. 21; 957-965, 2004.

[55] Ge Z.-M. and Wu H.-W. "Chaos synchronization and chaos anticontrol of a suspended track with moving loads", Journal of Sound and Vibration Vol. 270; 685-712, 2004.

[56] Ge Z.-M. and Yu C.-Y. and Chen Y.-S. "Chaos synchronization and chaos anticontrol of a rotational supported simple pendulum", JSME International Journal,

Series C, Vol. 47; No. 1, 233-41, 2004.

[57] Ge Z.-M. and Leu W.-Y. "Anti-control of chaos of two-degree-of-freedom louderspeaker system and chaos system of different order system", Chaos, Solitons and Fractals Vol. 20; 503-21, 2004.

[58] Ge Z.-M., Cheng J.-W. and Chen Y.-S. "Chaos anticontrol and synchronization of three time scales brushless DC motor system", Chaos, Solitons and Fractals Vol. 22; 1165-82, 2004.

[59] Ge Z.-M. and Lee C.-I "Anticontrol and synchronization of chaos for an autonomous rotational machine system with a hexagonal centrifugal governor", Chaos, Solitons and Fractals Vol. 282; 635-48, 2005.

[60] Ge Z.-M. and Lee C.-I "Control, anticontrol and synchronization of chaos for an autonomous rotational machine system with time-delay", Chaos, Solitons and Fractals Vol. 23; 1855-64, 2005.

[61] Codreanu S. "Desynchronization and chaotification of nonlinear dynamical systems", Chaos, Solitons & Fractals 13: 839-43, 2002.

[62] Tang K-S, Man KF, Zhong G-Q, Chen G. "Generating chaos via x|x|", IEEE Trans Circ Syst I 48:636–41, 2001.

[63] Wang X-F, Chen G. "Generating topological conjugate chaotic systems via feedback control". IEEE Trans Circ Syst I 50:812-7, 2003.

[64] Oldham K.B., Spanier J. *The fractional Calculus. San Diego*, CA: Academic, 1974.

[65] Oustaloup A., Sabatier J., Lanusse P. "From fractal robustness to CRONE control", Fract Calculus Appl Anal 2: 1–30, 1999.

[66] Podlubny I., Petras I., Vinagre B. M., O'Leary P., Dorcak L. "Analogue realizations of fractional-order controllers", Nonlinear Dyn 29: 281–96, 2002.

[67] Chen Y. Q., Moore K. "Discretization schemes for fractional-order

differentiators and integrators", IEEE Trans CAS-I 49: 363–7, 2002.

[68] Hwang C., Leu J.-F., Tsay S.-Y. "A note on time-domain simulation of feedback fractional-order systems", IEEE Trans Auto Contr 47: 625–31, 2002.

[69] Charef A., Sun H. H., Tsao Y. Y., Onaral B. "Fractal System as Represented by Singularity Function", IEEE Transactions on Automatic control Vol 37, No 9, 1992.

[70] Tom T. Hartley, Carl F. Lorenzo, Helen Killory Qammer "Chaos in Fractional Order Chua's System", IEEE, Tran. on circuit and systems Vol 42, No 8, 1995.

[71] van der Pol, B. "On relaxation oscillations", Philosophical Magazine 2, 978-92, 1926.

[72] van der Pol, B. and van der Mark, J. "Frequency demultiplication", Nature 120, 363-4, 1927.

[73] van der Pol, B. and van der Mark, J. "The heartbeat considered as a relaxarion oscillation and an electrical model of the heart", Philosophical Magazine 6, 763-75, 1928.

[74] Ge, Z.M., Yi, C.X., "Chaos in a nonlinear damped Mathieu system, in a nano resonator system and in its fractional order system", Chaos, Solitons and Fractals 2006, in press.

Appendix

Table 1. FRACTIONAL OPERATORS WITH APPROXIMATELY 2 db ERROR FROM ω = 10–2 TO 102 rad/sec

$\frac{1}{s^{0.1}} \approx \frac{220.4s^4 + 5004s^3 + 503s^2 + 234.5s + 0.484}{s^5 + 359.8s^4 + 5742s^3 + 4247s^2 + 147.7s + 0.2099}$
$\frac{1}{s^{0.2}} \approx \frac{60.95s^4 + 816.9s^3 + 582.8s^2 + 23.24s + 0.04934}{s^5 + 134s^4 + 956.5s^3 + 383.5s^2 + 8.953s + 0.01821}$
$\frac{1}{s^{0.3}} \approx \frac{23.76s^4 + 224.9s^3 + 129.1s^2 + 4.733s + 0.01052}{s^5 + 64.51s^4 + 252.2s^3 + 63.61s^2 + 1.104s + 0.002267}$
$\frac{1}{s^{0.4}} \approx \frac{25s^4 + 558.5s^3 + 664.2s^2 + 44.15s + 0.1562}{s^5 + 125.6s^4 + 840.6s^3 + 317.2s^2 + 7.428s + 0.02343}$
$\frac{1}{s^{0.5}} \approx \frac{15.97s^4 + 593.2s^3 + 1080s^2 + 135.4s + 1}{s^5 + 134.3s^4 + 1072s^3 + 543.4s^2 + 20.1s + 0.1259}$
$\frac{1}{s^{0.6}} \approx \frac{8.579s^4 + 255.6s^3 + 405.3s^2 + 35.93s + 0.1696}{s^5 + 94.22s^4 + 472.9s^3 + 134.8s^2 + 2.639s + 0.009882}$
$\frac{1}{s^{0.7}} \approx \frac{4.406s^4 + 177.6s^3 + 209.6s^2 + 9.179s + 0.0145}{s^5 + 88.12s^4 + 279.2s^3 + 33.3s^2 + 1.927s + 0.0002276}$
$\frac{1}{s^{0.8}} \approx \frac{5.235s^3 + 1453s^2 + 5306s + 254.9}{s^4 + 658.1s^3 + 5700s^2 + 658.2s + 1}$
$\frac{1}{s^{0.9}} \approx \frac{1.766s^2 + 38.27s + 4.914}{s^3 + 36.15s^2 + 7.789s + 0.01}$

Paper List

[1] Ge Z.-M. and Zhang A.-R., “Chaos in a Modified Heartbeat System and in Its Fractional order Systems”, Chaos, Solitons and Fractals, Dec. 2005, accepted and proofed.(SCI, Impact Factor:1.938)

[2] Ge Z.-M. and Zhang A.-R., “Parameter Excited Chaos Synchronizations of Integral and Fractional Order Modified Heartbeat Systems”, submitted to Chaos, Solitons and Fractals, 2006.

[3] Ge Z.-M. and Zhang A.-R., “Anticontrol of Chaos of the Fractional Order Modified Heartbeat Systems”, submitted to Chaos, Solitons and Fractals, 2006.

[4] Ge Z.-M. and Zhang A.-R., “Parameter Excited Chaotization of Integral and Fractional Order Modified Heartbeat Systems”, submitted to Chaos, Solitons and Fractals, 2006.